Diffraction Grating Handbook

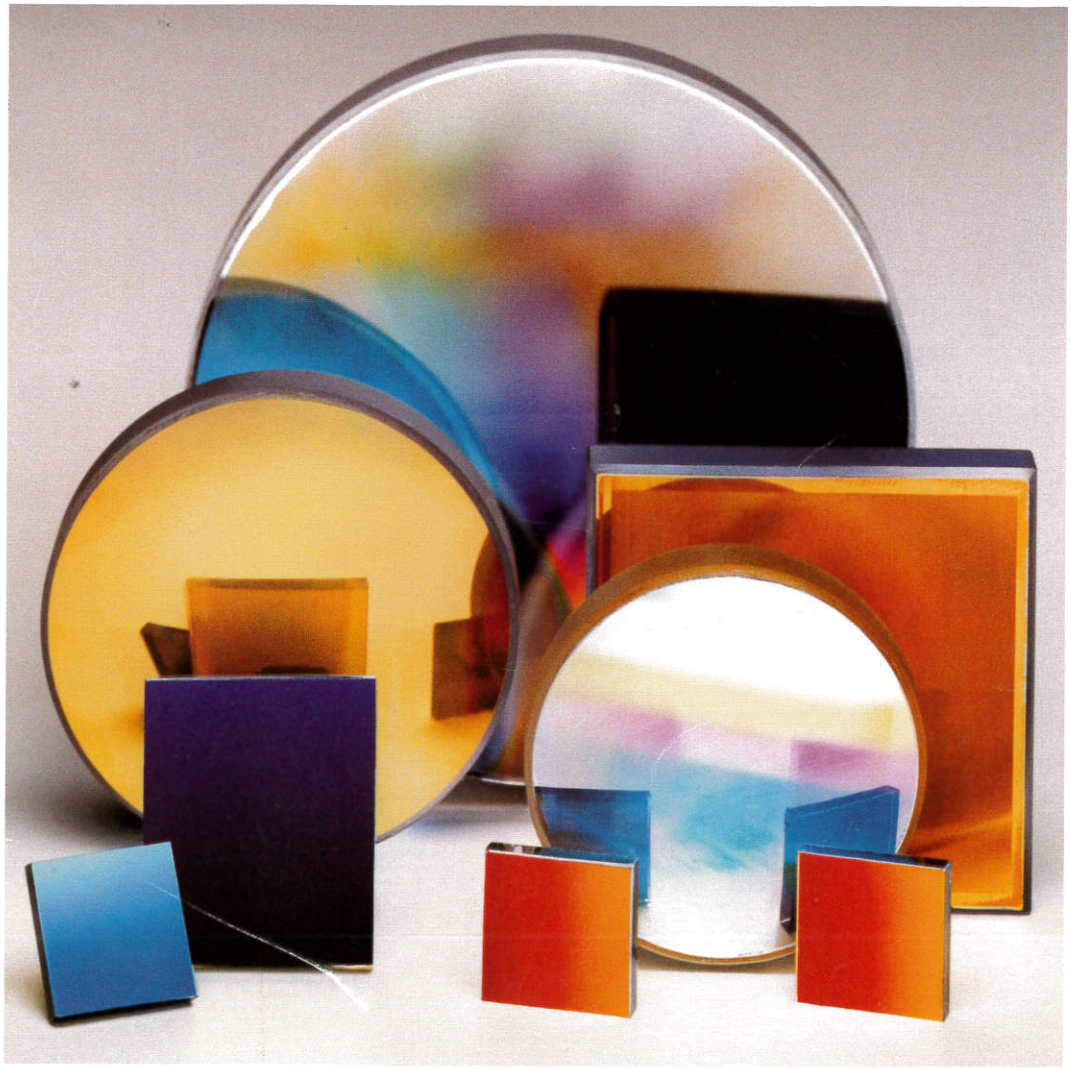

Richardson Grating Laboratory

Spectronic Instruments

DIFFRACTION GRATING HANDBOOK

third edition

Christopher Palmer
Editor

Erwin Loewen
Editor (first edition)

RICHARDSON GRATING LABORATORY
820 Linden Avenue, Rochester, New York 14625 USA
phone: (716) 262-1331, fax: (716) 454-1568
e-mail: gratings@spectronic.com
Web Site: http://www.gratinglab.com

The Richardson Grating Laboratory is a unit of Spectronic Instruments,

TABLE OF CONTENTS

I. SPECTROSCOPY AND GRATINGS 1
The Diffraction Grating 1
A Brief History of Grating Development 1
The Richardson Grating Laboratory 2

II. THE PHYSICS OF DIFFRACTION GRATINGS 3
The Grating Equation 3
Diffraction Orders 5
Existence of Diffraction Orders 5
Overlapping of Diffracted Spectra 5
Dispersion 6
Angular dispersion 6
Linear dispersion 7
Resolving Power, Spectral Resolution, and Bandpass 7
Resolving power 7
Spectral resolution 8
Bandpass 8
Resolving power vs. resolution 9
Focal Length and *f*/number 9
Anamorphic Magnification 10
Free Spectral Range 10
Energy Distribution (Grating Efficiency) 11
Stray Light 11
Grating stray light 11
Instrumental stray light 11
Signal-to-Noise Ratio (SNR) 12

III. RULED GRATINGS 13
Grating Ruling Engines 13
The Michelson engine 13
The Mann engine 13
The 'B' engine 13
The Ruling Process 14
Varied Line-space (VLS) Gratings 14

IV. INTERFERENCE (HOLOGRAPHIC) GRATINGS 15
Principle of Manufacture 15
Formation of an interference pattern 15
Formation of the grooves 16
Classification of Interference Gratings 16
Single-beam interference 16
Double-beam interference 16
The Recording Process 17
Differences between Ruled and Interference Gratings 18
Differences in stray light 18
Differences and limitations in the groove profile 18
Limitations in obtainable groove frequencies 18
Differences in the groove patterns 19
Differences in the substrate shapes 19
Differences in generation time for master gratings 19

V. REPLICATED GRATINGS 21
The Replication Process 21
Certified Precision Diffraction Gratings 21

VI. PLANE GRATINGS AND THEIR MOUNTS 23
Grating Mount Terminology 23
Plane Grating Mounts 23
The Czerny-Turner Monochromator 23
The Ebert-Fastie Monochromator 24
The Monk-Gillieson Monochromator 24
The Littrow Mount 24
Double Monochromators 25
Triple Monochromators 25

VII. CONCAVE GRATINGS AND THEIR MOUNTS 27
Classification of Grating Types 27
Groove patterns 27
Blank shapes 27
Classical Concave Grating Imaging 28
Nonclassical Concave Grating Imaging 31
Reduction of Aberrations 32
Concave Grating Mounts 32
Rowland Circle Spectrographs 32
The Wadsworth Spectrograph 33
Flat Field Spectrographs 33
Constant-Deviation Monochromators 34

VIII. IMAGING PROPERTIES OF GRATING SYSTEMS 35
Characterization of Imaging Quality 35
Geometric Raytracing & Spot Diagrams 35
Linespread Calculations 36
Instrumental Imaging 36
Magnification of the entrance aperture 36
Effects of the entrance aperture dimensions 37
Effects of the exit aperture dimensions 38

IX. EFFICIENCY OF DIFFRACTION GRATINGS 41
Grating Efficiency and Groove Shape 42
Triangular-groove gratings 43
Sinusoidal-groove gratings 45
The effects of finite conductivity 47
Distribution of Energy by Diffraction Order 47
Useful Wavelength Range 49
Blazing of Ruled Transmission Gratings 49

Overcoating of Reflection Gratings.....49

X. TESTING AND CHARACTERIZATION OF GRATINGS.....51
Spectral Defects.....51
Rowland Ghosts.....51
Lyman Ghosts.....52
Satellites.....52
Efficiency Measurement.....52
Foucault Knife-edge Test.....53
Direct Wavefront Testing.....53
Scattered Light.....54

XI. SELECTION OF DISPERSING SYSTEMS.....55
Reflection Grating Systems.....55
Plane reflection grating systems.....55
Concave reflection grating systems.....55
Transmission Grating Systems.....56
Grating Prisms (Grisms).....56
Grazing Incidence Systems.....57
Echelles.....57

XII. GRATINGS FOR SPECIAL PURPOSES.....59
Astronomical Gratings.....59
Filter Gratings.....59
Gratings for Electron Microscope Calibration.....59
Gratings for Laser Tuning.....59
Gratings as Beam Dividers.....60
Space-borne Spectrometry.....60
Special Gratings.....60

XIII. ADVICE TO GRATING USERS.....61
Choosing a Specific Grating.....61
Care in Handling Gratings.....61
Grating Cleaning Service.....61
Recoating.....62
Appearance.....62
Ruled gratings.....62
Interference gratings.....62
Grating Mounting.....62

BIBLIOGRAPHY.....63

REFERENCES.....63

RICHARDSON GRATING LABORATORY TECHNICAL PUBLICATIONS.....64

INDEX.....65

PREFACE

In July 1995, Life Sciences International plc of London, England, acquired Spectronic Instruments, Inc., including the Richardson Grating Laboratory, from Milton Roy Company.

Spectronic Instruments is proud to build upon the heritage of technical excellence which began when the Laboratory was a unit of Bausch & Lomb with the production of the first high-quality grating in 1949. A high-fidelity replication process was subsequently developed to make duplicates of the tediously generated master gratings. This process became the key to converting diffraction gratings from academic curiosities to catalogue items, which in turn enabled gratings to almost completely replace prisms as the optical dispersing element of choice.

The *Diffraction Grating Handbook* is supplemented by the Richardson Grating Laboratory's *Grating Catalog*, which lists the standard plane and concave gratings available. If the *Catalog* does not offer a diffraction grating which meets your requirements, please contact us for a listing of new gratings or a quotation for a custom-designed grating.

The Richardson Grating Laboratory remains committed to maintaining its proud traditions – using the most advanced technology available to produce high-quality precision diffraction gratings, and providing competent technical assistance in the choice and use of these gratings.

For further information regarding our diffraction gratings, please contact

RICHARDSON GRATING LABORATORY
Marketing and Sales Department
820 Linden Avenue
Rochester, New York 14625 USA

phone: 716-262-1331
800-654-9955

fax: 716-454-1568

e-mail: gratings@spectronic.com

Web site: http://www.gratinglab.com

ACKNOWLEDGMENT

The editor gratefully acknowledges the following people for their thorough and critical review of the manuscript:

Peter Gray
Anglo-Australian Observatory, Epping, New South Wales, Australia

W. R. Hunter
SFA Inc., Landover, Maryland

Robert P. Madden
National Institute of Standards and Technology, Gaithersburg, Maryland

Daniel J. Schroeder
Beloit College, Beloit, Wisconsin

"It is difficult to point to another single device that has brought more important experimental information to every field of science than the diffraction grating. The physicist, the astronomer, the chemist, the biologist, the metallurgist, all use it as a routine tool of unsurpassed accuracy and precision, as a detector of atomic species to determine the characteristics of heavenly bodies and the presence of atmospheres in the planets, to study the structures of molecules and atoms, and to obtain a thousand and one items of information without which modern science would be greatly handicapped."

- J. Strong , J. Opt. Soc. Am. ***50*** *, 1148-1152 (1960), quoting G. R. Harrison*

SPECTROSCOPY AND GRATINGS I

Spectroscopy is the study of electromagnetic spectra – the wavelength composition of light – due to atomic and molecular interactions. For many years, spectroscopy has been important in the study of physics, and it is now equally important in astronomical, biological, chemical, metallurgical and other analytical investigations. The first experimental tests of quantum mechanics involved verifying predictions regarding the spectrum of hydrogen with grating spectrometers. In astrophysics, diffraction gratings provide clues to the composition of and processes in stars and planetary atmospheres, as well as offer clues to the large-scale motions of objects in the universe. In chemistry, toxicology and forensic science, grating-based instruments are used to determine the presence of chemical species in samples.

The diffraction grating is of considerable importance in spectroscopy, due to its ability to separate (disperse) polychromatic light into its constituent monochromatic components. In recent years, the spectroscopic quality of diffraction gratings has greatly improved, and the Richardson Grating Laboratory has been a leader in this development.

The extremely high precision required of a modern diffraction grating dictates that the mechanical dimensions of diamond tools, ruling engines, and optical recording hardware, as well as their environmental conditions, be controlled to the very limit of that which is physically possible. Anything less results in gratings which are ornamental but have little technical or scientific value. The challenge to produce precision diffraction gratings has attracted the attention of some of the world's most capable scientists and technicians. Only a few have met with any appreciable degree of success, each limited by the technology available.

THE DIFFRACTION GRATING

A *diffraction grating* is a collection of reflecting (or transmitting) elements separated by a distance comparable to the wavelength of light under study. It may be thought of as a collection of diffracting elements, such as a pattern of transparent slits (or apertures) in an opaque screen, or a collection of reflecting grooves on a substrate. A *reflection grating* consists of a grating superimposed on a reflective surface, whereas a *transmission grating* consists of a grating superimposed on a transparent optical surface. An electromagnetic wave incident on a grating will, upon diffraction, have its electric field amplitude (or phase, or both) modified in a predictable manner.

A BRIEF HISTORY OF GRATING DEVELOPMENT

The first diffraction grating was made by an American astronomer, David Rittenhouse, in 1785, who reported constructing a half-inch wide grating with fifty-three apertures. Apparently he developed this prototype no further, and there is no evidence that he tried to use it for serious scientific experiments.

In 1821, unaware of the earlier American report, Joseph von Fraunhofer began his work on diffraction gratings. His research was given impetus by his insight into the value that grating dispersion could have for what we now call the science of spectroscopy. Fraunhofer's persistence resulted in gratings of sufficient quality to enable him to measure the absorption lines of the solar spectrum. He also derived the equations that govern the dispersive behavior of gratings. Fraunhofer was interested only in making gratings for his own experiments, and upon his death, his equipment disappeared.

By 1850, F. A. Nobert, a Prussian instrument maker, began to supply scientists with gratings far superior to Fraunhofer's. About 1870, the scene of grating development returned to America, where L. M. Rutherfurd, a New York lawyer with an avid interest in astronomy, became interested in gratings.

In just a few years, Rutherfurd learned to rule reflection gratings in speculum metal that were larger and better than any Nobert had made. For the first time, the performance of diffraction gratings surpassed even that of the

most powerful prisms. Rutherfurd made few gratings, though, and their uses were limited due to their high ghost intensities.

Rutherfurd's dedication, impressive as it was, could not match the tremendous strides made by H. A. Rowland, professor of physics at the Johns Hopkins University. Rowland's work established the grating as the primary optical element of spectroscopic technology.

Rowland not only constructed sophisticated ruling engines but also invented the concave grating, a device of spectacular value to modern spectroscopists. He continued to rule gratings until his death in 1901.

After Rowland's great success, others set out to rule diffraction gratings. With some success, they sharpened the scientific demand for gratings. As the advantages of gratings over prisms and interferometers for spectroscopic work became more apparent, the demand for diffraction gratings far exceeded the supply.

In 1947, Bausch & Lomb decided to make precision gratings available commercially for the first time. In 1950, through the encouragement of George R. Harrison of MIT, David Richardson and Robert Wiley of Bausch & Lomb succeeded in producing their first high quality grating. This was ruled on a rebuilt engine which had its origins in the University of Chicago laboratory of Albert A. Michelson. A high fidelity replication process was subsequently developed, which was crucial to making *replicas*, duplicates of the tediously generated master gratings. Since then, the Richardson Grating Laboratory has produced thousands of master gratings and many times that number of high quality replicas. In 1985, Milton Roy Company acquired Bausch & Lomb's gratings and spectrometer operations, and in 1995 sold the unit to Life Sciences International plc as part of Spectronic Instruments, Inc. Spectronic has continued to uphold the traditions of precision and quality established by Bausch & Lomb fifty years ago.

A most useful feature of modern gratings is the availability of an enormous range of sizes and groove spacings (up to 10800 grooves per millimeter), and their enhanced quality is now almost taken for granted. In particular, the control of groove shape (or blazing) has increased spectral efficiency to its theoretical limits. In addition, interferometric and servo control systems have made it possible to break through the accuracy barrier previously set by the mechanical constraints inherent in the lead screws of ruling engines.

The Richardson Grating Laboratory

The Richardson Grating Laboratory is a unique, integrated facility in Rochester, New York, housing not only the Richardson ruling engines but the associated testing and production facilities.

To achieve gratings of the highest practical resolution, a precision of better than 1 nm (0.001 μm) in the spacing of the grooves must be maintained. Such high precision requires extreme control over temperature fluctuation and vibration in the ruling engine environment. This control has been established at the Laboratory by construction of an underground grating ruling laboratory equipped with temperature control to better that ±0.01 °C, and a modern vibration isolation system that suppresses amplitudes to less than 0.025 μm. The installation can maintain reliable control over the important environmental factors for periods in excess of six weeks, the time required to rule large, finely-spaced gratings.

The Richardson Grating Laboratory contains facilities for coating and testing master and replica blanks, as well as special areas for the controlled replication itself. In order to produce the finest gratings with maximum control and efficiency, even storage, packing and shipping of finished gratings are part of the same facility.

In addition to mechanically burnishing gratings with a diamond tool, photographic recording of an optical interference pattern can be used to produce gratings. Master interference gratings require strict maintenance of the recording optical system to obtain the best contrast and fringe structure. The Richardson Grating Laboratory produces interference (holographic) gratings in its dedicated recording facility, in whose controlled environment thermal gradients and air currents are minimized and fine particulates are filtered from the air. These master gratings are replicated in a process identical to that for ruled master gratings.

THE GRATING EQUATION

When monochromatic light is incident on a grating surface, it is diffracted into discrete directions. We can picture each grating groove as being a very small, slit-shaped source of diffracted light. The light diffracted by each groove combines to form a diffracted wavefront. The usefulness of a grating depends on the fact that there exists a unique set of discrete angles along which, for a given spacing d between grooves, the diffracted light from each facet is in phase with the light diffracted from any other facet, so they combine constructively.

Diffraction by a grating can be visualized from the geometry in Figure II-1, which shows a light ray of wavelength λ incident at an angle α and diffracted by a grating (of *groove spacing d*) along angles β_m. These angles are measured from the grating normal, which is the dashed line perpendicular to the grating surface at its center. The sign convention for these angles depends on whether the light is diffracted on the same side or the opposite side of the grating as the incident light. In diagram (a), which shows a *reflection grating*, the angles $\alpha > 0$ and $\beta_1 > 0$ (since they are measured counter-clockwise from the grating normal) while the angles $\beta_0 < 0$ and $\beta_{-1} < 0$ (since they are measured clockwise from the grating normal). Diagram (b) shows the case for a *transmission grating*.

By convention, angles of incidence and diffraction are measured *from* the grating normal *to* the beam. This is shown by arrows in the diagrams. In both diagrams, the sign convention for angles is shown by the plus and minus symbols located on either side of the grating normal. For either reflection or transmission gratings, the algebraic signs of two angles differ if they are measured from opposite sides of the grating normal. Other sign conventions exist, so care must be taken in calculations to ensure that results are self-consistent.

Another illustration of grating diffraction, using wavefronts (surfaces of constant phase), is shown in Figure II-2. The geo-

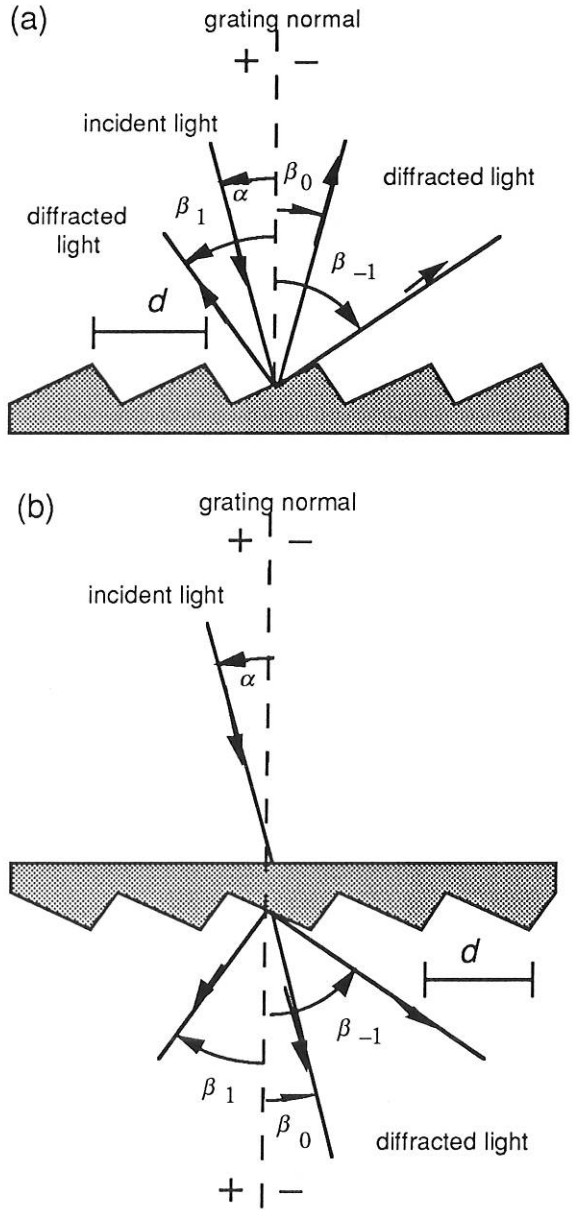

Figure II-1. Diffraction by a plane grating. A beam of monochromatic light of wavelength λ is incident on a grating and diffracted along several discrete paths. The triangular grooves come out of the page; the rays lie in the plane of the page. The sign convention for the angles α and β is shown by the + and – signs on either side of the grating normal. (a) A *reflection grating*: the incident and diffracted rays lie on the same side of the grating. (b) A *transmission grating*: the incident and diffracted rays lies on opposite sides of the grating.

metrical path difference between light from adjacent grooves is seen to be $d \sin\alpha + d \sin\beta$. [Since $\beta < 0$, the latter term is actually negative.] The principle of interference dictates that only when this difference equals the wavelength λ of the light, or some integral multiple thereof, will the light from adjacent grooves be in phase (leading to constructive interference). At all other angles β, there will be some measure of destructive interference between the wavelets originating from the groove facets.

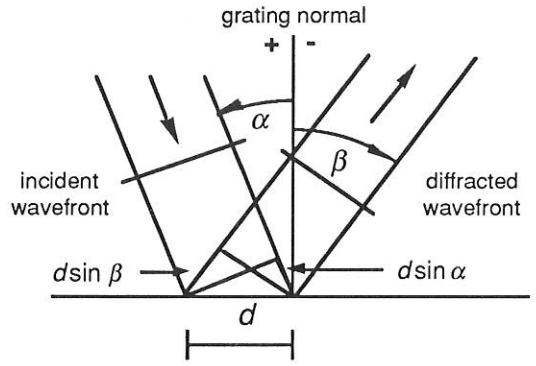

Figure II-2. Geometry of diffraction, for planar wavefronts. The terms in the path difference, $d \sin\alpha$ and $d \sin\beta$, are shown.

These relationships are expressed by the *grating equation*

$$m\lambda = d\,(\sin\alpha + \sin\beta), \qquad (2\text{-}1)$$

which governs the angles of diffraction from a grating of groove spacing d. Here m is the *diffraction order* (or *spectral order*), which is an integer. For a particular wavelength λ, all values of m for which $|m\lambda/d| < 2$ correspond to physically realizable diffraction orders. It is sometimes convenient to write the grating equation as

$$Gm\lambda = \sin\alpha + \sin\beta, \qquad (2\text{-}1')$$

where $G = 1/d$ is the *groove frequency*, *groove density* or *pitch*, more commonly called "grooves per millimeter".

[Eq. (2-1) and its equivalent Eq. (2-1') are the common forms of the grating equation, but their validity is restricted to cases in which the incident and diffracted rays are perpendicular to the grooves (at the center of the grating). The vast majority of grating systems fall within this category, which is called *classical* (or *in-plane*) *diffraction*. If the incident light beam is not perpendicular to the grooves, though, the grating equation must be modified:

$$Gm\lambda = \cos\varepsilon\,(\sin\alpha + \sin\beta). \qquad (2\text{-}1'')$$

Here ε is the angle between the incident light path and the plane perpendicular to the grooves at the grating center (the plane of the page in Figure II-2). If the incident light lies in this plane, $\varepsilon = 0$ and Eq. (2-1") reduces to the more familiar Eq. (2-1'). In geometries for which $\varepsilon \neq 0$, the diffracted spectra lie on a cone rather than in a plane, so such cases are termed *conical diffraction*.]

For a grating of groove spacing d, there is a purely mathematical relationship between the wavelength and the angles of incidence and diffraction. In a given spectral order m, the different wavelengths of polychromatic wavefronts incident at angle α are separated in angle:

$$\beta(\lambda) = \arcsin(m\lambda/d - \sin\alpha). \qquad (2\text{-}2)$$

When $m = 0$, the grating acts as a mirror, and the wavelengths are not separated ($\beta = -\alpha$ for all λ); this is called *specular reflection* or simply the *zero order*.

A special but common case is that in which the light is diffracted back toward the direction from which it came (*i.e.*, $\alpha = \beta$); this is called the *Littrow configuration*, for which the grating equation becomes

$$m\lambda = 2d \sin\alpha, \qquad \text{in Littrow.} \qquad (2\text{-}3)$$

In many applications (such as constant-deviation monochromators), the wavelength λ is changed by rotating the grating about the axis coincident with its central ruling, with the directions of incident and diffracted light remaining unchanged. The *deviation angle* $2K$ between the incidence and diffraction directions (also called the *angular deviation*) is

$$2K = \alpha - \beta = \text{constant}, \qquad (2\text{-}4)$$

while the *scan angle* ϕ, which is measured from the grating normal to the bisector of the beams, is

$$2\phi = \alpha + \beta. \qquad (2\text{-}5)$$

Note that ϕ changes with λ (as do α and β). In this case, the grating equation can be expressed in terms of ϕ and the *half deviation angle K* as

$$m\lambda = 2d \cos K \sin\phi. \qquad (2\text{-}6)$$

This version of the grating equation is useful for monochromator mounts (see Chapter VII). Eq. (2-6) shows that the wavelength diffracted by a grating in a monochromator mount is directly proportional to the sine of the angle ϕ through which the grating rotates, which is the basis for monochromator drives in which a *sine bar* rotates the grating to scan wavelengths (see Figure II-3).

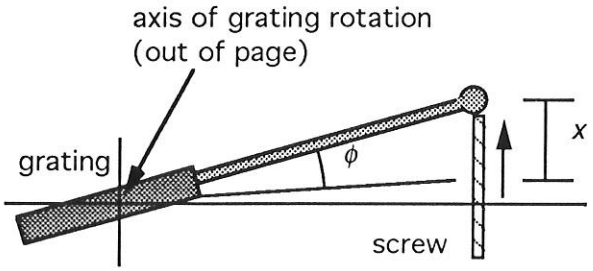

Figure II-3. A sine bar mechanism for wavelength scanning. As the screw is extended linearly by the distance x shown, the grating rotates through an angle ϕ in such a way that $\sin\phi$ is proportional to x.

DIFFRACTION ORDERS

Existence of Diffraction Orders. For a particular set of values of the groove spacing d and the angles α and β, the grating equation (2-1) is satisfied by more than one wavelength. In fact, subject to restrictions discussed below, there may be several discrete wavelengths which, when multiplied by successive integers m, satisfy the condition for constructive interference. The physical significance of this is that the constructive reinforcement of wavelets diffracted by successive grooves merely requires that each ray be retarded (or advanced) in phase with every other; this phase difference must therefore correspond to a real distance (path difference) which equals an integral multiple of the wavelength. This happens, for example, when the path difference is one wavelength, in which case we speak of the positive first diffraction order ($m = 1$) or the negative first diffraction order ($m = -1$), depending on whether the rays are advanced or retarded as we move from groove to groove. Similarly, the second order ($m = 2$) and negative second order ($m = -2$) are those for which the path difference between rays diffracted from adjacent grooves equals two wavelengths.

The grating equation reveals that only those spectral orders for which $|m\lambda/d| < 2$ can exist; otherwise, $|\sin\alpha + \sin\beta| > 2$, which is physically meaningless. This restriction prevents light of wavelength λ from being diffracted in more than a finite number of orders. Specular reflection ($m = 0$) is always possible; that is, the *zero order* always exists (it simply requires $\beta = -\alpha$). In most cases, the grating equation allows light of wavelength λ to be diffracted into both negative and positive orders as well. Explicitly, spectra of all orders m exist for which

$$-2d < m\lambda < 2d, \qquad m \text{ an integer.} \qquad (2\text{-}7)$$

For $\lambda/d << 1$, a large number of diffracted orders will exist.

As seen from Eq. (2-1), the distinction between negative and positive spectral orders is that

$$\beta > -\alpha \text{ for positive orders } (m > 0),$$

$$\beta < -\alpha \text{ for negative orders } (m < 0), \qquad (2\text{-}8)$$

$$\beta = -\alpha \text{ for specular reflection } (m = 0).$$

This sign convention for m requires that $m > 0$ if the diffracted ray lies to the left (the counter-clockwise side) of the zero order ($m = 0$), and $m < 0$ if the diffracted ray lies to the right (the clockwise side) of the zero order. This convention is shown graphically in Figure II-4.

Overlapping of Diffracted Spectra. The most troublesome aspect of multiple order behavior is that successive spectra overlap, as shown in Figure II-5. It is evident from the grating equation that, for any grating instrument configuration, the light of wavelength λ diffracted in the $m = 1$ order will coincide with the light of wave-

length $\lambda/2$ diffracted in the $m = 2$ order, *etc.*, for all m satisfying inequality (2-7). In this example, the red light (600 nm) in the first spectral order will overlap the ultraviolet light (300 nm) in the second order. A detector sensitive at both wavelengths would see both simultaneously. This superposition of wavelengths, which would lead to ambiguous spectroscopic data, is inherent in the grating equation itself and must be prevented by suitable filtering (called *order sorting*), since the detector cannot generally distinguish between light of different wavelengths incident on it (within its range of sensitivity). [See also **FREE SPECTRAL RANGE**, below.]

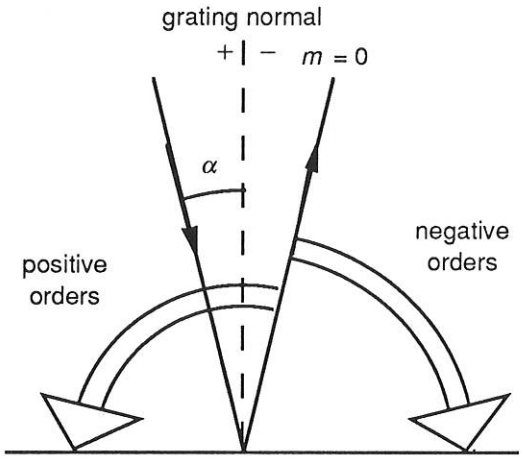

Figure II-4. Sign convention for the spectral order m. In this example α is positive.

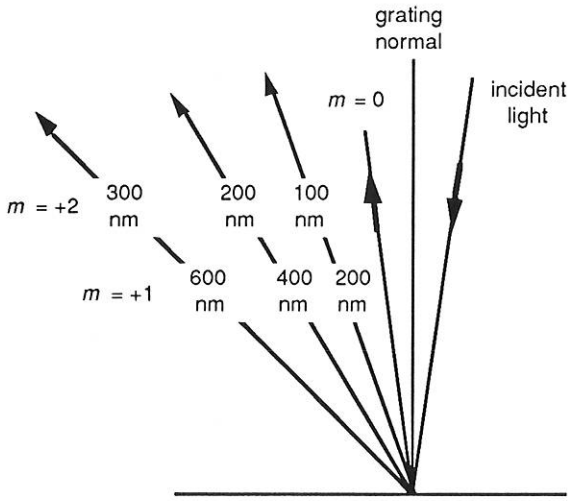

Figure II-5 - Overlapping of spectral orders. The light for wavelengths 100, 200 and 300 nm in the second order is diffracted in the same direction as the light for wavelengths 200, 400 and 600 nm in the first order. In this diagram, the light is incident from the right, so $\alpha < 0$.

DISPERSION

The primary purpose of a diffraction grating is to disperse light spatially by wavelength. A beam of white light incident on a grating will be separated into its component colors upon diffraction from the grating, with each color diffracted along a different direction. *Dispersion* is a measure of the separation (either angular or spatial) between diffracted light of different wavelengths. Angular dispersion expresses the spectral range per unit angle, and linear resolution expresses the spectral range per unit length.

Angular dispersion. The angular spread $d\beta$ of a spectrum of order m between the wavelength λ and $\lambda + d\lambda$ can be obtained by differentiating the grating equation, assuming the incidence angle α to be constant. The change D in diffraction angle per unit wavelength is therefore

$$D = \frac{d\beta}{d\lambda} = \frac{m}{d\cos\beta} = \frac{m}{d}\sec\beta = G m \sec\beta, \quad (2\text{-}9)$$

where β is given by Eq. (2-2). The ratio $D = d\beta/d\lambda$ is called the *angular dispersion*. As the groove frequency $G = 1/d$ increases, the angular dispersion increases (meaning that the angular separation between wavelengths increases for a given order m).

In Eq. (2-9), it is important to realize that the quantity m/d is not a ratio which may be chosen independently of other parameters; substitution of the grating equation into Eq. (2-9) yields the following general equation for the angular dispersion:

$$D = \frac{d\beta}{d\lambda} = \frac{(\sin\alpha + \sin\beta)}{\lambda\cos\beta}. \quad (2\text{-}10)$$

For a given wavelength, this shows that the angular dispersion may be considered to be solely a function of the angles of incidence and diffraction. This becomes even more clear when we consider the Littrow configuration ($\alpha = \beta$), in which case Eq. (2-10) reduces to

$$D = \frac{d\beta}{d\lambda} = \frac{2}{\lambda}\tan\beta, \qquad \text{in Littrow.} \quad (2\text{-}11)$$

When $|\beta|$ increases from 10° to 63° in Littrow use, the angular dispersion increases by a factor of ten, regardless of the spectral order or wavelength under consideration. Once β has been determined, the choice must be made whether a fine-pitch grating (small d) should be used in a low order, or a course-pitch grating (large d) such as an echelle grating should be used in a high order. [The fine-pitched grating, though, will provide a larger free spectral range; see below.]

Linear dispersion. For a given diffracted wavelength λ in order m (which corresponds to an angle of diffraction β), the *linear dispersion* of a grating system is the product of the angular dispersion D and the effective focal length $r'(\beta)$ of the system:

$$r'D = r'\frac{d\beta}{d\lambda} = \frac{m\,r'}{d\cos\beta} = \frac{m\,r'}{d}\sec\beta$$

$$= Gmr'\sec\beta. \quad (2\text{-}12)$$

The quantity $r'\,d\beta = dl$ is the change in position along the spectrum (a real distance, rather than a wavelength). We have written $r'(\beta)$ for the focal length to show explicitly that it may depend on the diffraction angle β (which, in turn, depends on λ).

The *reciprocal linear dispersion*, also called the *plate factor* P, is more often considered; it is simply the reciprocal of $r'D$, usually measured in nm/mm:

$$P = \frac{d\cos\beta}{m\,r'}. \quad (2\text{-}12')$$

P is a measure of the change in wavelength (in nm) corresponding to a change in location along the spectrum (in mm). It should be noted that the terminology *plate factor* is used by some authors to represent the quantity $1/\sin\Phi$, where Φ is the angle the spectrum makes with the line perpendicular to the diffracted rays (see Figure II-6); in order to avoid confusion, we call the quantity $1/\sin\Phi$ the *obliquity factor*. When the image plane for a particular wavelength is not perpendicular to the diffracted rays (*i.e.*, when $\Phi \neq 90°$), P must be multiplied by the obliquity factor to obtain the correct reciprocal linear dispersion in the image plane.

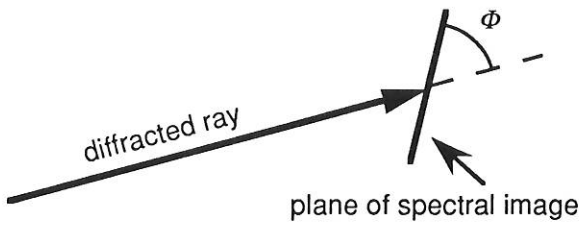

Figure II-6. The obliquity angle Φ. The spectral image recorded need not lie in the plane perpendicular to the diffracted ray (i.e., $\Phi \neq 90°$).

Resolving Power, Spectral Resolution, and Bandpass

Resolving power. The resolving power R of a grating is a measure of its ability to separate adjacent spectral lines of average wavelength λ. It is usually expressed as the dimensionless quantity

$$R = \lambda/\Delta\lambda. \quad (2\text{-}13)$$

Here $\Delta\lambda$ is the *limit of resolution*, the difference in wavelength between two lines of equal intensity which can be distinguished (that is, the peaks of two wavelengths λ_1 and λ_2 for which $|\lambda_1 - \lambda_2| < \Delta\lambda$ will be ambiguous). The theoretical resolving power of a planar diffraction grating is given in elementary optics textbooks as

$$R = mN, \quad (2\text{-}14)$$

where m is the diffraction order and N is the total number of grooves illuminated on the surface of the grating. For negative orders ($m < 0$), the absolute value of R is considered.

A more meaningful expression for R is derived below. The grating equation can be used to replace m in Eq. (2-14):

$$R = Nd\,(\sin\alpha + \sin\beta)/\lambda. \quad (2\text{-}15)$$

If the groove spacing d is uniform over the surface of the grating, and if the grating blank is planar, the quantity Nd is simply the ruled width W of the grating, so

$$R = W\,(\sin\alpha + \sin\beta)/\lambda. \qquad (2\text{-}16)$$

As expressed by Eq. (2-16), R is not dependent explicitly on the spectral order or the number of grooves; these parameters are contained within the ruled width and the angles of incidence and diffraction. Since

$$|\sin\alpha + \sin\beta| < 2 \qquad (2\text{-}17)$$

the maximum attainable resolving power is

$$R_{MAX} = 2W/\lambda, \qquad (2\text{-}18)$$

regardless of the order m or number of grooves N. This maximum condition corresponds to the grazing Littrow configuration, i.e., $\alpha \approx \beta$ (Littrow), $|\alpha| \approx 90°$ (grazing).

It is useful to consider the resolving power as being determined by the maximum phase retardation of the extreme rays diffracted from the grating. Measuring the difference in optical path lengths between the rays diffracted from opposite sides of the grating provides the maximum phase retardation; dividing this quantity by the wavelength λ of the diffracted light gives the resolving power R.

The degree to which the theoretical resolving power is attained depends not only on the angles α and β, but also on the optical quality of the grating surface, the uniformity of the groove spacing, the quality of the associated optics, and the width of the slits and/or detector elements. Any departure greater than $\lambda/10$ from flatness for a plane grating, or sphericity for a concave grating, will result in a loss of resolving power. The grating groove spacing must be kept constant to within about 1% of the wavelength at which theoretical performance is desired. Experimental details, such as slit width, air currents, and vibrations can seriously interfere with obtaining optimal results.

The practical resolving power is limited by the spectral half-width of the lines emitted by the source. This explains why systems with revolving powers greater than 500 000 are usually required only in the study of spectral line shapes, Zeeman effects, and line shifts, and are not needed for separating individual spectral lines.

A convenient test of resolving power is to examine the isotopic structure of the mercury emission line at 546.1 nm. Another test for resolving power is to examine the line profile generated in a spectrograph or scanning spectrometer when a single mode laser is used as the light source. Line width at half intensity (or other fractions as well) can be used as the criterion. Unfortunately, resolving power measurements are the convoluted result of all optical elements in the system, including the locations and dimensions of the entrance and exit slits and the auxiliary lenses and mirrors, as well as the quality of these optics. Their effects constitute the *instrument function* and are necessarily superimposed on those of the grating.

Spectral resolution. While resolving power can be considered a characteristic of the grating and the angles at which it is used, the ability to resolve two wavelengths λ_1 and $\lambda_2 = \lambda_1 + \Delta\lambda$ generally depends not only on the grating but on the dimensions and locations of the entrance and exit slits (or detector elements), the aberrations in the images, and the magnification of the images. The minimum wavelength difference $\Delta\lambda$ (also called the *limit of resolution*, or simply *resolution*) between two wavelengths which can be resolved unambiguously can be determined by convoluting the image of the entrance aperture (at the image plane) with the exit aperture (or detector element). This measure of the ability of a grating system to resolve nearby wavelengths is arguably more relevant than is resolving power, since it takes into account the image effects of the system. While resolving power is a dimensionless quantity, resolution has spectral units (usually nanometers).

Bandpass. The *bandpass* B of a spectroscopic system is the wavelength interval of the light that passes through the exit slit (or falls onto a detector element). It is often defined as the difference in wavelengths between the points of half-maximum intensity on either side of an intensity maximum. An estimate for bandpass is the product of the exit slit width w' and the reciprocal linear dispersion P:

$$B \approx w'\,P. \qquad (2\text{-}19)$$

An instrument with smaller bandpass can resolve wavelengths that are closer together than an instrument with a larger bandpass. Bandpass can be reduced by decreasing the width of the exit slit (to a certain limit; see Chapter VIII), but usually at the expense of decreasing light intensity as well.

Bandpass is sometimes called *spectral bandwidth*, though some authors assign distinct meanings to these terms.

Resolving power *vs.* resolution. In the literature, the terms *resolving power* and *resolution* are sometimes interchanged. While the word *power* has a very specific meaning (energy per unit time), the phrase *resolving power* does not involve *power* in this way; as suggested by Hutley, though, we may think of resolving power as 'ability to resolve'.

The comments above regarding resolving power and resolution pertain to planar classical gratings used in collimated light (plane waves). The situation is complicated for gratings on concave substrates or with groove patterns consisting of unequally spaced lines, which restrict the usefulness of the previously defined simple formulæ, though they may still yield useful approximations. Even in these cases, though, the concept of maximum retardation is still a useful measure of the resolving power.

FOCAL LENGTH AND *f*/NUMBER

For gratings (or grating systems) which image as well as diffract light, or disperse light which is not collimated, a *focal length* may be defined. If the beam diffracted from a grating of a given wavelength λ and order m converges to a focus, then the distance between this focus and the grating center is the focal length $r'(\lambda)$. [If the diffracted light is collimated, and then focused by a mirror or lens, the focal length is that of the refocusing mirror or lens and not the distance to the grating.] If the diffracted light is diverging, the focal length may still be defined, although by convention we take it to be negative (indicating that there is a virtual image behind the grating). Similarly, the incident light may diverge toward the grating (so we define the incidence or entrance slit distance $r(\lambda) > 0$) or it may converge toward a focus behind the grating (for which $r(\lambda) < 0$). Usually gratings are used in configurations for which r does not depend on wavelength (though in such cases r' usually depends on λ).

In Figure II-7, a typical concave grating configuration is shown; the monochromatic incident light (of wavelength λ) diverges from a point source at A and is diffracted toward B. Points A and B are distances r and r', respectively, from the grating center O. In this figure, both r and r' are positive.

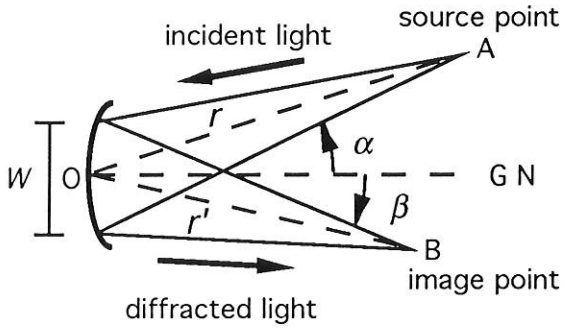

Figure II-7. Geometry for focal distances and focal ratios (f/numbers). GN is the grating normal (perpendicular to the grating at its center, O).

Calling the width (or diameter) of the grating (in the dispersion plane) W allows the *input* and *output f/numbers* (also called *focal ratios*) to be defined:

$$f/\mathrm{no}_{\mathrm{INPUT}} = \frac{r}{W}, \quad f/\mathrm{no}_{\mathrm{OUTPUT}} = \frac{r'(\lambda)}{W}. \quad (2\text{-}20)$$

Usually the input f/number is matched to the f/number of the light cone leaving the entrance optics (*e.g.*, an entrance slit or fiber) in order to use as much of the grating surface for diffraction as possible. This increases the amount of diffracted energy while not overfilling the grating (which would generally contribute to stray light).

For oblique incidence or diffraction, Eqs. (2-20) are often modified by replacing W with the projected width of the grating:

$$f/\mathrm{no}_{\mathrm{INPUT}} = \frac{r}{W\cos\alpha}, \quad f/\mathrm{no}_{\mathrm{OUTPUT}} = \frac{r'(\lambda)}{W\cos\beta}. \quad (2\text{-}21)$$

These equations account for the reduced width of the grating as seen by the entrance and exit slits; moving toward oblique angles (*i.e.*, increasing $|\alpha|$ or $|\beta|$) decreases the projected width and therefore increases the f/number.

The focal length is an important parameter in the design and specification of grating spectrometers, since it governs the overall size of the optical system (unless folding mirrors are used). The ratio between the input and output focal lengths determines the projected width of the entrance slit which must be matched to the exit slit width or detector element size. The f/number is also important, as it is generally true that spectral aberrations decrease as f/number increases. Unfortunately, increasing the input f/number results in the grating subtending a smaller solid angle as seen from the entrance slit; this will reduce the amount of light energy the grating collects and consequently reduce the intensity of the diffracted beams. This trade-off prohibits the formulation of a simple rule for choosing the input and output f/numbers, so sophisticated design procedures have been developed to minimize aberrations while maximizing collected energy. See chapter VII for a discussion of the imaging properties and chapter VIII for a description of the efficiency characteristics of grating systems.

Anamorphic Magnification

For a given wavelength λ, we may consider the ratio of the width of a collimated diffracted beam to that of a collimated incident beam to be a measure of the effective magnification of the grating (see Figure II-8). From this figure we see that this ratio is

$$\frac{b}{a} = \frac{\cos\beta}{\cos\alpha} . \qquad (2\text{-}22)$$

Since α and β depend on λ through the grating equation (2-1), this magnification will vary with wavelength. The ratio b/a is called the *anamorphic magnification*; for a given wavelength λ, it depends only on the angular configuration in which the grating is used.

The magnification of an object not located at infinity (so that the incident rays are not collimated) is discussed in chapter VIII.

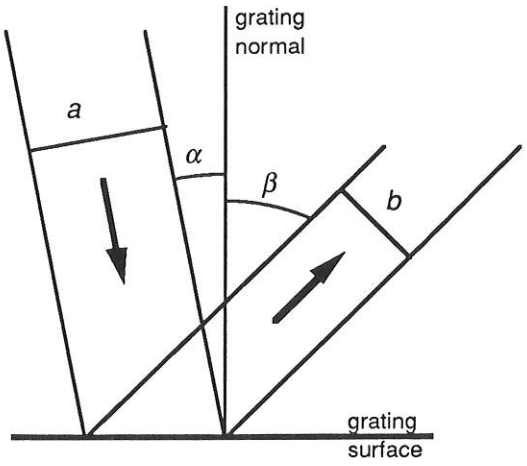

Figure II-8. Anamorphic magnification. The ratio of the beam widths b/a equals the anamorphic magnification.

Free Spectral Range

For a given set of incidence and diffraction angles, the grating equation is satisfied for a different wavelength for each integral diffraction order m. Thus light of several wavelengths (each in a different order) will be diffracted along the same direction: light of wavelength λ in order m is diffracted along the same direction as light of wavelength $\lambda/2$ in order $2m$, *etc.*

The range of wavelengths in a given spectral order for which superposition of light from adjacent orders does not occur is called the *free spectral range* F_λ. It can be calculated directly from its definition: in order m, the wavelength of light which diffracts along the direction of λ_1 in order m+1 is $\lambda_1 + \Delta\lambda$, where

$$\lambda_1 + \Delta\lambda = \frac{m+1}{m}\,\lambda_1, \qquad (2\text{-}23)$$

from which

$$F_\lambda = \Delta\lambda = \lambda_1/m. \qquad (2\text{-}24)$$

The concept of free spectral range applies to all gratings capable of operation in more than one diffraction order, but it is particularly important in the case of echelles,

because they operate in high orders with correspondingly short free spectral ranges.

Free spectral range and order sorting are intimately related, since grating systems with greater free spectral ranges may have less need for filters (or cross-dispersers) which absorb or diffract light from overlapping spectral orders. This is one reason why first-order applications are widely popular.

Energy Distribution (Grating Efficiency)

The intensity of light of a given wavelength diffracted by a grating into a given spectral order depends on many parameters, including the intensity and polarization of the incident light, the angles of incidence and diffraction, the (complex) index of refraction of the metal (or glass or dielectric) of the grating, and the groove spacing. A complete treatment of grating efficiency requires the vector formalism of electromagnetic theory (Maxwell's equations), which has been studied in detail over the past few decades. While the theory does not yield conclusions easily, certain rules of thumb can be useful in making approximate predictions. The topic of grating efficiency is addressed more fully in chapter IX.

Stray Light

All light which reaches the image plane from anywhere other than the grating, by any means other than diffraction as governed by Eq. (2-1), is called *stray light.* All components in an optical system contribute stray light, as will any baffles, apertures, and partially reflecting surfaces.

Grating stray light. Of the radiation incident on the surface of a diffraction grating, some will be diffracted and some will be absorbed by the grating itself. The remainder is unwanted energy called *grating stray light.* Stray light may arise from several factors, including imperfections in the shape and spacing of the grooves and roughness on the surface of the grating.

Diffuse stray light is scattered into the hemisphere in front of the grating surface. It is due mainly to grating surface microroughness. It is the primary cause of stray light in interference gratings. For monochromatic light incident on a grating, the intensity of diffuse stray light is higher near the diffraction orders for that wavelength than between the diffracted orders. M. C. Hutley (National Physical Laboratory, United Kingdom) found this intensity to be proportional to slit area, and probably proportional to $1/\lambda^4$.

In-plane scatter is unwanted energy in the dispersion plane. Due primarily to random variations in the groove spacing or groove depth, its intensity is directly proportional to slit area and probably inversely proportional to the square of the wavelength.

Ghosts are caused by periodic errors in the groove spacing. Characteristic of ruled gratings, interference gratings are free from ghosts when properly made.

Stray light can be reduced greatly through the use of a double grating spectrometer, in which light diffracted from one grating is incident on another.

Instrumental stray light. Stray light for which the grating cannot be blamed is called *instrumental stray light.* Most important is the ever-present light reflected into the zero order, which must be trapped so that it does not contribute to stray light. Diffraction from sharp edges and apertures causes light to propagate along directions other than those predicted by the grating equation. Reflection from instrument chamber walls and mounting hardware also contributes to the redirection of unwanted energy toward the image plane; generally, a smaller instrument chamber presents more significant stray light problems. Light incident on detector elements may be reflected back toward the grating and rediffracted; since the angle of incidence may now be different, light rediffracted along a given direction will generally be of a different wavelength than the light which originally diffracted along the same direction. Baffles, which trap diffracted energy outside the spectrum of interest, are intended to reduce the amount of light in other orders and in other wavelengths, but they may themselves diffract and reflect this light so that it ultimately reaches the image plane.

SIGNAL-TO-NOISE RATIO (SNR)

The *signal-to-noise ratio* (SNR) is the ratio of diffracted energy to unwanted light energy. While we might be tempted to think that increasing diffraction efficiency will increase SNR, stray light usually plays the limiting role in the achievable SNR for a grating system.

Replicated gratings from ruled master gratings generally have quite high SNRs, though interference gratings usually have even higher SNRs, since they have no ghosts due to periodic errors in groove location and lower interorder stray light.

In practical instruments, the effective noise will also depend on the spectral distribution of the light source and the spectral sensitivity of the detector. For example, a CsI detector has no sensitivity to light of wavelength above 160 nm, and therefore does not respond to long-wavelength scattered light.

The first diffraction gratings made for commercial use were mechanically ruled, manufactured by burnishing grooves individually with a diamond tool against a thin coating of evaporated metal applied to a plane or concave surface. Such *ruled gratings* comprise the majority of diffraction gratings used in spectroscopic instrumentation.

Grating Ruling Engines

The most vital component in the production of ruled diffraction gratings is the apparatus, called a *ruling engine*, on which master gratings are ruled. At present, the Richardson Grating Laboratory has three ruling engines in full-time operation, each producing substantial numbers of high-quality master gratings every year. Each of these systems produce gratings with very low Rowland ghosts and high resolving power.

Selected diamonds, whose crystal axis is oriented for optimum behavior, are used to shape the grating grooves. The ruling diamonds are carefully shaped by skilled diamond tool makers to produce the exact groove profile required for each grating. The carriage that carries the diamond back and forth during ruling must maintain its position to better than a few nanometers for ruling periods that may last for one day or as long as six weeks.

The mechanisms for advancing the grating carriages on all Laboratory engines are designed to make it possible to rule gratings with a wide choice of groove spacings. The current *Grating Catalog* shows the range of groove spacings available.

The Michelson engine. In 1947 Bausch & Lomb acquired its first ruling engine from the University of Chicago; this engine was originally designed by Albert Michelson in the 1910s and rebuilt by B. Gale. It underwent further refinement, which greatly improved its performance, and has produced a continuous supply of high quality gratings of up to 200 x 250 mm ruled area.

The Michelson engine originally used an interferometer system to plot, every few years, the error curve of the screw, from which an appropriate mechanical correction cam was derived. In 1990, this system was superceded by the addition of a digital computer servo control system based on a laser interferometer. The Michelson engine is unusual in that it covers the widest range of groove spacings of any ruling engine: it can rule both plane and concave gratings, as coarse as 20 grooves per millimeter (g/mm) and as fine as 10 800 g/mm.

The Mann engine. The second engine installed at the Laboratory has been producing gratings since 1953. It was originally built by David W. Mann of Lincoln, Massachusetts. Bausch & Lomb equipped it with an interferometric control system following Harrison's technique. The Mann engine can rule areas up to 100 x 110 mm, with virtually no ghosts and nearly theoretical resolving power.

While the lead screws of the ruling engines are lapped to the highest precision attainable, there are always residual errors in both threads and bearings which must be compensated to produce the highest quality gratings. The Mann engine is equipped with an automatic interferometer servo system that continually adjusts the grating carriage to the correct position as each groove is ruled. The servo system effectively simulates a perfect lead screw.

The 'B' engine. The third engine, built by George Harrison of MIT, was moved to Rochester in 1968. It has the capacity to rule plane gratings to the greatest precision ever achieved; these gratings may be up to 400 mm wide, with grooves (between 20 and 1500 per millimeter) up to 300 mm long. It uses a double interferometer control system, based on a frequency-stabilized laser, to monitor not only table position but to correct residual yaw errors as well. This engine produces gratings with nearly theoretical resolving powers, virtually

eliminating Rowland ghosts and minimizing stray light. It has also ruled almost perfect echelle gratings, the most demanding application of a ruling engine.

The Ruling Process

Master gratings are ruled on carefully selected well-annealed blanks of several different materials. The choice is generally between BK-7 optical glass, special grades of fused silica, or ZeroDur®. The optical surfaces of these blanks are polished to closer than $\lambda/10$ for green light (about 50 nm), then coated with a reflective film (usually aluminum or gold).

Temperature and pressure controls are especially important in the environment around a ruling engine. Room temperature must be held constant to within 0.01 °C for small ruling engines (and to within 0.005 °C for larger engines). Since the interferometric control of the ruling process uses monochromatic light, whose wavelength is sensitive to the changes of the refractive index of air with pressure fluctuations, atmospheric pressure must be compensated for by the system. A change in pressure of 2.5 mm Hg corresponds to a change in wavelength of one part per million, which (when allowed to accumulate over tens of thousands of grooves) will cause the interferometer to vary the groove spacing during ruling. The ruling engine must also be isolated from vibrations, which are easily transmitted to the diamond; this may be done by suspending the engine mount from springs which isolate vibrations between frequencies of 2 to 3 Hz (below which there is no concern) to about 60 Hz, above which vibrations are usually too small to have a noticeable effect.

The actual ruling of a master grating is a long, slow and painstaking process. The set-up of the engine, prior to the start of the ruling, requires great skill and patience. This critical alignment is impossible without the use of a high-power interference microscope, or an electron microscope for more finely spaced grooves.

After each microscopic examination, the diamond is readjusted until the operator is completely satisfied that the groove shape is the best possible for the particular grating being ruled. This painstaking adjustment, although time consuming, results in very "bright" gratings with nearly all the diffracted light energy concentrated in a specific angular range from the grating. This ability to concentrate the light selectively at a certain part of the spectrum is what distinguishes blazed diffraction gratings from all others.

Master gratings are carefully tested to be certain that they have met specifications completely. The wide variety of tests run to evaluate all the important properties include resolution, efficiency, Rowland ghost intensity, and surface accuracy. Wavefront interferometry is used when appropriate. If a grating meets all specifications, it is used as a master for the production of replica gratings.

Varied Line-space (VLS) Gratings

For the last century great effort has been expended in keeping the spacing between successive grooves uniform as a master grating is ruled. As early as 1875, A. Cornu realized that variations in the groove spacing modified the curvature of the diffracted wavefronts. While periodic and random variations were understood to produce stray light, a uniform variation in groove spacing across the grating surface was recognized by Cornu to change the location of the focus of the spectrum, which need not be considered a defect if properly taken into account. He determined that a planar classical grating, which by itself would have no focusing properties if used in collimated incident light, would focus the diffracted light if ruled with a systematic 'error' in its groove spacing. He was able to verify this by ruling three gratings whose groove positions were specified to vary as each groove was ruled. Such gratings, in which the pattern of straight parallel grooves has a variable yet well-defined (though not periodic) spacing between successive grooves, are now called *varied line-space (VLS) gratings*.

The Michelson engine, which has digital computer control, can readily rule VLS gratings. Any groove spacing $d(y)$ which varies reasonably as a function of position y along the grating surface can be programmed into the computer. The relationship between groove spacing (and curvature) and imaging is discussed in chapter VII.

INTERFERENCE (HOLOGRAPHIC) GRATINGS IV

Since the late 1960s, a method distinct from mechanical ruling has also been used to manufacture diffraction gratings. This method involves the photographic recording of a stationary interference fringe field. Such *interference gratings* are unfortunately known more commonly as *holographic gratings*, although holography is not involved in their generation or use. Interference gratings have several characteristics which distinguish them from ruled gratings.

In 1901 Aime Cotton produced experimental interference gratings, fifty years before the concepts of holography were developed by Gabor. A few decades later, Michelson considered the interferometric generation of diffraction gratings obvious, but recognized that an intense monochromatic light source and a photosensitive material of sufficiently fine granularity did not then exist. In the mid 1960s, ion lasers and photoresists (grainless photosensitive materials) became available; the former provided a strong monochromatic line, and the latter was photoactive at the molecular level, rather than at the crystalline level (unlike, for example, photographic film). In 1967 D. Rudolph and G. Schmahl at the University of Göttingen and A. Labeyrie and J. Flamand in France independently produced the first interference diffraction gratings of spectroscopic quality.

PRINCIPLE OF MANUFACTURE

Formation of an interference pattern. When two sets of coherent equally polarized monochromatic optical plane waves of equal intensity intersect each other, a standing wave pattern will be formed in the region of intersection if both sets of waves are of the same wavelength λ (see Figure IV-1). The combined intensity distribution forms a set of straight equally-spaced fringes (bright and dark lines). Thus a photographic plate would record a fringe pattern, since the regions of zero field intensity would leave the film unexposed while the regions of maximum intensity would leave the film maximally exposed. Regions between these extremes, for which the combined intensity is neither maximal nor zero, would leave the film partially exposed. The combined intensity varies sinusoidally with position as the interference pattern is scanned along a line. If the beams are not of equal intensity, the minimum intensity will no longer be zero, thereby decreasing the contrast between the fringe. As a consequence, all portions of the photographic plate will be exposed to some degree.

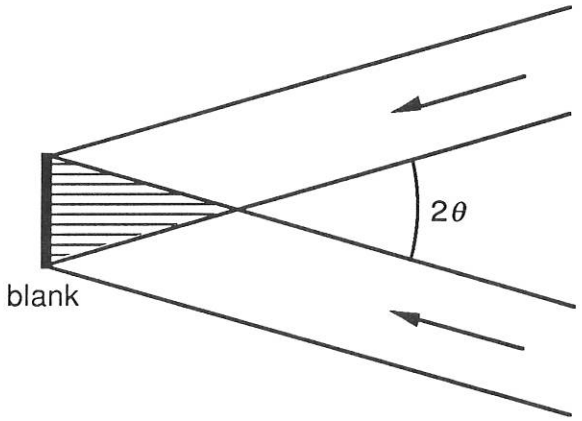

Figure IV-1. Formation of interference fringes. Two collimated beams of wavelength λ form an interference pattern composed of straight equally spaced planes of intensity maxima (shown as the horizontal lines). A sinusoidally varying interference pattern is found at the surface of a blank B placed perpendicular to these planes.

The centers of adjacent fringes (that is, adjacent lines of maximum intensity) are separated by a distance d, where

$$d = \lambda/(2 \sin\theta) \qquad (4\text{-}1)$$

and θ is the half the angle between the beams. A small angle between the beams will produce a widely spaced fringe pattern (large d), whereas a larger angle will produce a fine fringe pattern. The lower limit for d is $\lambda/2$, so for visible recording light, thousands of fringes per millimeter may be formed.

Formation of the grooves. Master interference diffraction gratings are recorded in photoresist, a material whose intermolecular bonds are either strengthened or weakened by exposure to light. Commercially available photoresists are more sensitive to some wavelengths than others; the recording laser line must be matched to the type of photoresist used. The proper combination of intense laser light and photoresist (with high sensitivity to this wavelength relative to other wavelengths from the same laser) will reduce exposure time.

Photoresist gratings are chemically developed after exposure to reveal the fringe pattern. A photoresist may be *positive* or *negative*, though the latter is rarely used. During chemical development, the portions of a blank covered in positive photoresist which have been exposed to light are dissolved, while for negative photoresist the unexposed portions are dissolved. Upon immersion in the chemical developer, a surface relief pattern is formed: for positive photoresist, valleys are formed where the bright fringes were, and ridges where the dark fringes were. At this stage a master interference grating has been produced; its grooves are sinusoidal ridges. This grating may be coated and replicated like master ruled gratings.

Classification of Interference Gratings

Single-beam interference. An interference pattern can be generated from a single collimated monochromatic coherent light beam if it is made to reflect back upon itself. A standing wave pattern will be formed, with intensity maxima forming planes parallel to the wavefronts. The intersection of this interference pattern with a photoresist-covered substrate will yield on its surface a pattern of grooves, whose spacing d depends on the angle θ between the blank surface and the planes of maximum intensity (see Figure IV-2); the relation between d and θ is identical to Eq. (4-1), though it must be emphasized that the recording geometry behind the single-beam interference grating (or *Sheridon grating*) is different from that of the double-beam geometry for which Eq. (4-1) was derived.

The groove depth h for a Sheridon grating is dictated by the separation between successive planes of maximum intensity (nodal planes); explicitly,

$$h = \lambda/2n, \qquad (4\text{-}2)$$

where λ is the wavelength of the recording light and n the refractive index of the photoresist. This severely limits the range of available blaze wavelengths, typically to those between 200 and 250 nm.

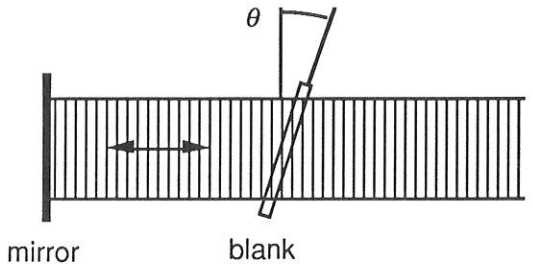

Figure IV-2. Sheridon recording method. A collimated beam of light, incident from the right, is retroreflected by a plane mirror, which forms a standing wave pattern whose intensity maxima are shown. A transparent blank, inclined at an angle θ to the fringes, will have its surfaces exposed to a sinusoidally varying intensity pattern.

Double-beam interference. The double-beam interference pattern shown in Figure IV-1 is a series of straight parallel fringe planes, whose intensity maxima (or minima) are equally spaced throughout the region of interference. Placing a substrate covered in photoresist in this region will form a groove pattern defined by the intersection of the surface of the substrate with the fringe planes. If the substrate is planar, the grooves will be straight, parallel and equally spaced, though their spacing will depend on the angle between the substrate surface and the fringe planes. If the substrate is concave, the grooves will be curved and unequally spaced, forming a series of circles of different radii and spacings. Regardless of the shape of the substrate, the intensity maxima are equally spaced planes, so the grating recorded will be a *classical equivalent interference grating* (more often called simply a *classical grating*). This name recognizes that the groove pattern

(on a planar surface) is identical to that of a planar classical ruled grating. Thus all interference gratings formed by the intersection of two sets of plane waves are called classical equivalents, even if their substrates are not planar. Producing such a grating requires high-grade collimating optics in the recording set-up.

If two sets of spherical wavefronts are used instead, as in Figure IV-3, a *first generation interference grating* is recorded. The surfaces of maximum intensity are now confocal hyperboloids (if both sets of wavefronts are converging, or if both are diverging) or ellipsoids (if one set is converging and the other diverging). This interference pattern can be obtained by focusing the recording laser light through pinholes (to simulate point sources); no optical elements are required between the pinholes and the grating blank. Even on a planar substrate, the fringe pattern will be a collection of unequally spaced curves. Such a groove pattern will alter the curvature of the diffracted wavefronts, regardless of the substrate shape, thereby providing focusing properties. Modification of the curvature and spacing of the grooves can be used to reduce aberrations in the spectral images (see chapter VI).

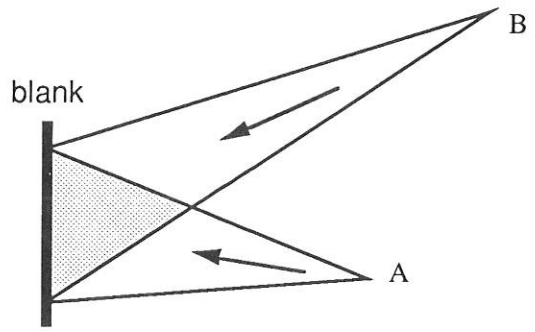

Figure IV-3. First-generation recording method. Laser light focused through pinholes at A and B diverges toward the grating blank. The standing wave region is shaded; the intensity maxima are confocal hyperboloids.

The addition of auxiliary concave mirrors or lenses into the recording beams can render the recording wavefronts toroidal (that is, their curvature in two perpendicular directions will generally differ). The grating thus recorded is called a *second generation interference grating*. The additional degrees of freedom in the recording geometry (*e.g.*, the location, orientation and radii of the auxiliary mirrors) provide for further aberration reduction above that of first generation interference gratings.

THE RECORDING PROCESS

Interference gratings are recorded by placing a light-sensitive surface in an interferometer. The generation of an interference grating of spectroscopic quality requires a stable optical bench and laser as well as precision optical components (mirrors, collimating optics, *etc.*). Ambient light must be eliminated so that fringe contrast is maximal. Thermal gradients and air currents, which change the local index of refraction in the beams of the interferometer, must be avoided. The Richardson Grating Laboratory records master interference gratings in its specially-designed facility.

During the recording process, the components of the optical system must be of nearly diffraction-limited quality, and mirrors, pinholes and spatial filters must be adjusted as carefully as possible. Any object in the optical system receiving laser illumination will scatter this light toward the grating, thus contributing to stray light. Proper masking and baffling during recording are essential to the successful generation an interference grating, as is single-mode operation of the laser throughout the duration of the exposure.

The blank on which the master interference grating is to be produced must be coated with a highly uniform, virtually defect-free coating of photoresist. Compared with photographic film, photoresists are much less sensitive to light during exposure, due to the molecular nature of their interaction with light. As a result, typical exposures may take from minutes to hours, during which time an extremely stable fringe pattern (and, therefore, optical system) is required. After exposure, the blank is immersed in a developing agent, which forms a surface relief fringe pattern; coating the blank with metal then produces a master interference diffraction grating.

Differences between Ruled and Interference Gratings

Due to the distinctions between the fabrication processes for ruled and interference gratings, each type has advantages and disadvantages relative to the other, some of which are described below.

Differences in stray light. Since interference gratings do not involve burnishing grooves into a thin layer of metal, the surface irregularities on its grooves differ from those of mechanically ruled gratings. Moreover, errors of ruling, which are a manifestation of the fact that ruled gratings have one groove formed after another, are nonexistent in interferometric gratings, for which all grooves are formed simultaneously. If properly made, then, interference gratings can be entirely free of both small periodic and random groove placement errors found on even the best mechanically ruled gratings. Interference gratings offer significant advantages to spectroscopic systems in which stray light is performance-limiting, such as in the study of the Raman spectra of solid samples.

Differences and limitations in the groove profile. The groove profile has a significant effect on the light intensity diffracted from the grating (see chapter VIII). While ruled gratings may have triangular or trapezoidal groove profiles, interference gratings usually have sinusoidal (or nearly sinusoidal) groove profiles (see Figure IV-4). A ruled grating and an interference grating, identical in every way except in groove profile, will have demonstrably different efficiencies (diffraction intensities) for a given wavelength and spectral order. Moreover, ruled gratings are more easily blazed (by choosing the proper shape of the burnishing diamond) than are interference gratings, which are usually blazed by ion bombardment (ion etching). Differences in the intensity diffracted into the order in which the grating is to be used implies differences in the intensities in all other orders as well; excessive energy in other orders usually makes the suppression of stray light more difficult.

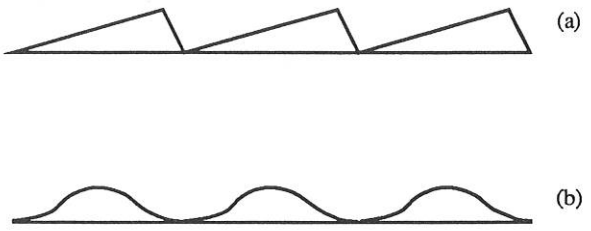

Figure IV-4. Groove profiles for ruled and interference gratings. (a) Triangular groove profile of a mechanically ruled grating. (b) Sinusoidal groove profile of an interference grating.

The distribution of groove profile characteristics across the surface of a grating may also differ between ruled and interference gratings. For a ruled concave grating, the blank curvature necessarily changes the groove angle across the grating, and with it the blaze wavelength. An interference grating, on the other hand, usually demonstrates much less variation in efficiency characteristics across its surface. Gratings have been ruled by changing the facet angle at different places on the blank during ruling. These so-called "multipartite" gratings, in which the ruling is interrupted and the diamond reoriented at different places across the width of the grating, demonstrate enhanced efficiency but do not provide the resolving power expected from an uninterrupted ruling (since each section of grooves may be out of phase with the others) [Hutley and Hunter 1981].

Limitations in obtainable groove frequencies. Limits on the number of grooves per millimeter differ between ruled and interference gratings: ruled gratings offer a much wider range of groove spacings. Below a few hundred grooves per millimeter the recording optical system necessary to generate interference gratings becomes cumbersome and the properties of photoresist are no longer adequate, while ruled gratings can have as few as twenty grooves per millimeter. For upper limits, interference gratings recorded with visible light are usually limited to 3600 grooves per millimeter, whereas ruled gratings have been produced with over 6000 grooves per millimeter.

Differences in the groove patterns. Classical ruled plane gratings, which constitute the vast majority of ruled gratings, have straight equally-spaced grooves. Classical ruled concave gratings have circumferential unequally-spaced grooves, but this groove pattern, when projected onto the plane tangent to the grating at its center, is still a set of straight equally spaced lines. [It is the projected groove pattern which governs imaging] Even ruled varied line-space (VLS) gratings (see chapter III) do not contain curved grooves, except on curved blanks. The aberration reduction possible with ruled gratings is therefore limited to that possible with straight grooves, though this limitation is due to the mechanical motions possible with present-day ruling engines rather than with the burnishing process itself.

Interference gratings, on the other hand, need not have straight grooves. Groove curvature can be modified slightly to reduce aberrations in the spectrum, thereby improving the throughput and resolution of imaging spectrometers. A fairly recent spectrometer mount is the *flat-field spectrograph*, in which the spectrum is imaged onto a flat detector array and several wavelengths are monitored simultaneously. Interference gratings can significantly improve the imaging of such a grating system, whereas classical ruled gratings are not suitable for forming well-focused planar spectra without auxiliary optics.

Differences in the substrate shapes. The interference pattern used to record interference gratings is not dependent on the substrate shape or dimension, so gratings of low *f*/number can be recorded interferometrically (mechanically ruled gratings are usually limited to curvatures above *f*/9). Consequently interference concave gratings lend themselves more naturally to systems with short focal lengths. Interference gratings of unusual curvature can be recorded easily; of course, there may still remain technical problems associated with the replication of such gratings.

Differences in generation time for master gratings. A ruled master grating is formed by burnishing each groove individually; to do so, the ruling diamond may traverse a very large distance to rule one grating. For example, a square grating of dimensions 100 x 100 mm with 1000 grooves per millimeter will require the diamond to move 10 km (over six miles) and takes several days to rule.

In the fabrication of a master interference grating, on the other hand, the grooves are created simultaneously. Exposure times vary from minutes to hours, depending on the intensity of the laser light used and the spectral response (sensitivity) of the photoresist at this wavelength. Even counting preparation and development time, interference master gratings are produced much more quickly than ruled master gratings. Of course, an extremely stable and clean optical recording environment is necessary to record precision interference gratings. For plane gratings, high-grade collimating optics are required, which can be a limitation for larger gratings.

Master interference gratings as large as 160 mm in diameter are made routinely at the Richardson Grating Laboratory, but with extra effort and care larger gratings can be produced.

REPLICATED GRATINGS V

Years of research and development pioneered at the Richardson Grating Laboratory have contributed to the process for manufacturing replicated diffraction gratings (*replicas*). This process is capable of producing duplicates of master gratings which equal the quality and performance of the master gratings. In certain gratings, inversion of the groove, which is the result of replication, increases efficiency significantly.

Exhaustive tests have shown that there is no loss of resolution between master and replica. There is no evidence of deterioration or change in replica gratings with age or when exposed to thermal variations from the boiling point of nitrogen (77 K = –196 °C) to 50 °C. Even the highest vacuum, such as that of outer space, has no effect on replica gratings. The most prominent hazard to a grating, either master or replica, is surface contamination from fingerprints; should this happen, a grating can sometimes be cleaned or recoated. However, accidentally evaporated contaminants, typical of vacuum spectrometry, can be especially harmful when baked on with ultraviolet radiation.

The process for making replica gratings results in a grating whose grooves are formed in a very thin layer of clear resin that adheres strongly to the surface of the substrate material. The optical surface of a reflection replica is usually coated with aluminum, but gold or platinum is recommended for greater diffracted energy in certain spectral regions. Transmission gratings are not subject to deterioration under normal working conditions. The ruled grooves of a grating can be damaged very easily by brushing, wiping or careless attempts at cleaning. The best rule, by far, is to refrain completely from touching the ruled surface of a grating and to provide this surface with adequate protection during handling and shipment.

Richardson Grating Laboratory replica gratings are shipped with their ruled surfaces protected by hard plastic covers. Plane gratings are equipped with edge standoffs on the cover to keep the covers from coming in contact with the grating surface. It is important to use care in removing the cover in order to avoid scratching the grating surface.

The Replication Process

The replication of a master diffraction grating is a four-step process. First, a parting agent is applied to the surface of the master grating; this layer provides poor adherence between the surface of the master grating and the evaporated metallic surface of the replica grating. A substrate is then cemented with a thin film of low-shrinkage epoxy to the grooved surface of the master grating; this layer is usually 10 to 25 microns in thickness. The epoxy is then cured, resulting in a groove profile that is a faithfully replica once the substrate and master are separated.

Certified Precision Diffraction Gratings

Every replica grating offered for sale by the Laboratory is marked "Certified Precision". This certification attests to the performance and precision of the replica grating, which is as good as, or better than, the master grating from which it was produced, both in performance and useful life.

The true value and usefulness of a replica grating depends on its quality. To be certain of no misunderstanding concerning quality, each "Certified Precision" grating is accompanied by a certificate which traces the origin of the replica to a specific master grating; this certificate identifies the grating by both catalogue and serial numbers. The certificate also shows the quality specifications for the grating.

When writing us in regard to a particular diffraction grating, please be certain to copy both grating numbers accurately so that it may be identified. The grating itself is identified by a sticker on the back which gives its essential characteristics as well as blaze direction.

PLANE GRATINGS AND THEIR MOUNTS VI

GRATING MOUNT TERMINOLOGY

The auxiliary collimating and focusing optics which modify the wavefronts incident on and diffracted by a grating, as well as the angular configuration in which it is used, is called its *mount*. Grating mounts are a class of *spectrometer*, a term which usually refers to any spectroscopic instrument, regardless of whether it scans wavelengths individually or entire spectra simultaneously, or whether it employs a prism or grating. For this discussion we consider grating spectrometers only.

A *monochromator* is a spectrometer that images a single wavelength band at a time onto an exit slit; the spectrum is scanned by the relative motion of the entrance (and/or exit) optics (usually slits) with respect to the grating, though in practice it is almost always the grating that rotates while the slits remain fixed.

A *spectrograph* is a spectrometer that images a range of wavelengths simultaneously, either onto photographic film or a series of detector elements, or through several exit slits (sometimes called a *polychromator*). The defining characteristic of a spectrograph is that an entire section of the spectrum is recorded at once.

PLANE GRATING MOUNTS

A *plane grating* is one whose surface is flat. Plane gratings are normally used in collimated incident light, which they disperse by wavelength but do not focus. These mounts require auxiliary optics, such as lenses or mirrors, to collect and focus the energy. Some simplified plane grating mounts illuminate the grating with converging light, though the focal properties of the system will then depend on wavelength. For simplicity, only plane reflection grating mounts are discussed below, though each mount may have a transmission grating analogue.

Concave grating mounts are discussed in Chapter VII.

The Czerny-Turner Monochromator. This design involves a classical plane grating illuminated by collimated light. The incident light is usually diverging from a source or slit, and collimated by a concave mirror (the *collimator*), and the diffracted light is focused by a second concave mirror (the *camera*); see Figure VI-1. Ideally, since the grating is planar and classical, and used in collimated incident light, no aberrations should be introduced into the diffracted wavefronts. In practice, aberrations are contributed by the off-axis use of the concave spherical mirrors.

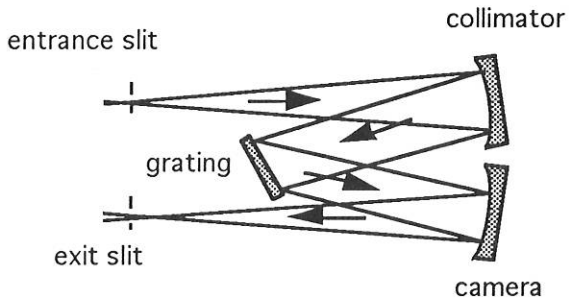

Figure VI-1. The Czerny-Turner mount. The plane grating provides dispersion and the concave mirrors provide focusing.

Like all monochromator mounts, the wavelengths are imaged individually. The spectrum is scanned by rotating the grating; this moves the grating normal relative to the incident and diffracted beams, which (by Eq. (2-1)) changes the wavelength diffracted toward the camera. For a Czerny-Turner monochromator, light incident and diffracted by the grating is collimated, so the spectrum remains at focus at the exit slit for each wavelength, since only the grating can introduce wavelength-dependent focusing properties.

Aberrations caused by the auxiliary mirrors include astigmatism and spherical aberration (each of which is contributed additively by the mirrors); as with all concave

mirror geometries, astigmatism increases as the angle of reflection increases. Coma can be eliminated at one wavelength through proper choice of the angles of reflection at the mirrors; due to the anamorphic (wavelength-dependent) tangential magnification of the grating, the images of the other wavelengths experience subsidiary coma (which becomes troublesome only in special systems).

The Ebert-Fastie Monochromator. This design is a special case of a Czerny-Turner mount in which a single relatively large concave mirror serves as both the collimator and the camera (Fig. VI-2). Its use is limited, since stray light and aberrations are more difficult to control.

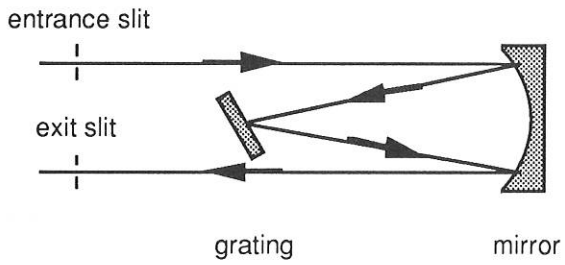

Figure VI-2. The Ebert-Fastie mount. A single concave mirror replaces the two concave mirrors found in Czerny-Turner mounts.

The Monk-Gillieson Monochromator. In this mount (see Figure VI-3), a plane grating is illuminated by converging light ($r < 0$). Usually light diverging from an entrance slit (or fiber) is rendered converging by off-axis reflection from a concave mirror (which introduces aberrations, so the light incident on the grating is not composed of perfectly spherical converging wavefronts). The grating diffracts the light, which converges toward the exit slit; the spectrum is scanned by rotating the grating to bring different wavelengths into focus at or near the exit slit. Often the angles of reflection (from the primary mirror), incidence and diffraction are small (measured from the appropriate surface normals), which keeps aberrations (especially off-axis astigmatism) to a minimum.

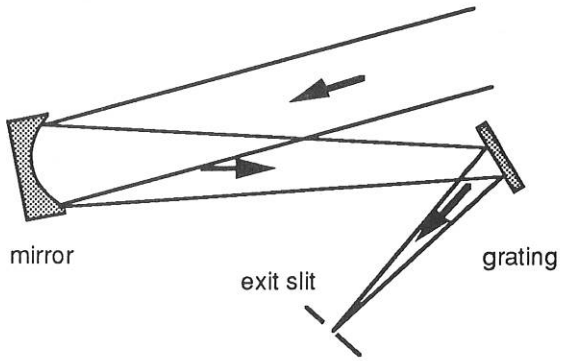

Figure VI-3. The Monk-Gillieson mount. A plane grating is used in converging light.

Since the incident light is not collimated, the grating introduces wavelength-dependent aberrations into the diffracted wavefronts (see chapter VII). Consequently the spectrum cannot remain in focus at a fixed exit slit when the grating is rotated (unless this rotation is about an axis displaced from the central groove of the grating, as pointed out by SCHROEDER [1970]). For low-resolution applications, the Monk-Gillieson mount enjoys a certain amount of popularity, since it represents a simple and inexpensive spectrometric system.

The Littrow Mount. A grating used in the Littrow or autocollimating configuration diffracts light of wavelength λ back along the incident light direction (Fig. VI-4). In a *Littrow monochromator*, the spectrum is scanned by rotating the grating; this reorients the grating normal, so the angles of incidence α and diffraction β change (even though $\alpha = \beta$ for all λ). The same auxiliary optics can be used as both collimator and camera, since the diffracted rays retrace the incident rays. The entrance slit and exit slit (or image plane) must be offset slightly along the direction parallel to the grooves so that they do not coincide, which generally introduces out-of-plane aberrations. The only true Littrow monochromator application is laser tuning (see chapter XII).

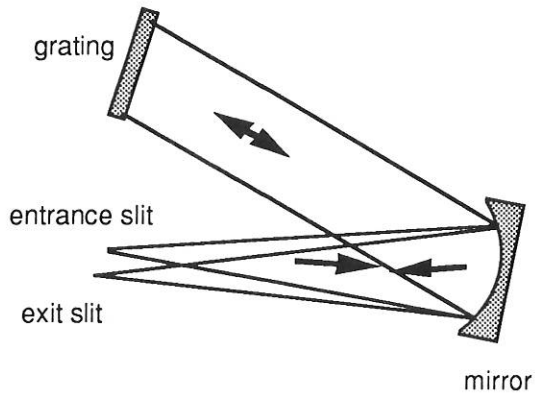

Figure VI-4. The Littrow monochromator mount. The entrance and exit slits are slightly above and below the dispersion plane, respectively; they are shown separated for clarity.

Double Monochromators. Two monochromator mounts used in series form a *double monochromator*. The exit slit of the first monochromator usually serves as the entrance slit for the second monochromator (see Figure VI-5). Stray light in a double monochromator is much lower than in a single monochromator: it is the product of ratios of stray light intensity to parent line intensity for each system. Also, the reciprocal linear dispersion P of the entire system is the sum of the reciprocal linear dispersions of each monochromator.

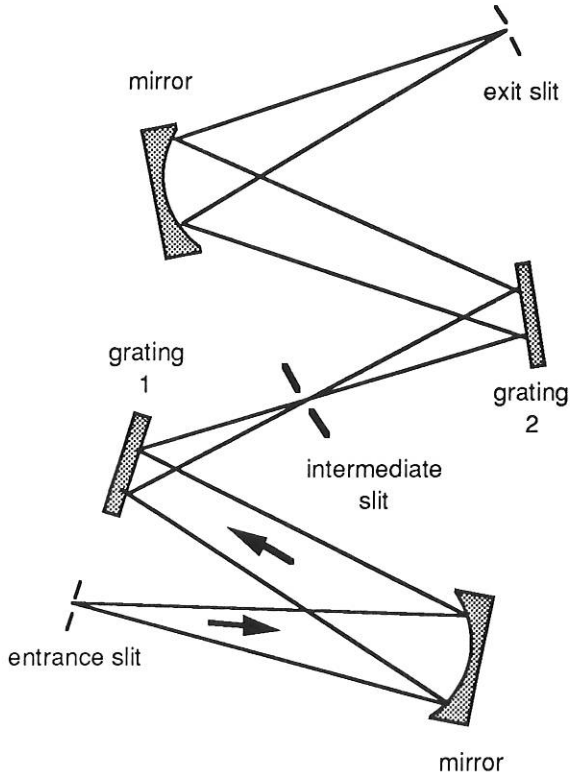

Figure VI-5. A double monochromator mount.

Triple Monochromators. A *triple monochromator* mount consists of three monochromators in series. These mounts are used only when the demands to reduce stray light are extraordinarily severe (*e.g.*, Raman spectroscopy of solid samples).

CONCAVE GRATINGS AND THEIR MOUNTS VII

A concave reflection grating can be modelled as a concave mirror which diffracts; it can be thought to reflect light by virtue of its concavity, and to disperse light by virtue of its groove pattern.

Since their invention by Henry Rowland in 1883, concave diffraction gratings have played an important role in spectrometry. Compared with plane gratings, they offer one important advantage: they provide the focusing (imaging) properties to the grating which otherwise must be supplied by separate optical elements. For spectroscopy below 110 nm, for which the reflectivity of available mirror coatings is low, concave gratings allow for systems free from focusing mirrors that would reduce throughput two or more orders of magnitude.

Many configurations for concave spectrometers have been proposed. Some are variations of the Rowland circle, while some place the spectrum on a flat field, which is more suitable for charge-coupled device (CCD) array instruments. The Seya-Namioka concave grating monochromator is especially suited for scanning the spectrum by rotating the grating around its own axis.

Classification of Grating Types

The imaging characteristics of a concave grating system are governed by the size, location and orientation of the entrance and exit optics (the *mount*), the aberrations due to the grating, and the aberrations due to any auxiliary optics in the system. [In this chapter we address only simple systems, in which the concave grating is the single optical element; auxiliary mirrors and lenses are not considered.] The imaging properties of the grating itself are determined completely by the shape of its blank (its *curvature* or *figure)* and the spacing and curvature of the grooves (its *groove pattern*).

Gratings are classified both by their groove patterns and by their blank curvatures. In the previous chapter we restricted our attention to plane classical gratings and their mounts. In this chapter, more general gratings and grating systems are considered.

Groove patterns. A *classical grating* is one whose grooves, when projected onto the tangent plane, form a set of straight equally-spaced lines. Until the last few decades, the vast majority of gratings were classical, in that any departure from uniform spacing, groove parallelism or groove straightness was considered a flaw. Classical gratings are made routinely both by mechanical ruling and interferometric recording.

A *first generation interference grating* has its grooves formed by the intersection of a family of confocal hyperboloids (or ellipsoids) with the grating blank. When projected onto the tangent plane, these grooves have both unequal spacing and curvature. First generation interference gratings are formed by recording the master grating in a field generated by two sets of spherical wavefronts, which may emanate from a point source or be focused toward a virtual point.

A *second generation interference grating* has the light from its point sources reflected by concave mirrors so that the recording wavefronts are toroidal.

A *varied line-space (VLS) grating* is one whose grooves, when projected onto the tangent plane, form a set of straight parallel lines whose spacing varies from groove to groove. Varying the groove spacing across the surface of the grating moves the tangential focal curve, while keeping the groove straight and parallel keeps the sagittal focal curve fixed.

Blank shapes. A *concave grating* is one whose surface is concave, regardless of its groove pattern or profile, or the mount in which it is used. Examples are spherical blanks (whose surfaces are portions of a sphere, which are definable with one radius) and toroidal blanks (definable by two radii). Spherical blanks are by far the most common concave substrates, since they are easily manufactured and toleranced, and can be replicated in a straightforward manner.

Toroidal substrates are much more difficult to align, tolerance and replicate. More general blank shapes are also possible, such as ellipsoidal or paraboloidal blanks, but tolerancing and replication complications relegate these grating surfaces out of the mainstream.

The shape of a concave grating can be characterized either by its radii or its curvatures. The radii of the slice of the blank in the principal (dispersion) plane is called the *tangential radius R*, while that in the plane parallel to the grooves at the grating center is called the *sagittal radius* ρ. Equivalently, we can define tangential and sagittal curvatures $1/R$ and $1/\rho$, respectively.

A *plane grating* is one whose surface is planar. While plane gratings can be thought of as a special case of concave gratings (for which the radii of curvature of the blank become infinite), we treat them separately here (see the previous chapter).

Classical Concave Grating Imaging

In Figure VII-1, a classical grating is shown; the Cartesian axes are defined as follows: the x-axis is the outward *grating normal* to the grating surface at its center (point O), the y-axis is tangent to the grating surface at O and perpendicular to the grooves there, and the z-axis completes the right-handed triad of axes (and is therefore parallel to the grooves at O). Light from point source A(ξ, η, 0) is incident on a grating at point O; light of wavelength λ in order m is diffracted toward point B(ξ', η', 0). Since point A was assumed, for simplicity, to lie in the xy plane, to which the grooves are perpendicular at point O, the image point B will lie in this plane as well; this plane is called the *principal plane* (also called the *tangential plane* or the *dispersion plane* (see Figure VII-2). Ideally, any point P(x, y, z) located on the grating surface will also diffract light from A to B.

The plane through points O and B perpendicular to the principal plane is called the *sagittal plane*, which is unique for this wavelength. The *grating tangent plane* is the plane tangent to the grating surface at its center point O (*i.e.*, the yz plane). The imaging effects of the groove spacing and curvature can be completely separated from those due to the curvature of the blank if the groove pattern is projected onto this plane.

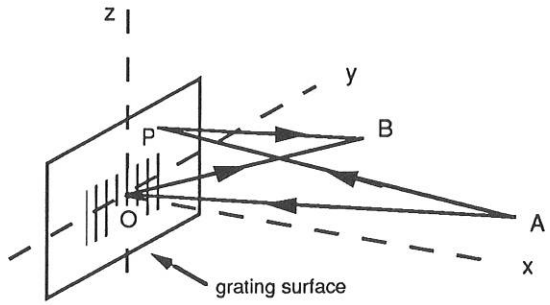

Figure VII-1. Use geometry. The grating surface centered at O diffracts light from point A to point B. P is a general point on the grating surface.

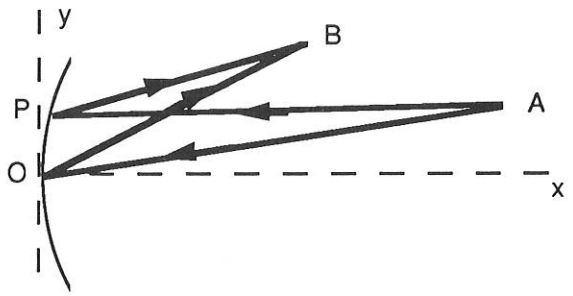

Figure VII-2. Use geometry – the principal plane. Points A, B and O lie in the xy (principal) plane; the general point P on the grating surface may lie outside this plane. The z-axis comes out of the page at O.

The imaging of this optical system can be investigated by considering the optical path difference *OPD* between the *pole ray* AOB (where O is the center of the grating) and the *general ray* APB (where P is an arbitrary point on the grating surface). Application of Fermat's principle to this path difference, and the subsequent expansion of the results in power series of the coördinates of the tangent plane (y and z), yields expressions for the aberrations of the system.

The optical path difference is

$$OPD = \langle APB \rangle - \langle AOB \rangle + Nm\lambda, \qquad (7\text{-}1)$$

where <APB> and <AOB> are the geometric lengths of the general and pole rays, respectively (both multiplied by the index of refraction), m is the diffraction order, and N is the number of grooves on the grating surface between points O and P. The last term in Eq. (7-1) accounts for the fact that the distances <APB> and <AOB> need not be exactly equal for the light along both rays to be in phase at B: due to the wave nature of light, the light is in phase at B even if there are an integral number of wavelengths between these two distances. If points O and P are one groove apart ($N = 1$), the number of wavelengths in the difference <APB> – <AOB> determines the order of diffraction m.

From geometric considerations, we find

$$\begin{aligned} \langle APB \rangle &= \langle AP \rangle + \langle PB \rangle \\ &= \sqrt{(\xi - x)^2 + (\eta - y)^2 + z^2} \\ &\quad + \sqrt{(\xi' - x)^2 + (\eta' - y)^2 + z^2}, \end{aligned} \qquad (7\text{-}2)$$

and similarly for <AOB>, if the medium of propagation is air ($n \approx 1$). The optical path difference can be expressed more simply if the coördinates of points A and B are plane polar rather than Cartesian: letting

$$\langle AO \rangle = r, \quad \langle OB \rangle = r', \qquad (7\text{-}3)$$

we may write

$$\begin{aligned} \xi &= r\cos\alpha, \ \eta = r\sin\alpha; \\ \xi' &= r'\cos\beta, \ \eta' = r'\sin\beta, \end{aligned} \qquad (7\text{-}4)$$

where the angles of incidence and diffraction (α and β) follow the sign convention described in chapter II.

The power series for OPD can be written in terms of the grating surface point coördinates y and z:

$$OPD = \sum_{i=0}^{\infty} \sum_{j=0}^{\infty} F_{ij}\, y^i z^j, \qquad (7\text{-}5)$$

where F_{ij}, the expansion coefficient of the (i,j) term, describes how the rays (or wavefronts) diffracted from point P toward the ideal image point B differ (in direction, or curvature, *etc.*) in proportion to $y^i z^j$ from those from point O. The x-dependence of OPD has been suppressed by writing

$$x = x(y,z) = \sum_{i=0}^{\infty} \sum_{j=0}^{\infty} a_{ij}\, y^i z^j. \qquad (7\text{-}6)$$

This equation makes use of the fact that the grating surface is usually a regular function of position, so x is not independent of y and z (*i.e.*, if it is a spherical surface of radius R, then $(x - R)^2 + y^2 + z^2 = R^2$).

By analogy with the terminology of lens and mirror optics, we call each term in series (7-5) an *aberration*, and F_{ij} its *aberration coefficient*. An aberration is absent from the image of a given wavelength (in a given diffraction order) if its associated coefficient F_{ij} is zero.

Since we have imposed a plane of symmetry on the system (the principal (xy) plane), all terms F_{ij} for which j is odd vanish. Moreover, $F_{00} = 0$, since the expansion (7-5) is about the origin O. The lowest-(first-) order term F_{10} in the expansion, when set equal to zero, yields the grating equation:

$$m\lambda = d\,(\sin\alpha + \sin\beta). \qquad (2\text{-}1)$$

By Fermat's principle, we may take this equation to be satisfied for all images, which leaves the second-order aberration terms as those of lowest order which need not vanish. The generally accepted terminology is that a *stigmatic image* has vanishing second-order coefficients even if higher-order aberrations are still present.

The second order terms describe the tangential and sagittal focusing:

$$\begin{aligned} F_{20} &= \cos\alpha\left(\frac{\cos\alpha}{2r} - a_{20}\right) + \cos\beta\left(\frac{\cos\beta}{2r'} - a_{20}\right) \\ &\equiv T(r, \alpha) + T(r', \beta), \end{aligned} \qquad (7\text{-}7)$$

$$\begin{aligned} F_{02} &= \left(\frac{1}{2r} - a_{02}\cos\alpha\right) + \left(\frac{1}{2r'} - a_{02}\cos\beta\right) \\ &\equiv S(r, \alpha) + S(r', \beta), \end{aligned} \qquad (7\text{-}8)$$

F_{20} governs the tangential (or spectral) focusing of the grating system, while F_{02} governs the sagittal focusing. The associated

aberrations are called *defocus* and *astigmatism*, respectively. The two aberrations describe the extent of a monochromatic image: defocus pertains to the blurring of the image – its extent of the image along the dispersion direction (*i.e.*, in the tangential plane). Astigmatism pertains to the extent of the image in the direction perpendicular to the dispersion direction. In more common (but sometimes misleading) terminology, defocus applies to the "width" of the image in the spectral (dispersion) direction, and astigmatism applies to the "height" of the spectral image; these terms imply that the *xy (tangential)* plane be considered as "horizontal" and the *yz* (sagittal) plane as "vertical".

Actually *astigmatism* more correctly defines the condition in which the tangential and sagittal foci are not coincident, which implies a line image at the tangential focus. It is a general result of the off-axis use of a concave mirror (and, by extension, a concave reflection grating as well). A complete three-dimensional treatment of *OPD* shows that the image is actually an arc; image points away from the center of the ideal image are diffracted toward the longer wavelengths. This effect, which technically is not an aberration, is called *(spectral) line curvature*, and is most noticeable in the spectra of Paschen-Runge mounts (see later in this chapter). Figure VII-3 shows astigmatism in the image of a wavelength diffracted off-axis from a concave grating, ignoring line curvature.

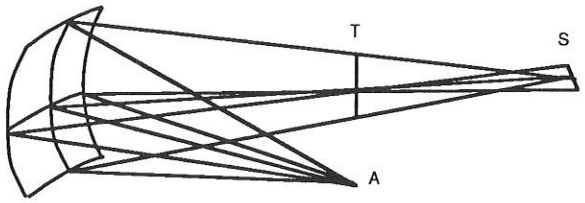

Figure VII-3. Astigmatic focusing of a concave grating. Light from point A is focused into a line parallel to the grooves at T (the tangential focus) and perpendicular to the grooves at S (the sagittal focus). Spectral resolution is maximized at T.

Since grating images are generally astigmatic, the focal distances r' in Eqs. (7-7) and (7-8) should be distinguished. Calling r'_T and r'_S the *tangential* and *sagittal focal distances*, respectively, we may set these equations equal to zero and solve for the focal curves $r'_T(\lambda)$ and $r'_S(\lambda)$:

$$r'_T(\lambda) = \frac{\cos^2\beta}{A + B\cos\beta}, \qquad (7\text{-}9)$$

$$r'_S(\lambda) = \frac{1}{D + E\cos\beta}. \qquad (7\text{-}10)$$

Here we have defined

$$A = B\cos\alpha - \frac{\cos^2\alpha}{r}, \quad B = 2a_{20},$$
$$D = E\cos\alpha - \frac{1}{r}, \quad E = 2a_{02}, \qquad (7\text{-}11)$$

where a_{20} and a_{02} are the coefficients in Eq. (7-6) (*e.g.*, $a_{20} = a_{02} = 1/(2R)$ for a spherical grating of radius R). These expressions are completely general for classical grating systems; that is, they apply to any type of grating mount or configuration.

Of the two primary (second-order) focal curves, that corresponding to defocus (F_{20}) is of greater importance in spectroscopy, since it is spectral resolution which is most crucial to grating systems. For this reason we do not concern ourselves with locating the image plane at the "circle of least confusion"; rather, we try to place the image plane at or near the tangential focus (where $F_{20} = 0$). For concave gratings ($a_{20} \neq 0$), there are two well-known solutions to the defocus equation $F_{20} = 0$.

The *Rowland circle* is a circle whose diameter is equal to the tangential radius of the grating blank, and which passes through the grating center (point O in Figure VII-5). If the point source A is placed on this circle, the tangential focal curve also lies on this circle. This solution is the basis for Rowland circle and Paschen-Runge mounts. For the Rowland circle mount,

$$r = \cos\alpha/2a_{20} = R\cos\alpha,$$
$$r'_T = \cos\beta/2a_{20} = R\cos\beta. \qquad (7\text{-}12)$$

The sagittal focal curve is

$$r'_S = \left[\frac{\cos\alpha + \cos\beta}{\rho} - \frac{1}{R\cos\alpha}\right]^{-1} \qquad (7\text{-}13)$$

(where ρ is the sagittal radius of the grating), which is always greater than r'_T (even for a spherical blank, for which $\rho = R$) unless $\alpha = \beta = 0$. Consequently this mount suffers from astigmatism, which in some cases is considerable.

The *Wadsworth mount* is one in which the source light is collimated ($r \to \infty$), so that the tangential focal curve is given by

$$r'_T = \frac{\cos^2\beta}{2\,a_{20}\,(\cos\alpha + \cos\beta)} = \frac{R\cos^2\beta}{\cos\alpha + \cos\beta}. \qquad (7\text{-}14)$$

The sagittal focal curve is

$$r'_S = \frac{1}{2\,a_{02}\,(\cos\alpha + \cos\beta)} = \frac{\rho}{\cos\alpha + \cos\beta}. \qquad (7\text{-}15)$$

In this mount, the imaging from a classical spherical grating ($\rho = R$) is such that the astigmatism of the image is zero only for $\beta = 0$, though this is true for any incidence angle α.

While higher-order aberrations are usually of less importance than defocus and astigmatism, they can be prohibitively large in common circumstances. The third-order aberrations, *primary* or *tangential coma* F_{30} and *secondary* or *sagittal coma* F_{12}, are given by

$$F_{30} = \frac{\sin\alpha}{r}\,T(r,\,\alpha) + \frac{\sin\beta}{r'}\,T(r',\,\beta) - a_{30}\,(\cos\alpha + \cos\beta), \qquad (7\text{-}16)$$

$$F_{12} = \frac{\sin\alpha}{r}\,S(r,\,\alpha) + \frac{\sin\beta}{r'}\,S(r',\,\beta) - a_{12}\,(\cos\alpha + \cos\beta), \qquad (7\text{-}17)$$

where T and S are defined in Eqs. (7-7) and (7-8). Often one or both of these third-order aberrations is significant in a spectral image, and must be minimized with the second-order aberrations.

NONCLASSICAL CONCAVE GRATING IMAGING

For nonclassical groove patterns, the aberration coefficients F_{ij} must be generalized to account for the image-modifying effects of the variations in curvature and spacing of the grooves, as well as for the focusing effects of the concave blank:

$$F_{ij} = M_{ij} + \frac{m\,\lambda}{\lambda_0}\,H_{ij} \equiv M_{ij} + H'_{ij}. \qquad (7\text{-}18)$$

The terms M_{ij} are simply the F_{ij} coefficients for classical concave grating mounts, discussed above. The H'_{ij} coefficients describe the groove pattern. For classical gratings, $H'_{ij} = 0$ for all terms of order two or higher ($i + j \geq 2$). The tangential and sagittal focal distances (Eqs. (7-9) and (7-10)) must now be generalized:

$$r'_T(\lambda) = \frac{\cos^2\beta}{A + B\cos\beta + C\sin\beta}, \qquad (7\text{-}19)$$

$$r'_S(\lambda) = \frac{1}{D + E\cos\beta + F\sin\beta}, \qquad (7\text{-}20)$$

where in addition to Eqs. (7-11) we have

$$C = -2\,H'_{20}, \quad F = -2\,H'_{02}. \qquad (7\text{-}21)$$

Here H'_{20} and H'_{02} being the terms which govern the effect of the groove pattern on the tangential and sagittal focusing. For a first generation interference grating, for example, the H_{ij} coefficients may be written in terms of the parameters of the recording geometry (see Figure VII-4):

$$H'_{20} = -T(r_C,\,\gamma) + T(r_D,\,\delta), \qquad (7\text{-}22)$$

$$H'_{02} = -S(r_C,\,\gamma) + S(r_D,\,\delta), \qquad (7\text{-}23)$$

where $C(r_C,\,\gamma)$ and $D(r_D,\,\delta)$ are the plane polar coördinates of the recording points. These equations are quite similar to Eqs. (7-7) and (7-8), due to the similarity in Figures VII-4 and VII-2.

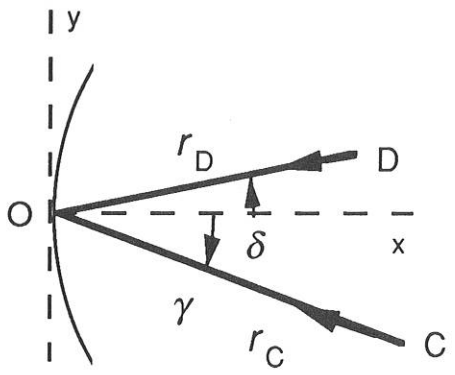

Figure VII-4. Recording parameters. Spherical waves emanate from point sources C and D; the interference pattern forms fringes on the concave blank centered at O.

For VLS gratings (see chapter IV), the terms H_{ij} are written in terms of the groove spacing coefficients rather than in terms of recording coördinates.

More details on the imaging properties of gratings systems can be found in NAMIOKA [1959] and NODA *et al.* [1974].

REDUCTION OF ABERRATIONS

In the design of grating systems, there exists several degrees of freedom whose values may be chosen to optimize image quality. For monochromators, the locations of the entrance slit A and exit slit B relative to the grating center O provide three degrees of freedom (or four, if no plane of symmetry is imposed); the missing degree of freedom is restricted by the grating equation, which sets the angular relationship between the lines AO and BO. For spectrographs, the location of the entrance slit A as well as the location, orientation and curvature of the image field provide degrees of freedom (though the grating equation must be satisfied). In addition, the curvature of the grating blank provides freedom, and the aberration coefficients H'_{ij} for an interference grating (or the equivalent terms for a VLS grating) can be chosen to improve imaging. Even in systems for which the grating use geometry has been specified, there exist several degrees of freedom due to the aberration reduction possibilities of the grating itself.

Algebraic techniques can find sets of design parameters which minimize image size at one or two wavelengths, but to optimize the imaging of an entire spectral range is usually so complicated that computer implementation of a design procedure is essential. The Richardson Grating Laboratory has developed a set of proprietary computer programs which are used to design and analyze grating systems. These programs allow selected sets of parameters governing the use and recording geometries to vary within prescribed limits. Optimal imaging is found by comparing the imaging properties for systems with different sets of parameters values.

CONCAVE GRATING MOUNTS

Rowland Circle Spectrographs. The first concave gratings of spectroscopic quality were ruled by Rowland, who invented them in 1881, also designing their first mounting. Placing the ideal source point on the Rowland circle forms spectra on that circle free from defocus and primary coma at all wavelengths (*i.e.*, $F_{20} = F_{30} = 0$ for all λ); while spherical aberration is residual and small, astigmatism is usually severe. Originally a Rowland circle spectrograph employed a photographic plate bent along a circular arc on the Rowland circle to record

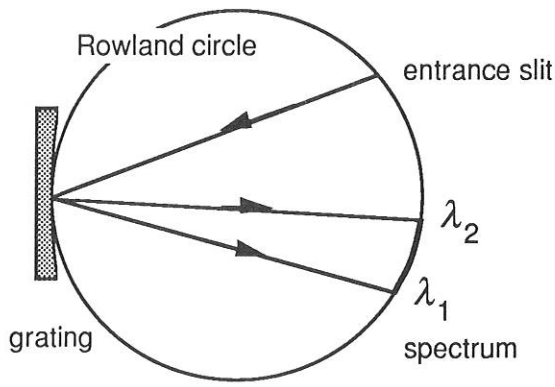

Figure VII-5. The Rowland Circle spectrograph. Both the entrance slit and the diffracted spectrum lie on the Rowland circle, whose diameter equals the tangential radius of curvature R of the grating and which passes through the grating center. Light of two wavelengths is shown focused at different points on the Rowland circle.

the spectrum in its entirety. Today it is more common for a series of exit slits to be cut into a circular mask to allow the recording of several discrete wavelengths photoelectrically; this system is called the *Paschen-Runge mount*. Other configurations based on the imaging properties of the Rowland circle are the *Eagle mount* and the *Abney mount*, both of which are described by Hutley and by Meltzer.

Unless the exit slits (or photographic plates) are considerably taller than the entrance slit, the astigmatism of Rowland circle mounts usually prevents more than a small fraction of the diffracted light from being recorded, which greatly decreases the efficiency of the instrument. Increasing the exit slit heights helps collect more light, but since the images are curved, the exits slits would have to be curved as well to maintain optimal resolution. To complicate matters further, this curvature depends on the diffracted wavelength, so each exit slit would require a unique curvature. Few instruments have gone to such trouble, so most Rowland circle grating mounts collect only a small portion of the light incident on the grating. For this reason these mounts are adequate for strong sources (such as the observation of the solar spectrum) but not for less intense sources (such as stellar spectra).

The imaging properties of instruments based on the Rowland circle spectrograph, such as direct readers and atomic absorption instruments, can be improved by the use of nonclassical gratings. Replacing the usual concave classical gratings with concave aberration-reduced gratings, astigmatism can be improved substantially. Rowland circle mounts modified in this manner direct more diffracted light through the exit slits without degrading resolution.

The Wadsworth Spectrograph. When a classical concave grating is illuminated with collimated light (rather than from a point source on the Rowland circle), spectral astigmatism on and near the grating normal is greatly reduced. Such a grating system is called the *Wadsworth mount*. The wavelength-dependent aberrations of the grating are compounded by the aberration of the collimating optics, though use of a paraboloidal mirror illuminated on-axis will eliminate off-axis aberrations and spherical aberrations. The Wadsworth mount suggests itself in situations in which the light incident on the grating is naturally collimated (from, for example, synchrotron radiation sources). In other cases, an off-axis parabolic mirror would serve well as the collimating element.

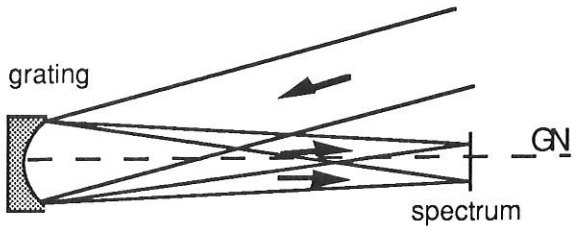

Figure VII-6. The Wadsworth spectrograph. Collimated light is incident on a concave grating; light of two wavelengths is shown focused at different points. GN is the grating normal.

Flat Field Spectrographs. One of the advantages of changing the groove pattern (as on a first- or second- generation interference grating or a VLS grating) is that the focal curves can be modified, yielding grating mounts which differ from the classical ones. A logical improvement of this kind on the Rowland circle spectrograph is the *flat-field spectrograph*, in which the tangential focal curve is removed from the Rowland circle and rendered nearly linear over the spectrum of interest (see Figure VII-7). While a grating cannot be made which images a spectrum perfectly on a line, one which forms a spectrum on a sufficiently flat surface is ideal for use in linear detector array instruments of moderate resolution. This development has had a significant effect on spectrograph design.

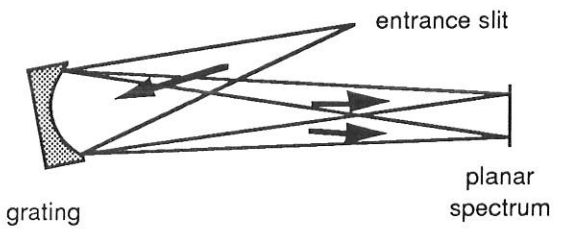

Figure VII-7. A flat-field spectrograph.

The relative displacement between the tangential and sagittal focal curves can also be reduced via VLS or interferometric modification of the groove pattern. In this way, the resolution of a flat-field spectrometer can be maintained (or improved) while its astigmatism is decreased; the latter effect allows more light to be transmitted through the exit slit (or onto the detector elements). An example of the process of aberration reduction is shown in Figure VII-8.

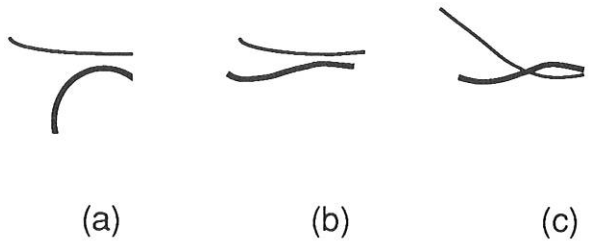

Figure VII-8. Modification of focal curves. The primary tangential focal curve ($F_{20} = 0$) is thick; the primary sagittal focal curve ($F_{02} = 0$) is thin. (a) Focal curves for a classical ($H_{20} = H_{02} = 0$) concave grating, illuminated off the normal ($\alpha \neq 0$) – the dark curve is an arc of the Rowland circle. (b) Choosing a suitable nonzero H_{20} value moves the tangential focal arc so that part of it is nearly linear, suitable for a flat-field spectrograph detector. (c) Choosing a suitable nonzero value of H_{02} moves the sagittal focal curve so that it crosses the tangential focal curve, providing a stigmatic image.

Constant-Deviation Monochromators. In a constant-deviation monochromator, the angle $2K$ between the entrance and exit arms is held constant as the grating is rotated (thus scanning the spectrum; see Figure VII-9). This angle is called the *deviation angle* or *angular deviation*. While plane or concave gratings can be used in constant-deviation mounts, only in the latter case can imaging be made acceptable over an entire spectrum without auxiliary focusing optics.

The *Seya-Namioka monochromator* is a very special case of constant-deviation mount using a classical spherical grating, in which the deviation angle $2K$ between the beams and the entrance and exit slit distances (r and r') are given by

$$2K = 70°30',$$
$$r = r' = R\cos(70°30'/2), \qquad (7\text{–}24)$$

where R is the radius of the spherical grating blank. The only moving part in this system is the grating, through whose rotation the spectrum is scanned. Resolution may be quite good in part of the spectrum, though it degrades farther from the optimal wavelength; astigmatism is high, but at an optimum. Replacing the grating with a classical toroidal grating can reduce the astigmatism, if the minor radius of the toroid is chosen judiciously. The reduction of astigmatism by suitably designed interference gratings is also helpful, though the best way to optimize the imaging of a constant-deviation monochromator is to relax the restrictions (7-24) on the use geometry.

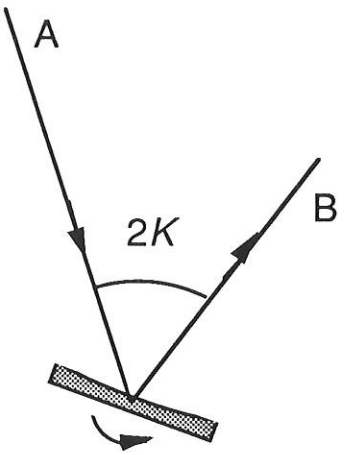

Figure VII-9. Constant-deviation monochromator geometry. To scan wavelengths, the entrance slit A and exit slit B remain fixed as the grating rotates. The deviation angle $2K$ is measured from the exit arm to the entrance arm.

IMAGING PROPERTIES OF GRATING SYSTEMS VIII

CHARACTERIZATION OF IMAGING QUALITY

In the previous chapter, we formulated the optical imaging properties of a grating system in terms of wavefront aberrations. After arriving at a design, though, this approach is not ideal for observing the imaging properties of the system. Two tools of image analysis – spot diagrams and line-spread functions – are discussed below.

Geometric Raytracing & Spot Diagrams. Raytracing (using the laws of geometrical optics) is superior to wavefront aberration analysis in the determination of image quality. Aberration analysis is an approximation to image analysis, since it involves expanding quantities in infinite power series and considering only a few of its terms. Raytracing, on the other hand, does not involve approximations, but shows (in the absence of the diffractive effects of physical optics) where each ray of light incident on the grating will diffract. It would be more exact to design grating systems with a raytracing procedure as well, though to do so would be computationally demanding.

The set of intersections of the diffracted rays and the image plane forms a set of points, called a *spot diagram.* In Figure VIII-1, several simple spot diagrams are shown; their horizontal axes are in the plane of dispersion (the tangential plane), and their vertical axes are in the sagittal plane. In (a) an uncorrected (out-of-focus) image is shown; (b) shows good tangential focusing, and (c) shows virtually point-like imaging. All three of these images are simplistic in that higher-order aberrations (such as coma and spherical aberration) render typical spot diagrams asymmetric, as in (d).

A straightforward method of evaluating the imaging properties of a spectrometer at a given wavelength is to measure the tangential and sagittal extent of an image (often called the width w' and height h' of the image, respectively).

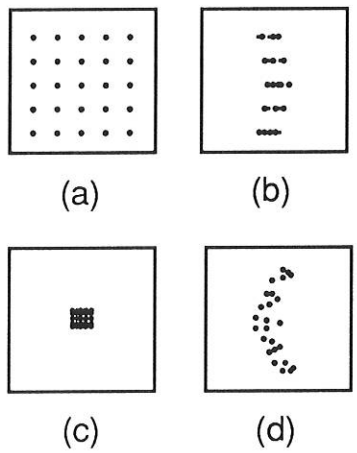

Figure VIII-1. Spot diagrams. In (a) the image is out of focus. In (b), the image is well focused in the tangential plane only; the line curvature inherent to grating-diffracted images is shown. In (c) the image is well focused in both directions – the individual spots are not discernable. In (d) a more realistic image is shown.

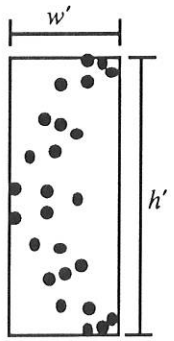

Figure VIII-2. Image dimensions. The width w' and height h' of the image in the image plane are the dimensions of the smallest rectangle which contains the spots.

Geometric raytracing provides spot diagrams in good agreement with observed spectrometer images, except for well-focused images, in which the wave nature of light

dictates a minimum size for the image. Even if the image of a point object is completely without aberrations, it is not a point image, due to the diffraction effects of the pupil (which is usually the perimeter of the grating). The minimal image size, called the *diffraction limit*, can be easily estimated for a given wavelength as the diameter a of the Airy disk for a mirror in the same geometry:

$$a = 2.44\lambda\, f/\mathrm{no}_{\mathrm{OUTPUT}} = 2.44\lambda \frac{r'(\lambda)}{W\cos\beta}. \qquad (8\text{-}1)$$

Here $f/\mathrm{no}_{\mathrm{OUTPUT}}$ is the output focal ratio, $r'(\lambda)$ is the focal distance for this wavelength, and W is the width of the grating (see Eq. (2-20), chapter II). Results from raytrace analyses which use the laws of geometrical optics only should not be considered valid if the dimensions of the image are found to be near or below the diffraction limit calculated from Eq. (8-1).

Linespread Calculations A fundamental problem with geometric raytracing procedures (other than that they ignore the variations in energy density throughout a cross-section of the diffracted beam and the diffraction efficiency of the grating) is its ignorance of the effect that the size and shape of the exit aperture has on the measured resolution of the instrument.

An alternative to merely measuring the extent of a spectral image is to compute its *linespread function*, which is the convolution of the (monochromatic) image of the entrance slit with the exit aperture (the exit slit in a monochromator, or a detector element in a spectrograph). A close physical equivalent is scanning the monochromatic image by moving the exit aperture past it in the image plane, and recording the light intensity passing through the slit as a function of position in this plane.

The linespread calculation thus described accounts for the effect that the entrance and exit slit dimensions have on the resolution of the grating system.

Instrumental Imaging

With regard to the imaging of actual optical instruments, it is not sufficient to state that ideal performance (in which geometrical aberrations are completely eliminated and the diffraction limit is ignored) is to focus a point object to a point image. All real sources are extended sources – that is, they have finite widths and heights. The ideal imaging of a square light source is not even a square image, since the magnification of the object (in both directions) is a natural and unavoidable consequence of diffraction from a grating.

Magnification of the entrance aperture. The image of the entrance slit, ignoring aberrations and the diffraction limit, will not have the same dimensions as the entrance slit itself. Calling w and h the width and height of the entrance slit, and w' and h' the width and height of the image, the *tangential* and *sagittal magnifications* χ_T and χ_S are

$$\chi_T \equiv \frac{w'}{w} = \frac{r'\cos\alpha}{r\cos\beta}, \qquad \chi_S \equiv \frac{h'}{h} = \frac{r'}{r}. \qquad (8\text{-}2)$$

These relations, which indicate that the size of the image of the entrance slit will usually differ from that of the entrance slit itself, are derived below.

Figure VIII-3 shows the plane of dispersion. The grating center is at O; the x-axis is the grating normal and the y-axis is the line through the grating center perpendicular to the grooves at O. Monochromatic light of wavelength λ leaves the entrance slit (of width w) located at the polar coördinates (r, α) from the grating center O and is diffracted

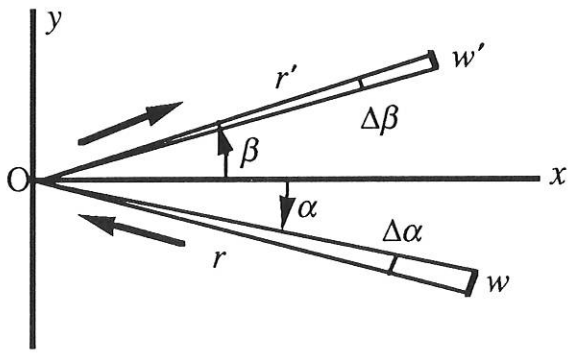

Figure VIII-3. Geometry showing tangential magnification. Monochromatic light from the entrance slit, of width w, is projected by the grating to form an image of width w'.

along angle β. When seen from O, the entrance slit subtends an angle $\Delta\alpha = w/r$ in the dispersion (xy) plane. Rays from one edge of the entrance slit have incidence angle α, and are diffracted along β; rays from the other edge have incidence angle $\alpha + \Delta\alpha$, and are diffracted along $\beta - \Delta\beta$. The image (located a distance r' from O), therefore subtends an angle $\Delta\beta$ when seen from O, has width $w' = r'\,\Delta\beta$. The ratio $\chi_T = w'/w$ is the tangential magnification.

We may apply the grating equation to the rays on either side of the entrance slit:

$$Gm\lambda = \sin\alpha + \sin\beta, \qquad (8\text{-}3)$$

$$Gm\lambda = \sin(\alpha+\Delta\alpha) + \sin(\beta-\Delta\beta). \qquad (8\text{-}4)$$

Here G (= $1/d$) is the pitch of the grating (the grooves frequency along the y-axis at O) and m is the diffraction order. Expanding $\sin(\alpha+\Delta\alpha)$ in Eq. (8-4) in a Taylor series about $\Delta\alpha = 0$, we obtain

$$\sin(\alpha+\Delta\alpha) = \sin\alpha + (\cos\alpha)\Delta\alpha + \ldots, \qquad (8\text{-}5)$$

where terms of order two or higher in $\Delta\alpha$ have been truncated. Using Eq. (8-5) (and its analogue for $\sin(\beta-\Delta\beta)$) in Eq. (8-4), and subtracting it from Eq. (8-3), we obtain

$$\cos\alpha\,\Delta\alpha = \cos\beta\,\Delta\beta, \qquad (8\text{-}6)$$

and therefore

$$\frac{\Delta\beta}{\Delta\alpha} = \frac{\cos\alpha}{\cos\beta}, \qquad (8\text{-}7)$$

from which the first of Eqs. (8-2) follows.

Figure VIII-4 shows the same situation in the sagittal plane, which is perpendicular to the principal plane and contains the pole diffracted ray. The entrance slit is located below the principal plane; consequently, its image is above this plane. A ray from the top of the center of the entrance slit is shown. Since the grooves are parallel to the sagittal plane at O, the grating acts as a mirror in this plane, so the angles ϕ and ϕ' are equal in magnitude. Ignoring signs, their tangents are equal as well:

$$\tan\phi = \tan\phi' \;\rightarrow\; \frac{z}{r} = \frac{z'}{r'}, \qquad (8\text{-}8)$$

where z and z' are the distances from the entrance and exit slit points to the principal plane. A ray from an entrance slit point a distance $|z + h|$ from this plane will image toward a point $|z' + h'|$ from this plane, where h' now defines the height of the image. As this ray is governed by reflection as well,

$$\tan\psi = \tan\psi' \;\rightarrow\; \frac{z+h}{r} = \frac{z'+h'}{r'}. \qquad (8\text{-}9)$$

Simplifying this using Eq. (8-8) yields the latter of Eqs. (8-2).

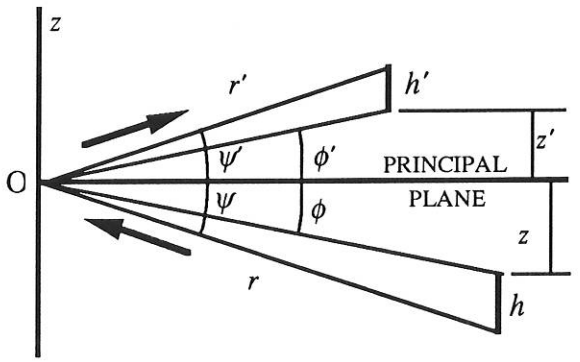

Figure VIII-4. Geometry showing sagittal magnification. Monochromatic light from the entrance slit, of height h, is projected by the grating to form an image of height h'.

Effects of the entrance aperture dimensions. In most instances, good approximations to the width w' and height h' of the image of an entrance slit of width w and height h are given by

$$w' = \chi_T\, w + \delta w', \qquad h' = \chi_S\, h + \delta h', \qquad (8\text{-}10)$$

where $\delta w'$ and $\delta h'$ are the width and height of the image of a point source. This equation allows the imaging properties of a grating system with an entrance slit of finite area to be estimated quite well from the imaging properties of the system in which an infinitesimally small object point is considered. In effect, rays need only be traced from one point in the entrance slit (which deter-

mines $\delta w'$ and $\delta h'$), from which the image dimensions for an extended entrance slit can be calculated using Eqs. (8-10). These approximations ignore subtle out-of-plane imaging effects which occur when the object point A lies outside of the principal plane, though such effects are usually negligible if the center of the entrance slit lies in this plane and if the entrance slit dimensions are small compared with the distance r between the entrance slit and the grating center.

Effects of the exit aperture dimensions. The linespread function for a spectral image, as defined above, depends on the width of the exit aperture as well as on the width of the diffracted image itself. In determining the optimal width of the exit slit (or single detector element), a rule of thumb is that the width w'' of the exit aperture should roughly match the width w' of the image of the entrance aperture, as explained below.

Typical linespread curves for the same diffracted image scanned by three different exit slit widths are shown in Figure VIII-5. For simplicity, we have assumed $\chi_T = 1$ for these examples. The horizontal axis is position along the image plane, in the plane of dispersion. This axis can also be thought of as a wavelength axis (that is, in spectral units); the two axes are related via the dispersion. The vertical axis is relative light intensity at the image plane; its bottom and top represent no intensity and total intensity (or no rays entering the slit and all rays entering the slit), respectively. Changing the horizontal coördinate represents scanning the monochromatic image by moving the exit slit across it, in the plane of dispersion. This is approximately equivalent to changing the wavelength while keeping the exit slit fixed in space.

An exit slit less wide than the image ($w'' < w'$) will result in a linespread graph such as that seen in Figure VIII-5 (a). In no position of the exit slit (or, for no diffracted wavelength) does the totality of diffracted rays fall within the slit, as it is not wide enough; the relative intensity does not reach its maximum value of unity. In (b), the exit slit width matches the width of the image: $w'' = w'$. At exactly one point during the scan, all of the diffracted light is contained within the exit slit; this point is the peak (at a relative intensity of unity) of the curve. In (c) the exit slit is wider than the image ($w'' > w'$). The exit slit contains the entire image for many positions of the exit slit.

In these figures the quantities FWZH and FWHM are shown. These are abbreviations for *full width at zero height* and *full width at half maximum*. The FWZH is simply the total extent of the linespread function, usually expressed in spectral units. The FWHM is the spectral extent between the two extreme points on the linespread graph which are at half the maximum value. The FWHM is often used as a quantitative measure of image quality in grating systems; it is often called the *effective spectral bandwidth*. The FWZH is sometimes called the *full spectral bandwidth*. It should be noted that the terminology is not universal among authors and is sometimes quite confusing.

As the exit slit width w' is decreased, the effective bandwidth will generally decrease. If w' is roughly equal to the image width w, though, further reduction of the exit slit width will not reduce the bandwidth appreciably. This can be seen in Figure VIII-5, in which reducing w' from case (c) to case (b) results in a decrease in the FWHM, but further reduction of w' to case (a) does not reduce the FWHM.

The situation in $w'' < w'$ is undesirable in that diffracted energy is lost (the peak relative intensity is low) since the exit slit is too narrow to collect all of the diffracted light at once. The situation $w'' > w'$ is also undesirable, since the FWHM is excessively large (or, similarly, an excessively wide band of wavelengths is accepted by the wide slit). The situation $w'' = w'$ seems optimal: when the exit slit width matches the width of the spectral image, the relative intensity is maximized while the FWHM is minimized. An interesting curve is shown in Figure VIII-6, in which the ratio FWHM/FWZH is shown *vs.* the ratio w''/w' for a typical grating system. This ratio reaches its single minimum near $w'' = w'$.

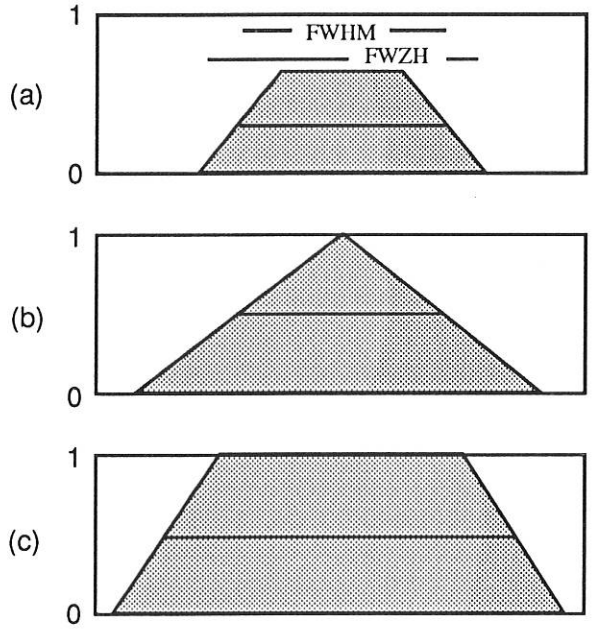

Figure VIII-5. Linespread curves for different exit slit widths. The vertical axis is relative intensity at the exit aperture, and the horizontal axis is position along the image plane (in the plane of dispersion). For a given curve, the dark horizontal line shows the FWHM (the width of that portion of the curve in which its amplitude exceeds its half maximum); the FWZH is the width of the entire curve. (a) $w''' < w'$; (b) $w''' = w'$; (c) $w'' > w'$. In (a) the peak is below unity. In (a) and (b), the FWHM are approximately equal. Severely aberrated images will yield linespread curves which differ from those above (in that they will be asymmetric), although their overall shape will be similar.

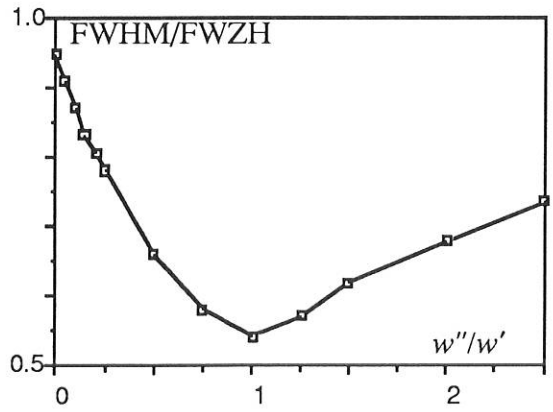

Figure VIII-6. FWHM/FWZH vs. w''/w' for a typical system.

The height of the exit aperture has a more subtle effect on the imaging properties of the spectrometer, since by 'height' we mean extent in the direction perpendicular to the plane of dispersion. If the exit slit height is less than the height (sagittal extent) of the image, some diffracted light will be lost, as it will not pass through the aperture. Since diffracted images generally display curvature, truncating the sagittal extent of the image by choosing a short exit slit also reduces the width of the image (see Figure VIII-7). This latter effect is especially noticeable in Paschen-Runge mounts.

In this discussion we have ignored the diffraction effects of the grating aperture: the comments above consider only the effects of geometrical optics on instrumental imaging. For cases in which the entrance and exit slits are equal in width, and this width is two or three times the diffraction limit, the linespread function is approximately Gaussian in shape rather than the triangle shown in Figure VIII-5(b).

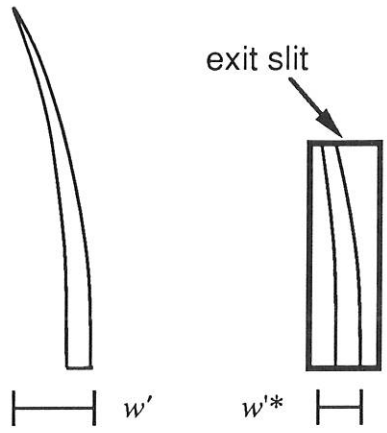

Figure VIII-7. Effect of exit slit height on image width. Both the width and the height of the image are reduced by the exit slit chosen. Even if the width of the exit slit is greater than the width of the image, truncating the height of the image yields $w'^* < w'$. [Only the top half of each image is shown.]

EFFICIENCY OF DIFFRACTION GRATINGS IX

This chapter is based on LOEWEN *et al.* [1977].

Efficiency and its variation with wavelength and spectral order are important characteristics of a diffraction grating. For a reflection grating, efficiency is defined as the intensity of monochromatic light diffracted into the order being measured, relative either to the intensity of the incident light (*absolute efficiency*) or to the specular reflection from a polished mirror blank coated with the same material (*relative efficiency*). Efficiency is defined similarly for transmission gratings, except that an uncoated substrate is used in the measurement of relative efficiency.

High efficiency gratings are desirable for several reasons. A grating with high efficiency is more useful than one with lower efficiency in measuring weak transition lines in optical spectra. A grating with high efficiency may allow the reflectivity and transmissivity specifications for the other components in the spectrometer to be relaxed. Moreover, higher diffracted energy may imply lower instrumental stray light due to other diffracted orders, as the total intensity leaving the grating is conserved (being equal to the light incident on it).

Control over the magnitude and variation of diffracted energy with wavelength is called *blazing*, and it involves the manipulation of the micro-geometry of the grating grooves. In the 1888 edition of *Encyclopædia Brittanica*, Lord Rayleigh recognized that the energy distribution (by wavelength) of a diffraction grating could be altered by modifying the shape of the grating grooves. A few decades later, R.W. Wood showed this to be true when he ruled a grating on which he had controlled the groove shape, thereby producing the first deliberately blazed diffraction grating.

The choice of an optimal efficiency curve for a grating depends on the specific application. Often the desired instrumental efficiency is linear; that is, the intensity of light transformed into signal at the image plane must be constant across the spectrum. To approach this as closely as possible, the spectral emissivity of the light source and the spectral response of the detector should be considered, from which the desired grating efficiency curve can be derived. Usually this requires peak grating efficiency in the region of the spectrum where the detectors are least sensitive; for example, a visible-light spectrometer using a silicon detector would be much less sensitive in the blue than in the red, suggesting that the grating itself be blazed to yield a peak efficiency in the blue.

A typical *efficiency curve* (a plot of absolute or relative diffracted efficiency *vs.* diffracted wavelength λ) is shown in Figure IX-1. Usually such a curve shows a single maximum, at the *peak wavelength* (or *blaze wavelength*) λ_B. This curve corresponds to a given diffraction order m; the peak of the curve decreases in magnitude and shifts toward shorter wavelengths as $|m|$ increases. The efficiency curve also depends on the angles of use (*i.e.*, the angles of incidence and diffraction). Moreover, the curve depends on the groove spacing d (more appropriately, on the dimensionless parameter λ/d) and the material with which the grating is coated (for reflection gratings) or made (for transmission gratings).

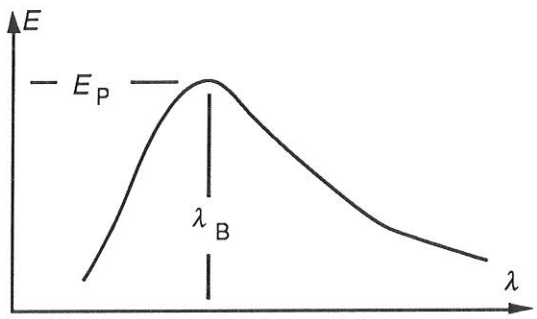

Figure IX-1. A typical (simplified) efficiency curve. This curve shows the efficiency E of a grating in a given spectral order m, measured *vs.* the diffracted wavelength λ. The peak efficiency E_P occurs at the blaze wavelength λ_B.

In many instances the light intensity diffracted from a grating depends on the polarization of the incident light. *P-plane* or *TE polarized light* is polarized parallel to the grating grooves, while *S-plane* or *TM polarized light* is polarized perpendicular to the grating grooves (see Figure IX-2). For completely unpolarized incident light, the efficiency curve will be exactly halfway between the P and S efficiency curves.

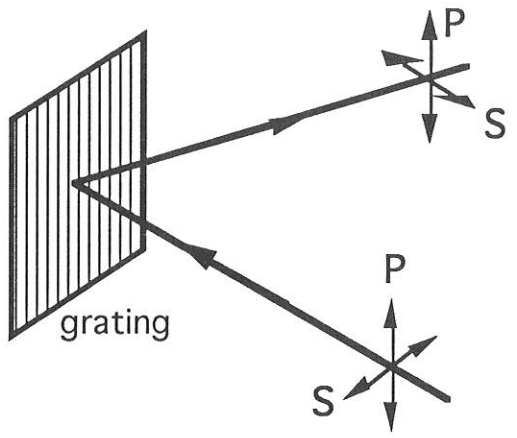

Figure IX-2. S and P polarizations The P polarization components of the incident and diffracted beams are polarized parallel to the grating grooves; the S components are polarized perpendicular to the P components. Both the S and P components are perpendicular to the propagation directions.

Usually light from a single spectral order m is used in a spectroscopic instrument, so a grating with ideal efficiency characteristics would diffract all of the light incident on it into this order (for the wavelength range considered). In practice, this is never true: the distribution of the light diffracted by the grating depends in a complicated way on the groove spacing and profile, the spectral order, the wavelength, and the grating material.

Anomalies are locations on an efficiency curve (efficiency plotted *vs.* wavelength) at which the efficiency changes abruptly. First observed by R. W. Wood, these sharp peaks and troughs in an efficiency curve are sometimes referred to as Wood's anomalies. Anomalies are rarely observed in P polarization efficiency curves, but they are often seen in S polarization curves (see Figure IX-3).

Lord Rayleigh predicted the locations (in the spectrum) where such anomalies would be found: he suggested that anomalies occur when light of a given wavelength λ' and spectral order m' is diffracted at $|\beta| = 90°$ from the grating normal (*i.e.*, it passes over the grating horizon). For wavelengths $\lambda < \lambda'$, $|\beta| < 90°$, so diffraction is possible in order m' (and all lower orders), but for $\lambda > \lambda'$ no diffraction is possible in order m' (but it is still possible in lower orders). Thus there is a discontinuity in the diffracted energy *vs.* λ in order m' at wavelength λ, and the energy that would diffract into this order for $\lambda > \lambda'$ is redistributed among the other spectral orders. This causes abrupt changes in the energy diffracted into these other orders.

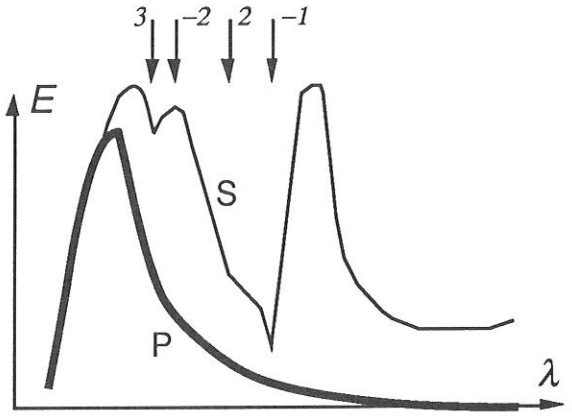

Figure IX-3. Anomalies in the first order for a typical grating with triangular grooves. The P efficiency curve (thick line) is smooth, but anomalies are evident in the S curve (thin line). The passing-off locations are identified by their spectral order at the top of the figure.

The Rayleigh explanation does not cover the extension towards longer wavelengths, where anomalies are due to resonance effects. The position of an anomaly depends to a slight degree on the optical constants of the reflecting material of the grating surface.

Grating Efficiency and Groove Shape

The maximum efficiency of a grating is typically obtained with a simple smooth tri-

angular groove profile, as shown in Figure IX-4, when the groove (or blaze) angle θ is such that the specular reflection angle for the angle of incidence is equal (in magnitude and opposite in sign) to the angle of diffraction. Ideally, the groove facet should be flat with smooth straight edges, and be generally free from irregularities on a scale comparable to the small fraction (< 1/10) of the wavelength of light being diffracted.

Fraunhofer was well aware that the distribution of light among the various diffraction orders depended on the shape of the individual grating grooves. Wood, many decades later, was the first to achieve a degree of control over the groove shape, thereby concentrating spectral energy into one angular region. Wood's gratings were seen to light up, or 'blaze', when viewed at the correct angle. The Richardson Grating Laboratory takes special pride in continuing its long tradition of advancing the technology of blazing so that its gratings have efficiencies near that theoretically attainable.

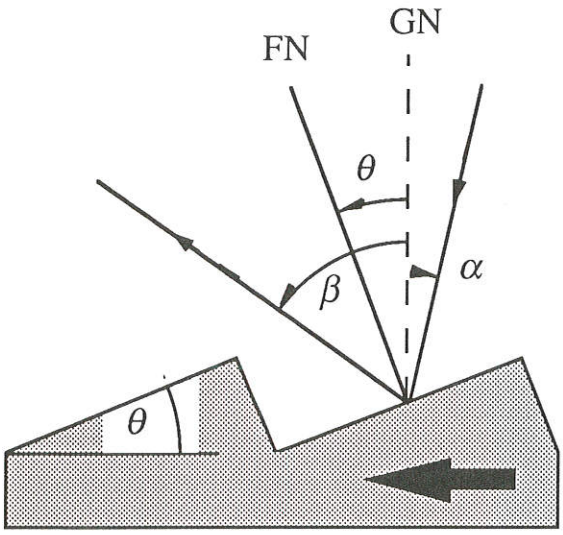

Figure IX-4. Triangular groove geometry. The angles of incidence α and diffraction β are shown in relation to the facet angle θ for the blaze condition. GN is the grating normal and FN is the facet normal. The facet normal bisects the angle between the incident and diffracted rays. The blaze arrow (shown) points from GN to FN.

Triangular-groove gratings. Gratings with triangular grooves can be generated by mechanical ruling, or by blazing sinusoidal groove profiles by ion etching. The efficiency behavior of gratings with triangular groove profiles (*i.e.*, blazed gratings) may be divided into six families, depending on the blaze angle:

family	*blaze angle*
very low blaze angle	$\theta < 5°$
low blaze angle	$5° \le \theta < 10°$
medium blaze angle	$10° \le \theta < 18°$
special low anomaly	$18° \le \theta < 22°$
high blaze angle	$22° \le \theta < 38°$
very high blaze angle	$\theta \ge 38°$

Very low blaze angle gratings ($\theta < 5°$) exhibit efficiency behavior which is almost perfectly scalar; that is, polarization effects are virtually nonexistent. In this region, a simple picture of blazing is applicable, in which each groove facet can be considered a simple flat mirror. The diffracted efficiency is greatest for that wavelength which is diffracted by the grating in the same direction as it would be reflected by the facets. This efficiency peak occurs at $\lambda/d = 2 \sin\theta$ (provided the angle between the incident and diffracted beams is not excessive). At $\lambda_B/2$, where λ_B is the blaze wavelength, the diffracted efficiency will be virtually zero (Figure IX-5) since for this wavelength the second-order efficiency will be at its peak. Fifty-percent absolute efficiency is obtained from roughly $0.67\lambda_B$ to $1.8\lambda_B$.

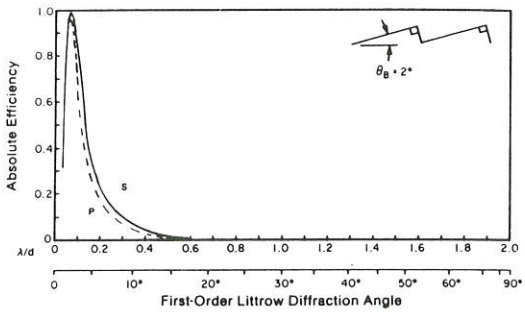

Figure IX-5. First-order theoretical efficiency curve: 2° blaze angle and Littrow mounting (2K = 0). Solid curve, S-plane; dashed curve, P-plane.

For *low blaze angle* gratings ($5° \leq \theta < 10°$), polarization effects will occur within their useable range (see Figure IX-6). In particular, a strong anomaly is seen near $\lambda/d = 2/3$. Also observed is the theoretical S-plane theoretical efficiency peak of 100% exactly at the nominal blaze, combined with a P-plane peak which is lower and at a shorter wavelength. It is characteristic of all P-plane curves to decrease monotonically from their peak toward zero as $\lambda/d \rightarrow 2$, beyond which diffraction is not possible (see Eq. (2-1)). Even though the wavelength band over which 50% efficiency is attained in unpolarized light is from $0.67\lambda_B$ to $1.8\lambda_B$, gratings of this type (with 1200 groove per millimeter, for example) are widely used, because they most effectively cover the wavelength range between 200 and 800 nm (in which most ultraviolet-visible (UV-Vis) spectrophotometers operate).

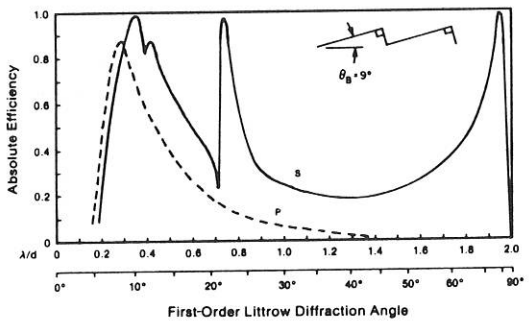

Figure IX-6. Same as Figure IX-5, except 9° blaze angle.

A typical efficiency curve for a *medium blaze angle* grating ($10° \leq \theta < 18°$) is shown in Figure IX-7. As a reminder that for unpolarized light the efficiency is simply the arithmetic average of the S- and P-plane efficiencies, such a curve is shown in this figure only, to keep the other presentations simple.

The *low-anomaly blaze angle* region ($18° \leq \theta < 22°$) is a special one. Due to the fact that the strong anomaly that corresponds to the –1 and +2 orders passing off ($\lambda/d = 2/3$) occurs just where these gratings have their

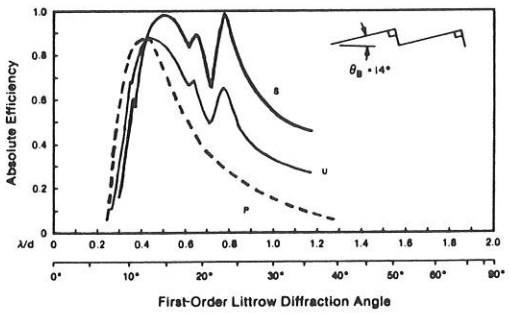

Figure IX-7. Same as Figure IX-5, except 14° blaze angle. The curve for unpolarized light (marked U) is also shown; it lies exactly halfway between the S and P curves.

peak efficiency, this anomaly ends up being severely suppressed (Figure IX-8). This property is quite well maintained over a large range of angular deviations (the angle between the incident and diffracted beams), namely up to 25°, but it depends on the grooves having an apex angle near 90°. The relatively low P-plane efficiency of this family of blazed gratings holds the 50% efficiency band from $0.7\lambda_B$ to $1.9\lambda_B$.

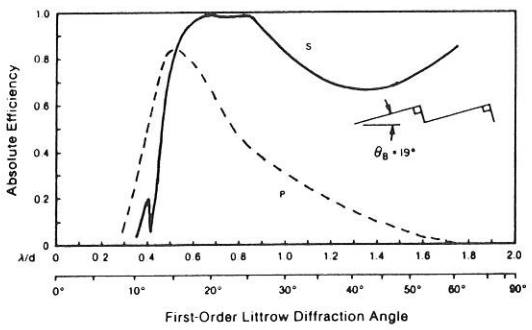

Figure IX-8. Same as Figure IX-5, except 19° blaze angle.

High blaze angle gratings ($22° \leq \theta < 38°$) are widely used, despite the presence of a very strong anomaly in their efficiency curves (Figure IX-9). For unpolarized light, the effect of this anomaly is greatly attenuated by its coincidence with the P-plane peak. An-

other method for reducing anomalies for such gratings is to use them at angular deviations above 45°, although this involves some

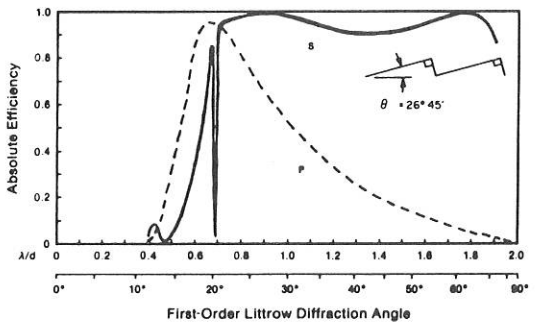

Figure IX-9. Same as Figure IX-5, except 26° 45' blaze angle.

sacrifice in efficiency and wavelength range. The 50% efficiency is theoretically attainable in the Littrow configuration from $0.6\lambda_B$ to $2\lambda_B$, but in practice the long-wavelength end corresponds to such an extreme angle of diffraction that instrumental difficulties arise.

Theoretically, all gratings have a second high-efficiency peak in the S-plane at angles corresponding to the complement of the blaze angle ($90° - \theta$); in practice, this peak is fully developed only on steeper groove-angle gratings, and then only when the steep face of the groove is not too badly deformed by the lateral plastic flow inherent in the diamond tool burnishing process. The strong polarization observed at all high angles of diffraction limits the useable efficiency in unpolarized light, but it makes such gratings very useful for tuning lasers, especially molecular lasers. The groove spacing may be chosen so that the lasing band corresponds to either the first or second of the S-plane high-efficiency plateaus. The latter will give at least twice the dispersion (in fact the maximum possible), as it is proportional to the tangent of the angle of diffraction under the Littrow conditions typical of laser tuning.

Very-high blaze angle gratings ($\theta \geq 38°$) are rarely used in the first order; their efficiency curves are interesting only because of the high P-plane values (Figure IX-10). In high orders they are often used in tuning dye lasers, where high dispersion is important

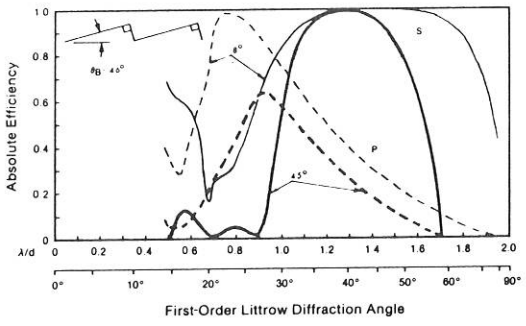

Figure IX-10. Same as Figure IX-5, except 46° blaze angle and 8° and 45° between the incident and diffracted beams (shown as light and heavy lines, respectively).

and where tuning through several orders can cover a wide spectral region with good efficiency. Efficiency curves for this family of gratings are shown for two configurations. With an angular deviation of 8°, the efficiency does not differ too much from Littrow; when this angle is 45°, the deep groove results in sharp reductions in efficiency. Some of the missing energy shows up in the zeroth order, but some of it can be absorbed by the grating.

Sinusoidal-groove gratings. A sinusoidal-groove grating can be obtained by the interferometric (holographic) recording techniques described in Chapter IV. Sinusoidal gratings have a somewhat different diffracted efficiency behavior than do triangular-groove gratings, and are treated separately.

It is convenient to consider five domains of sinusoidal-groove gratings, with progressively increasing modulation μ, where

$$\mu = h/d, \qquad (9\text{-}1)$$

h is the groove height and d is the groove spacing:

domain	*modulation*
very low	$\mu \leq 0.05$
low	$0.05 < \mu \leq 0.15$
medium	$0.15 < \mu \leq 0.25$
high	$0.25 < \mu \leq 0.4$
very high	$\mu > 0.4$

Very low modulation gratings ($\mu < 0.05$) operate in the scalar domain, where the theoretical efficiency peak for sinusoidal grooves is only 33.8% (Figure IX-11). This figure may be readily scaled, and specification is a simple matter as soon as it becomes clear that the peak wavelength always occurs at $\lambda_B = 3.4h = 3.4\mu d$. A blazed grating with an equivalent peak wavelength will require a groove depth 1.7 times greater.

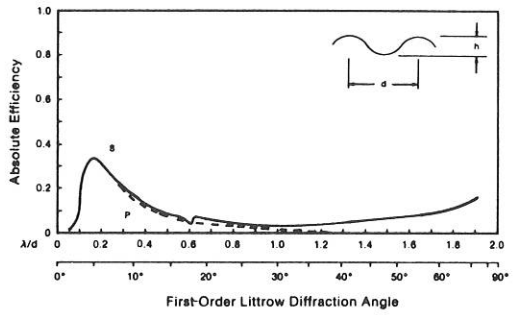

Figure IX-11. First-order theoretical efficiency curve: sinusoidal grating, $\mu = h/d = 0.05$ and Littrow mounting ($2K = 0$). Solid curve, S-plane; dashed curve, P-plane.

Low modulation gratings ($0.05 \leq \mu < 0.15$) are quite useful in that they have a low but rather flat efficiency over a λ/d band from 0.35 to 1.4 (Figure IX-12). This figure includes not only the infinite conductivity values shown on all previous ones, but includes the effects of finite conductivity by adding the curves for an 1800 g/mm aluminum surface. The most significant effect is in the behavior of the anomaly, which is the typical result of the finite conductivity of real metals.

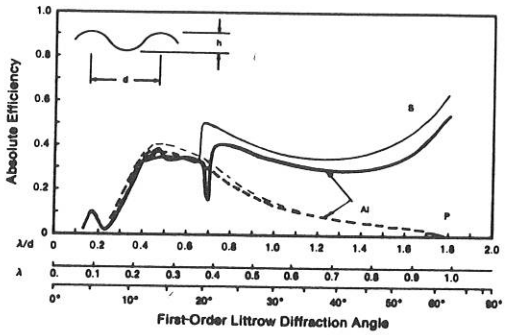

Figure IX-12. First-order theoretical efficiency curve: sinusoidal grating, aluminum coating, 1800 grooves per millimeter, $\mu = 0.14$ and Littrow mounting. Solid curves, S-plane; dashed curves, P-plane. For reference, the curves for a perfectly conducting surface are shown as well (light curves).

Figure IX-13 is a good example of a *medium modulation* grating ($0.15 \leq \mu < 0.25$). It demonstrates an important aspect of such sinusoidal gratings, namely that reasonable efficiency requirements confine first-order applications to values of $\lambda/d > 0.45$,

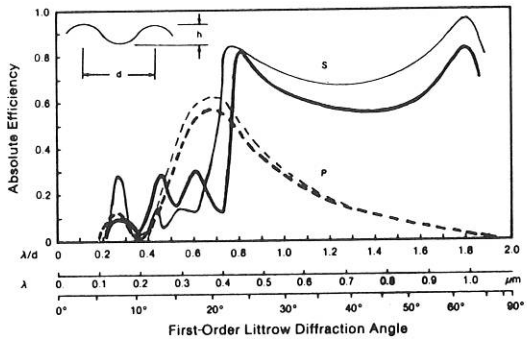

Figure IX-13. Same as Figure IX-12, except $\mu = 0.22$ and 8° between incident and diffracted beams ($2K = 8°$).

which eliminates them from systems with wide wavelength ranges. Over this restricted region, however, efficiencies are comparable to those of triangular grooves, including the high degree of polarization. This figure also

demonstrates how a departure from Littrow to an angular deviation of 8° splits the anomaly into two branches, corresponding to the new locations of the –1 and +2 order passing-off conditions.

High modulation gratings ($0.25 \leq \mu < 0.40$), such as shown in Figure IX-14, have the maximum useful first-order efficiencies of sinusoidal-groove gratings. Provided they are restricted to the domain in which higher orders diffract (*i.e.*, $\lambda/d > 0.65$), their efficiencies are very similar to those of triangular-groove gratings having similar groove depths (*i.e.*, $26° < \theta < 35°$).

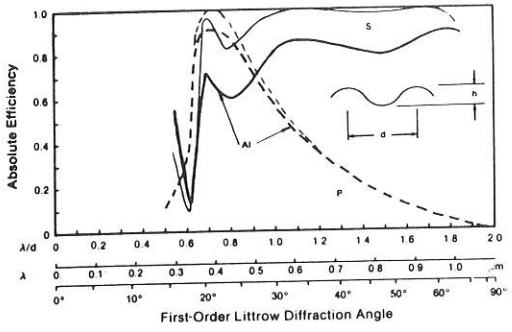

Figure IX-14. Same as Figure IX-12, except μ = 0.36.

Very-high modulation gratings ($\mu > 0.40$), in common with equivalent triangular-groove gratings, have little application in the first order due to their relatively low efficiencies except perhaps for grazing incidence applications.

The effects of finite conductivity. For metal-coated reflection gratings, the finite conductivity of the metal is of little importance for wavelengths of diffraction above 4 μm, but the complex nature of the dielectric constant and the index of refraction begin to effect efficiency behavior noticeably for wavelengths below 1 μm, and progressively more so as the wavelength decreases. In the P-plane, their effect is a simple reduction in efficiency, in direct proportion to the reflectance. In the S-plane, the effect is more complicated, especially for deeper grooves and shorter wavelengths.

Figure IX-15 shows the first-order efficiency curve for a widely-used grating: 1200 g/mm, triangular grooves, medium blaze angle (θ = 10°), coated with aluminum and used with an angular deviation of 8°. The finite conductivity of the metal cause a reduction in efficiency; also, severe modification of the anomaly is apparent. It is typical that the anomaly is broadened and shifted toward a longer wavelength with respect to the infinite conductivity curve. Even for an angular deviation as small as 8°, the single anomaly in the figure is separated into a double anomaly.

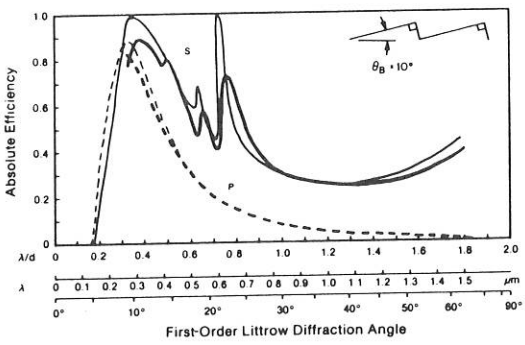

Figure IX-15. First-order theoretical efficiency curve: triangular-groove grating, aluminum coating, 1200 grooves per millimeter, 10° blaze angle and 2K = 8°. Solid curves, S-plane; dashed curves, P-plane. For reference, the curves for a perfectly conducting surface are shown as well (light curves).

For sinusoidal gratings, the situation is shown in Figures IX-12 and -14. Figure IX-13 is interesting in that it clearly shows a series of new anomalies that are traceable to the role of aluminum.

With scalar domain gratings (either $\theta < 5°$ or $\mu < 0.10$), the role of finite conductivity is simply to reduce the efficiency by the ratio of surface reflectance.

Distribution of Energy by Diffraction Order

Gratings are most often used in higher diffraction orders to extend the spectral range

of a single grating to shorter wavelengths than can be covered in lower orders. For blazed gratings, the second-order peak will be at one-half the wavelength of the nominal first-order peak, the third-order peak at one-third, *etc.* Since the ratio λ/d will be progressively smaller as $|m|$ increases, polarization effects will become less significant; anomalies are usually negligible in diffraction orders for which $|m| > 2$. Figure IX-16 and -17 show the second- and third-order heoretical Littrow efficiencies, respectively, for a blazed grating with $\theta = 26°45'$; they are plotted as a function of $m\lambda/d$ in order to demonstrate the proper angular ranges of use.

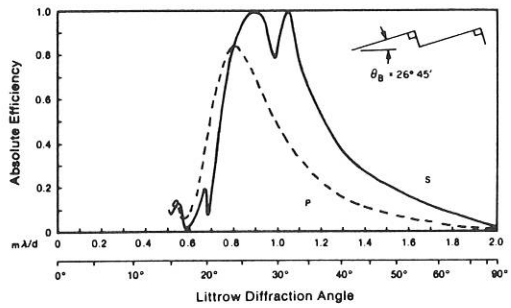

Figure IX-16. Second-order theoretical efficiency curve: 26° 45′ blaze angle and Littrow mounting. Solid curve, S-plane; dashed curve, P-plane.

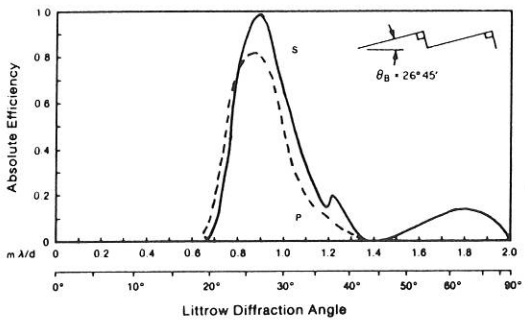

Figure IX-17. Same as Figure IX-16, except third order.

These curves should be compared with Figure IX-9 for corresponding first-order behavior.

For gratings with sinusoidally shaped grooves, higher orders can also be used, but if efficiency is important, the choice is likely to be a finer pitch first-order grating instead. When groove modulations are very low (so that the grating is used in the scalar domain), the second-order efficiency curve looks similar to Figure IX-18, except that the theoretical peak value is about 23% (instead of 33.8%) and occurs at a wavelength 0.6 times that of the first-order peak, which corresponds to $2.05h$ (instead of $3.41h$), where h

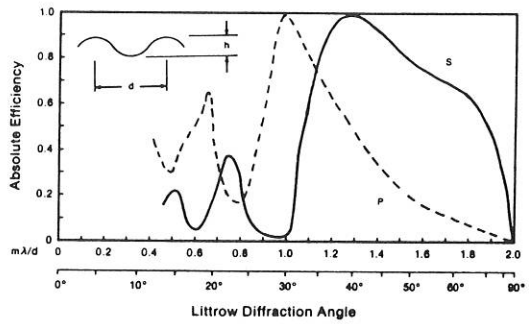

Figure IX-18. Second-order theoretical efficiency curve: sinusoidal grating, $\mu = 0.36$ and Littrow mounting. Solid curve, S-plane; dashed curve, P-plane.

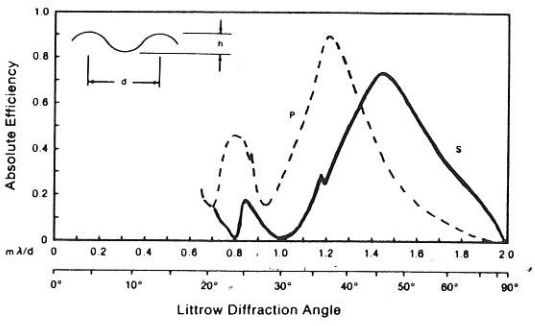

Figure IX-19. Same as Figure IX-18, except third order.

is the groove depth. Successive higher-order curves for gratings with sinusoidal grooves are not only closer together, but drop off more sharply with order than for gratings with triangular grooves. For sufficiently deeply modulated sinusoidal grooves, the second order can often be used effectively, though (as Figure IX-18 shows) polarization effects are relatively strong. The corresponding third-order theoretical curve is shown in Figure IX-19.

Useful Wavelength Range

A grating is of little use if high-grade imaging is not accompanied by sufficient diffraction efficiency. The laws governing diffracted efficiency are quite complicated, but a very rough rule of thumb can be used to estimate the useful range of wavelengths available on either side of the blaze (peak) wavelength for triangular-groove gratings.

For coarse gratings (for which $d \geq 2\lambda$), in the first diffraction order the efficiency is roughly half its maximum (which is at λ_B) at $2\lambda_B/3$ and $3\lambda_B/2$. Curves of similar shape are obtained in the second and third orders, but the efficiencies are typically 20% less everywhere, as compared with the first order.

Grating of fine pitch ($d \approx \lambda$) have a somewhat lower peak efficiency than do coarse gratings, though the useful wavelength range is greater.

Blazing of Ruled Transmission Gratings

Because they have no metallic overcoating, triangular-groove transmission gratings display far simpler efficiency characteristics than do their ruled counterparts. In particular, transmission gratings have efficiency curves almost completely free of polarization effects.

The peak wavelength generally occurs when the direction of refraction of the incident beam through a groove (thought of as a small prism) equals the direction dictated by the grating equation. [This is in direct analogy with the model of reflection grating blazing in which the grooves are thought of as small mirrors.] Due to the index of refraction of the grating, though, the groove angle exceeds the blaze angle for a transmission grating.

Blazing of Interference Reflection Gratings

A useful technique for rendering sinusoidal groove profiles more nearly triangular (thus enhancing their efficiency) is *ion etching*. By bombarding a surface with energetic ions, the material can be removed (etched) by an amount per unit time dependent on the angle between the beam and the local surface normal. The etching of a sinusoidal profile by an ion beam provides a continuously-varying angle between the ion beam and the surface normal, which preferentially removes material at some parts of the profile while leaving other parts hardly etched. The surface evolves toward a triangular groove profile as the ions bombard it.

Overcoating of Reflection Gratings

All standard reflection gratings are furnished with an aluminum (Al) reflecting surface. While no other metal has more general application, there are a number of special situations where alternative surfaces or coatings are recommended.

The metallic coating on a reflection grating is evaporated onto the blank. This produces a surface whose reflectivity is higher than that of the same metal electroplated onto the grating surface. The thickness of the metallic layer is chosen to enhance the diffraction efficiency throughout the spectral region of interest.

The reflectivity of aluminum drops rather sharply for wavelengths below 170 nm. While freshly deposited, fast-fired pure aluminum in high vacuum maintains its reflectivity to wavelengths shorter than 100 nm, the thin layer of oxide normally present absorbs wavelengths below about 170 nm.

Fortunately, a method developed in the late 1950s makes it possible to preserve the reflectivity of aluminum to shorter wavelengths. The process involves overcoating the grating with a thin layer of fast-fired aluminum, which is followed immediately by a coating of magnesium fluoride (MgF_2)

approximately 25 nm thick; the grating is kept at room temperature for both coatings. The main purpose of the MgF_2 coating is to protect the aluminum from oxidation. The advantage of this coating is especially marked in the region between 120 and 170 nm. While reflectivity drops off sharply below this region, it remains higher than that of gold and comparable to that of platinum, the most commonly used alternative materials, down to 70 nm.

On an experimental basis, the use of lithium fluoride (LiF) instead of MgF_2 has proved effective in maintaining relatively high reflectivity in the 100 to 110 nm region. Unfortunately, a LiF film deteriorates unless maintained in a low humidity environment, which has curtailed practical exploitations, though it can be protected by a very thin layer of MgF_2.

Gratings coated with gold (Au) and platinum (Pt) have been used for some time. Gold gratings have the great advantage that they can be replicated directly from either gold or aluminum master gratings, and are therefore most likely to maintain their groove profiles.

Overcoating gratings so that their surfaces are coated with two layers of different metals sometimes leads to a change in diffraction efficiency over time. HUNTER *et al.* [1972] have found the cause of this change to be intermetallic diffusion. For example, they measured a drastic decrease (over time) in efficiency at 122 nm for gratings coated in Au and then overcoated in Al + MgF_2; this decrease was attributed to the formation of intermetallic compounds, primarily $AuAl_2$ and Au_2Al. Placing a suitable dielectric layer such as SiO between the two metallic layers prevents this diffusion.

As mentioned elsewhere, fingerprints are a danger to aluminized optics. It is possible to overcoat such optics, both gratings and mirrors, with dielectrics like MgF_2, to prevent finger acids from attacking the aluminum. These MgF_2 coatings cannot be baked, as is customary for glass optics, and therefore must not be cleaned with water. Spectrographic-grade organic solvents are the only recommended cleaning agents, and they should be used sparingly and with care.

Multilayer dielectric overcoatings, which are so useful in enhancing plane mirror surfaces, are of little value on a typical diffraction grating used in the visible and infrared spectra, as these coatings lead to complex guided wave effects that are rarely useful. For wavelengths below 30 nm, though, in which grazing angles of incidence and diffraction are common, multilayer coatings can enhance efficiency considerably [RIFE *et al.* 1989].

TESTING AND CHARACTERIZATION OF GRATINGS X

SPECTRAL DEFECTS

It is fundamental to the nature of diffraction gratings that errors are relatively easy to measure, although not all attributes are equally detectable or sometimes even definable.

For example, an optically clean grating, *i.e.*, one with low background in the form of scatter or satellites, can be simply tested for Rowland ghosts on an optical bench. With a mercury lamp or a laser source, and a scanning slit connected to a detector and recorder, a ghost having intensity 0.002% of the intensity of the main line can be readily located. The periodic error in the groove spacing giving rise to such a ghost may be less than one nanometer, a mechanical precision seldom achieved with man-made machines.

Grating ghosts are measured at the Richardson Grating Laboratory by making the grating part of a scanning spectrometer and illuminating it with monochromatic light, such as that from a mercury isotope lamp (isotope 198 or 202) or a helium-neon laser. On scanning both sides of the parent line, using a chart recorder and calibrated attenuators, it is easy to identify all ghost lines and to measure their intensities relative to the parent line. The importance of ghosts in grating applications varies considerably. In most spectrophotometers, and in work with low-intensity sources, ghosts play a negligible role. In Raman spectroscopy, however, even the weakest ghost may appear to be a Raman line, especially when investigating solid samples, and hence these ghosts must be suppressed to truly negligible values.

Ghosts are usually classified as Rowland ghosts and Lyman ghosts. Another grating deficiency is the presence of satellites; if excessive, satellites lying within a line contour may reduce the attainable resolution, and hence are of great concern in high resolution spectroscopy. Satellites should be at a minimum for Raman spectroscopy.

Rowland Ghosts. Rowland ghosts are spurious lines seen in some grating spectra that result from periodic errors in the spacing of the grooves. These lines are usually located symmetrically with respect to each strong spectral line at a spectral distance from it which depends on the period of the error, and with an intensity which depends on the amplitude of this error.

If the curve of groove spacing error *vs.* position is not simply sinusoidal, there will be a number of ghosts on each side of the parent line representing the various orders from each of the harmonics of the error curve. On engines with mechanical drives, Rowland ghosts are associated primarily with errors in the lead or pitch of the precision screw, or with the bearings that hold the screw in place. As a consequence, their location depends upon the number of grooves ruled for each complete turn of the screw. For example, if the ruling engine has a pitch of 2 mm, and a ruling is made at 1200 grooves/mm, 2400 grooves will be ruled per turn of the screw, and the ghosts in the first order can be expected to lie at $\Delta\lambda = \pm \lambda/2400$ from the parent line λ, with additional ghosts located at integral multiples of $\Delta\lambda$. In gratings ruled on engines with interferometric feedback correction mechanisms, Rowland ghosts are usually much less intense, but they can arise from the mechanisms used in the correction system if care is not taken to prevent their occurrence.

If the character of the periodic errors in a ruling engine were simply harmonic, which is rarely true in practice, the ratio of the diffracted intensities of the first order Rowland ghost ($I_{RG\ (m\,=\,1)}$) to that of the parent line (I_{PL}) is

$$\frac{I_{RG\ (m\,=\,1)}}{I_{PL}} = 4\left(\frac{\pi A \sin\alpha}{\lambda}\right)^2, \qquad (10\text{-}1)$$

where A is the peak simple harmonic error amplitude, α is the angle of incidence, and λ is the diffracted wavelength. The second-

order Rowland ghost will be much less intense:

$$\frac{I_{RG\,(m=2)}}{I_{PL}} = 4\left(\frac{\pi A \sin\alpha}{\lambda}\right)^4. \qquad (10\text{-}2)$$

Higher-order Rowland ghosts would be virtually invisible. The ghost intensity is independent of the diffraction order m of the parent line, and of the groove spacing d. In the Littrow configuration, Eq. (10-1) becomes

$$\frac{I_{RG\,(m=1)}}{I_{PL}} = \left(\frac{\pi m A}{d}\right)^2, \quad \text{in Littrow,} \qquad (10\text{-}3)$$

an expression derived in 1893 by Rowland.

These simple mathematical formulæ do not always apply in practice when describing higher-order ghost intensities, since the harmonic content of actual error curves gives rise to complex amplitudes that must be added vectorially and then squared to obtain intensity functions. A fortunate result of this is that ghost intensities are generally smaller than those predicted from the peak error amplitude.

The order of magnitude of the fundamental harmonic error amplitude can be derived from Eq. (10-1) [or Eq. (10-3)]. For example, a 1200 g/mm grating used in the $m = 1$ order in Littrow will show a 0.14% first-order ghost intensity, compared with the parent line, for a fundamental harmonic error amplitude of 10 nm. For some applications this intensity is unacceptably high, which illustrates the importance of making a concerted effort to minimize periodic errors of ruling. For Raman gratings and echelles, the amplitude of the periodic error must not exceed one nanometer; the fact that this has been accomplished is a remarkable achievement.

Lyman Ghosts. Ghost lines observed at large spectral distances from their parent lines are called Lyman ghosts. They result from compounded periodic errors in the spacing of the grating grooves. Lyman ghosts differ from Rowland ghosts in that each period of Lyman ghosts contains relatively few grooves. Lyman ghosts can be said to be in fractional-order positions. Thus, if every other groove is misplaced so that the period contains just two grooves, ghosts are seen in the half-order positions. The number of grooves per period determines the fractional-order position of Lyman ghosts. Usually it is possible to find the origin of the error in the ruling engine once its periodicity is determined. It is important that Lyman ghosts be kept to a minimum, because they are not nearly as easy to identify as Rowland ghosts.

Satellites. Satellites are false spectral lines usually occurring very close to the parent line. Individual gratings vary greatly in the number and intensity of satellites which they produce. In a poor grating, they give rise to much scattered light, referred to as *grass* (so called since this low intensity scattered light appears like a strip of lawn when viewed with green mercury light). Satellites are absent in a "clean" grating. In contrast to Rowland ghosts, which usually arise from errors extending over large areas of the grating, each satellite usually originates from a small number of randomly misplaced grooves in a localized part of the grating. With laser illumination a relative background intensity of 10^{-7} is easily observable with the eye.

Efficiency Measurement

In our laboratory, grating efficiency measurements are performed with a double monochromator system. The first monochromator supplies monochromatic light derived from a tungsten lamp, mercury arc or deuterium lamp, depending on the spectral region involved. The grating being tested serves as the dispersing element in the second monochromator. In the normal mode of operation, the output is compared with that from a high grade mirror coated with the same material as the grating. The efficiency of the grating relative to that of the mirror is reported (relative efficiency), although absolute efficiency values can also be obtained (either by direct measurement or through knowledge of the variation of mirror reflectivity with wavelength). For plane reflection gratings, the wavelength region covered is usually 190 nm to 2.50 μm; gratings blazed farther into the infrared are measured in higher orders. Concave reflection gratings focus as well as disperse the light, so the entrance and exit slits of the second monochromator are placed at the positions for which the grating was designed (that is, concave grating efficiencies are measured in the

geometry in which the gratings are to be used). Transmission gratings are tested on the same equipment, with values given as the ratio of diffracted light to light falling directly on the detector, (*i.e.*, absolute efficiency).

A vacuum ultraviolet monochromator is available for testing plane and concave gratings, as well as mirrors, from 58.4 to 250 nm, for absolute and relative efficiency.

Curves of efficiency *vs.* wavelength for plane gratings are made routinely on all new master gratings, both plane and concave, with light polarized in the S and P planes to assess the presence and amplitudes (if any) of anomalies. Such curves are furnished on request.

Foucault Knife-edge Test

One of the most critical tests an optical system can undergo is the Foucault knife-edge test. This test not only reveals a great deal about wavefront deficiencies but also locates specific areas (or zones) where they originate. The test is suited equally well to plane and concave gratings (for the former, the use of very high grade collimating optics is required). The sensitivity of the test depends on the radius of the concave grating (or the focal length of the collimating system), and may easily exceed that of interferometric testing, although the latter is more quantitative.

By setting on ghost wavelengths, it is easy to see from which areas of the grating they originate. Errors of run, which are progressive changes in the groove spacing across the surface of the grating, are quite apparent to the practiced observer. This is also true of fanning error, which results when the groove spacing at the top of the grating differs from that at the bottom (resulting in a fan-shaped groove pattern). The sharper its knife-edge cutoff, the more likely that a grating will yield high resolution.

The Foucault test is a sensitive and powerful tool, but experience is required to interpret each effect that it makes evident. All Grating Laboratory master plane gratings, large plane replicas and large-radius concave gratings are checked by this method.

Direct Wavefront Testing

Any departure from perfect flatness of a plane grating, or perfect sphericity of a concave grating, as well as variations in the groove spacing, depth or parallelism, will result in a diffracted wavefront which is less than perfect. According to the Rayleigh criterion, resolution is lost whenever the deficiency exceeds $\lambda/4$, where λ is the wavelength of the light used in the test. To obtain an understanding of the magnitudes involved, it is necessary to consider the angle at which the grating is used. For simplicity, consider this to be the blaze angle, under Littrow conditions. Any surface figure error of height h will cause a wavefront deformation of $2h\cos\theta$, which decreases with increasing $|\theta|$. On the other hand, a groove position error p introduces a wavefront error of $2p\sin\theta$, which explains why ruling parameters are more critical for gratings used in high-angle configurations.

A plane grating may produce a slightly cylindrical wavefront if the groove spacing changes linearly, or if the surface figure is similarly deformed. In this special case, resolution is maintained, but focal distance will vary with wavelength.

Wavefront testing can be done conveniently by mounting a grating at its autocollimating angle (Littrow) in a Twyman-Green interferometer. Few such instruments exist that combine sufficiently high quality with large aperture. The Richardson Grating Laboratory instrument has an aperture of 150 mm (6 inch). With coherent laser light sources, however, it is possible to make the same measurements with a much simpler Fizeau interferometer, equipped with computer fringe analysis.

Periodic errors show up as zig-zag fringe displacements. A sudden change in groove position gives rise to a step in the fringe pattern; in the spectrum, this is likely to appear as a satellite. Curved fringes due to progressive ruling error can be distinguished from figure problems by observing fringes obtained in zero, first and higher orders. Fanning error (non-parallel grooves) will cause spreading fringes.

Experience has shown that the sensitivity of standard interferograms for grating deficiencies equals or exceeds that of other plane grating testing methods only for gratings

used at high angles. This is why the interferometric test is especially appropriate for the testing of echelles and other gratings used in high diffraction orders.

SCATTERED LIGHT

As discussed in chapter II, the composite of misplaced spectral energy is called *stray light* or *scattered light. Near scatter* is usually due to large numbers of satellites and ghosts; *far scatter* is due to every kind of groove position error as well as geometrical deficiencies such as the smoothness of the grooves and the edge effects at each groove. Such deficiencies show up more at shorter wavelengths as mechanical imperfections become large relative to the wavelength.

The practical importance of stray light depends on the specific application of the grating. In some cases, filters (or their equivalent in the form of narrow range detectors) can play an important role in suppressing the effects of stray light. Another method is to use double monochromators or crossed dispersion.

Measurement methods used to determine far scatter depend on filters to mask parts of the spectrum. Ratios of radiometric readings made with and without the filters serve as a measure of scattered light. The approach, while functional, is arbitrary, with results affected by the diffraction efficiency of the grating, the spectrometric system used, the light source, and the spectral response of the detecting system. Definition and subsequent measurement of far scatter is an active field of research.

The Richardson Grating Laboratory has a special apparatus to examine light scattered by small regions on the surface of a mirror or grating. This "scatter checker" provides several degrees of freedom, so that light scattered by a grating between diffraction orders can be attributed to areas on its surface. The scatter checker can also illuminate the entire grating, so that total grating stray light can be measured.

SELECTION OF DISPERSING SYSTEMS XI

Reflection Grating Systems

Reflection grating systems are much more common than transmission grating systems. Optical systems can be 'folded' with reflection gratings, which reflect as well as disperse, whereas transmission grating systems are 'in-line' and therefore usually of greater length. Moreover, reflection gratings are not limited by the transmission properties of the grating substrate (or resin), and can operate at much higher angles of diffraction.

Plane reflection grating systems. The choice of existing plane reflection gratings is extensive and continually increasing. Sizes as large as 12 x 16 inches (about 300 x 400 mm) have been ruled. For infrared spectra, plane reflection gratings are most suitable because of the availability of large gratings. While plane gratings have been used for visible and ultraviolet spectra for some time, they are also used increasingly for wavelengths as short as 110 nm, an extension made possible by special overcoatings that give satisfactory reflectivity even at such short wavelengths (see chapter IX).

The most popular arrangement for plane reflection gratings is the Czerny-Turner mount, which uses two spherical concave mirrors between the grating and the entrance and exit slits. A single mirror arrangement (the Ebert-Fastie mount) can also be used. Both achieve spectral scanning through rotation of the grating. Collimating lenses are rarely used, since mirrors are inherently achromatic.

For special purposes, plane reflection gratings can be made on unusual materials, such as ceramics or metals, given special shapes, or supplied with holes for Cassegrain and Coudé-type telescopic systems.

Concave reflection grating systems. The great advantage in using concave gratings lies in the fact that separate collimating optics are unnecessary. This is particularly important in the far vacuum ultraviolet region of the spectrum, for which there are no good reflectors. Two mirrors, each reflecting 20%, will reduce throughput by a factor of twenty-five. Hence, concave systems dominate the entire ultraviolet region, and at wavelengths less than 110 nm are used exclusively. Their chief deficiency lies in astigmatism, which limits the exit slit size (and, consequently, the energy throughput). The situation can be improved by using toroidal grating blanks; however, their use is restricted because of high costs.

Though most ruled gratings are flat, curved substrates can be ruled as well if their curvatures are not extreme (*c.* *f*/9 or greater). Concave gratings are not only more difficult to rule than plane gratings, since the tool must swing through an arc as it crosses the blank, but they require extremely tight control over the sphericity to the blank as well. Since each radius of curvature is a new parameter, there cannot be the large selection of rulings (in size and blaze angle) for any one given radius that there is with plane gratings.

Another limitation of ruled concave gratings appears when they are ruled at shallow groove angles. The ruled width is unfortunately limited by the radius of the blank, since the diamond cannot rule useful grooves when the slope angle of the blank exceeds the blaze angle. The automatic energy limitation that is thereby imposed can be overcome by ruling multipartite gratings, a Richardson Grating Laboratory development. Here the ruling is interrupted once or twice, so the tool can be reset at a different angle. The resulting bipartite or tripartite gratings are very useful, as available energy is otherwise low in the short wavelength regions. One must not expect such gratings to have a resolving power in excess of that of any single section, for such an achievement would require phase matching to a degree that is beyond the present state of the art.

The advent of the interference (holographic) method of generating gratings has made the manufacture of concave gratings commonplace. Since the fringe

pattern formed during the recording process is three-dimensional, a curved blank placed in this pattern will record fringes. Unlike ruled gratings, concave interference gratings can be generated on blanks whose radii are smaller than 100 mm.

Transmission Grating Systems

In certain types of instrumentation, transmission gratings are much more convenient to use than reflection gratings. The most common configuration involves converting cameras into simple spectrographs by inserting a grating in front of the lens. These are used particularly for studying the composition of falling meteors or the re-entry of space vehicles, where the distant luminous streak becomes the entrance slit. Another application where high-speed lenses and transmission gratings can be combined advantageously is in the determination of spectral sensitivity of photographic emulsions.

Transmission gratings can be made by stripping the aluminum film from the surface of a reflection grating. However, since the blank is now part of the imaging optics, special blanks are used, made to tighter specifications for parallelism, and those used in the visible region are given a magnesium fluoride (MgF_2) antireflection coating on the back to reduce light loss and internal reflections.

In most cases, relatively coarse gratings are preferred, although gratings up to 600 g/mm are furnished routinely. Experimentally, transmission gratings of 1200 g/mm have been used. Energy distribution on either side of the blaze peak is very similar to that of reflection gratings in the scalar domain. For wavelengths between 220 and 300 nm, transmission gratings are made on fused silica blanks with a special resin capable of high transmission for these wavelengths.

Since transmission gratings do not have a delicate metal film they are much more readily cleaned. However, they are limited to spectral regions where blanks and resins transmit, but their main drawback is that they do not fold the optical path conveniently as a reflection grating does. Moreover, to avoid total internal reflection, their diffraction angles cannot be extreme. Even though the blank surface is antireflection coated, internal reflections from the grating-air interface leads to some back reflection in several orders; this limits the maximum efficiency to 85% or less.

Grating Prisms (Grisms)

For certain applications, such as a direct vision spectroscope, it is very useful to have a dispersing element that will provide in-line viewing for one wavelength. This can be done by replicating a transmission grating onto the hypotenuse face of a right-angle prism. The light diffracted by the grating is bent back in-line by the refracting effect of the prism. The device is commonly called a *Carpenter prism* or *grism.*

The derivation of the formula for computing the required prism angle follows (refer to Figure XI-1). On introducing Snell's law, the grating equation becomes

$$m\lambda = d\,(n \sin\alpha + n' \sin\beta), \qquad (11\text{-}1)$$

where n and n' are the refractive indices of glass and air, respectively, and $\beta < 0$ since the diffracted ray lies on the opposite side of the normal from the incident rays ($\alpha > 0$).

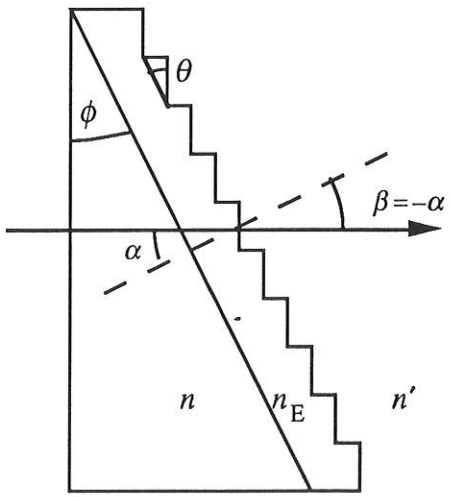

Figure XI-1. Grating prism (grism). Ray path for straight-through operation at one wavelength.

Taking $n' = 1$ for air, and setting $\alpha = -\beta = \phi$, the prism angle, Eq. (10-1) becomes

$$m\lambda = d\,(n-1)\,\sin\phi\,. \qquad (11\text{-}2)$$

In this derivation it is assumed that the refractive index n of the glass is the same (or very nearly the same) as the index n_E of the epoxy resin at the straight-through wavelength λ. While this is not likely to be true, the resulting error is often quite small.

The dispersion of a grating prism cannot be linear, owing to the fact that the dispersive effects of the prism are superimposed on those of the grating. The following steps are useful in designing a grism:

1. Select the prism material desired (*e.g.*, BK-7 glass for visible light or fused silica for ultraviolet light).
2. Obtain the index of refraction of the prism material for the straight-through wavelength.
3. Select the grating constant d for the appropriate dispersion desired.
4. Determine the prism angle ϕ from Eq. (11-2).
5. For maximum efficiency in the straight-through direction, select the grating from the catalogue with groove angle θ closest to ϕ.

Grazing Incidence Systems

For work in the x-ray region (1 to 25 nm), the need for high dispersion and the normally low reflectivity of materials both demand that concave gratings be used at grazing incidence (*i.e.*, $|\alpha| > 80°$, measured from the grating normal). Groove spacings of 600 to 1200 per millimeter are very effective, but exceptional groove smoothness is required on these rulings to achieve good results.

Echelles

A need has long existed for spectroscopic devices that give higher resolution and dispersion than ordinary gratings, but with a greater free spectral range than a Fabry-Perot étalon or a reflection echelon. This gap is admirably filled by the echelle grating, first suggested by Harrison. Physically, an echelle can be thought of as lying halfway between a grating and a reflection echelon. The echelon is so difficult to make, and has such a low free spectral range, that it is now little more than a textbook curiosity. Echelles, on the other hand, are becoming ever more popular tools as large high quality rulings become available. In particular, they lead to compact instruments with high reciprocal dispersion and high throughput.

Echelles are a special class of high-angle gratings, rarely used in orders below $|m| = 5$, and sometimes used in orders beyond 100. Because of order overlap, some type of filtering is normally required with higher-order grating systems. This can take several forms, such as cutoff filters, detectors insensitive to longer wavelengths, or cross-dispersion in the form of prisms or low-dispersion gratings. The latter approach leads to a square display format suitable for corresponding types of array detectors. In the case of dye laser tuning, the filtering is performed effectively by the choice of dyes.

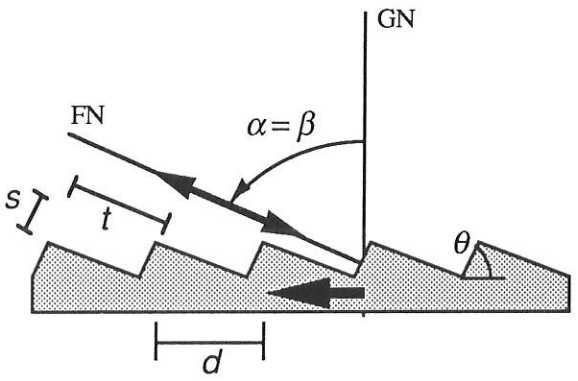

Figure XI-2. Echelle geometry. The groove spacing d, step width t and step height s are shown. GN is the grating normal and FN is the facet normal. The blaze arrow (shown) points from GN to FN.

As seen in Fig XI-2, an echelle looks like a coarse grating used at such a high angle (typically 63° from the normal) that the steep side of the groove becomes the optically active facet. Typical echelle groove spacings

are 31.6, 79 and 316 g/mm, all blazed at 63°26' (although 76° is available for greater dispersion). With these grating, resolving powers greater than 1 000 000 for near-UV wavelengths can be obtained, using an echelle 10 inches wide. Correspondingly high values can be obtained throughout the visible spectrum and to 20 μm in the infrared. Since echelles always operate close to the Littrow mode, the grating equation becomes

$$m\lambda = 2d \sin\beta = 2d \sin\theta = 2t, \qquad (11\text{-}3)$$

where β is the angle of diffraction, θ the groove (blaze) angle, and t is the width of one echelle step (see Fig XI-2).

The free spectral range is

$$F_\lambda = \lambda/m. \qquad (2\text{-}23)$$

From Figure XI-2, $m = 2t/\lambda$, so

$$F_\lambda = \lambda^2/2t; \qquad (11\text{-}4)$$

for an echelle used in Littrow. In terms of wavenumbers, the free spectral range is

$$F_\sigma = \Delta\lambda/\lambda^2 = 1/2t. \qquad (11\text{-}5)$$

The linear dispersion of the spectrum is, from Eq. (2-12),

$$r' \frac{d\beta}{d\lambda} = \frac{m\, r'}{d \cos\beta} = \frac{m\, r'}{s} = \frac{r'}{s}\left(\frac{2t}{\lambda}\right), \qquad (11\text{-}6)$$

where $s = d \cos\beta$ is the step height of the echelle groove (see Fig. XI-2). The useful length l of spectrum between two consecutive diffraction orders is equal to the product of the linear dispersion and the free spectral range:

$$l = r'\lambda/s. \qquad (11\text{-}7)$$

For example, consider a 300 g/mm echelle with a step height $s = 6.5$ μm, combined with an $r' =$ 1.0 meter focal length mirror, working at a wavelength of 500 nm. The useful length of one free spectral range of the spectrum is 77 mm.

Typically, the spectral efficiency reaches a peak in the center of each free spectral range, and drops to about half of this value at the ends of the range. An echelle remains blazed for all wavelengths in the free spectral range (for a given diffraction order).

The steep angles and the correspondingly high orders at which echelles are used makes their ruling much more difficult than ordinary gratings. Periodic errors of ruling must especially be limited to a few nanometers or even less, which is attainable only by using interferometric control of the ruling engine. The task is made even more difficult by the fact that the coarse, deep grooves require heavy loads on the diamond tool. Only ruling engines of exceptional rigidity can hope to rule echelles. This also explains why the problems escalate as the groove spacing increases.

Echelles are often referred to by their "R numbers". This number is the tangent of the blaze angle θ:

$$R\ number = \tan\theta = t/s \qquad (11\text{-}8)$$

(see Figure XI-2). An R2 echelle, for example, has a blaze angle of 63°.

GRATINGS FOR SPECIAL PURPOSES XII

Astronomical Gratings

Large gratings for astronomical purposes were formerly available only by ruling two adjacent sections. In 1972, the 'B' engine was modified to rule larger areas with a single diamond, and since then it has produced echelles and large gratings up to 308 mm x 408 mm in size. Even larger gratings can be achieved by high accuracy multiple replication onto a single blank.

Filter Gratings

It is frequently desirable to use diffraction gratings as reflectance filters when working in the far infrared, in order to remove the unwanted second- and higher- diffraction orders from the light. For this purpose, small plane gratings are used that are blazed for the wavelength of the unwanted shorter-wavelength radiation. The grating acts as a mirror, reflecting the desired light into the instrument while diffracting shorter wavelengths out of the beam.

Gratings for Electron Microscope Calibration

It is possible to make shadow-cast replicas from replica gratings that can be very useful for calibrating the magnification of electron microscopes. These are replica gratings made from lightly ruled master gratings so that a space is left between the grooves. Besides offering this type of grating with a variety of spacings, the Richardson Grating Laboratory can also rule gratings with two sets of grooves at right angles (*cross-rulings*), which forms a grid that will show distortion of the field in the electron microscope. Groove frequencies as high as 10 000 grooves per millimeter have been produced experimentally.

Gratings for Laser Tuning

External-cavity semiconductor diode lasers are often used for their single-mode operation and spectral tunability. Plane reflection gratings can be used in the Littrow configuration to tune the lasing wavelength, as shown in Fig. XII-1, or in the grazing-incidence mount. In some systems a telescope is used to expand the laser beam to fill the grating, which is necessary for high resolution. A set of prisms, though, can do the same job more simply. Grazing-incidence tuning with one grating associated with a mirror or a second grating can also be used to tune dye lasers.

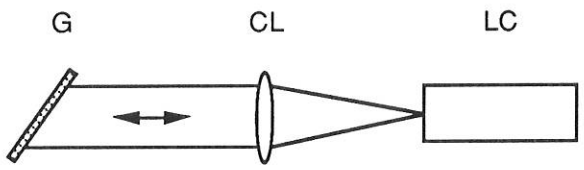

Figure XII-1. Littrow tuning of a dye laser. Light from the laser cavity [LC] diverges toward the collimating lens [CL], which directs it toward the grating [G], which is oriented so that light of the power wavelength is redirected back toward the lens, which focuses it into the laser cavity.

Molecular lasers, operating in either a pulsed or continuous-wave (cw) mode, have their output wavelength tuned by Littrow-mounted gratings. High efficiency is obtained by using the first diffraction order at diffraction angles $|\beta| > 20°$. The output is polarized in the S-plane, since the efficiency in the P plane is quite low.

Some molecular lasers operate at powers high enough to destroy gratings. For pulsed laser tuning, extra-thick replica films may help, but at maximum power only master gratings survive. Due to their far greater thermal conductivity, replica gratings on metal blanks are superior to glass for cw laser applications; in some cases, the grating

blanks must be water-cooled to prevent failure.

Gratings as Beam Dividers

Gratings ruled with symmetrical V-shaped grooves, as well as laminar transmission gratings, are capable of being used as beam dividers in conjunction with Moiré fringe applications or interferometers. A diffraction grating used as a beam divider provides higher efficiencies when its groove profile is rectangular, whereas a grating used for spectroscopic purposes should have a sinusoidal or triangular groove profile.

Space-borne Spectrometry

Neither master nor replica blanks suffer in any measurable way over extended periods of time in a space environment. The advantage of replicas lies not only in their greater availability and lower cost, but in making possible the provision of exact duplicates whenever needed.

Since most space work involves the study of ultraviolet (UV) and extreme ultraviolet (XUV) wavelengths, special problems exist in setting and aligning the optics. For this purpose the Grating Laboratory can rule gratings matching the XUV grating but with a groove spacing modified so that the mercury 546.1-nm line lies in the spectrum just where the main wavelength under study will lie. Another possibility is to rule a small section on the main grating with similar coarse spacings and then mask off this area when the alignment is complete. Sometimes special tolerances on blank radii are required for complete interchangeability.

Special Gratings

Usually some of the standard gratings offered in the latest *Grating Catalog* will satisfy a customer's requirements for groove spacing and blaze angle.

Blank size. Grating size is usually dictated by the light throughput desired (and, in the case of concave gratings, imaging and instrument size limitations as well). Should none of the standard blank sizes listed in the *Catalog* be suitable to match an instrument design, these same gratings can be supplied on special size blanks. Special elongated blank shapes are available for echelles and laser tuning gratings.

Blank material. The standard material for small and medium-sized grating blanks is specially annealed boro-silicate crown glass (BK-7). Low-expansion material, such as Zero-Dur® or fused silica, can be supplied upon request. For large gratings (approximately 135 x 265 mm or larger), low-expansion material is standard; BK-7 can be requested as well. For certain applications, it is possible to furnish metal substrates (*e.g.*, copper or aluminum) that are good heat sinks.

Blank coatings. While evaporated aluminum is the standard coating for reflection gratings, fast-fired aluminum with overcoatings of magnesium fluoride (MgF_2) can be used to enhance efficiency in the spectrum between 120 and 160 nm. For the extreme ultraviolet (below 50 nm), gold replica gratings are recommended, while platinum is recommended for 80–110 nm. Gold replicas also have higher reflectivity in most regions of the infrared spectrum.

ADVICE TO GRATING USERS XIII

Choosing a Specific Grating

If a diffraction grating is to be used only to disperse light (rather than provide focusing as well), then choosing the proper grating is often a simple matter involving the specification of the blaze angle and groove spacing. In other instances, the problem is one of deciding on the spectrometric system itself. The main parameters that must be specified are

Spectral region (wavelength range)
Speed (focal ratio) or throughput
Resolution or resolving power
Dispersion
Free spectral range
Output optics
Size limitations

To these should be added the question of whether an innovative design is required.

The spectral region will usually dictate the choice of plane *vs.* concave design, as well as the coating (if the grating is reflecting). Imaging (or spectral resolution) requirements and dispersion are also of primary importance. The size and weight of the system, the method of receiving output data, the intensity, polarization and spectral distribution of the energy available, *etc.*, must also be considered. The nature of the detection system, especially for array detectors, plays a major role in system design: its size, resolution, and image field flatness are critical issues in the specification of the optical system.

Resolving power depends on many aspects of the optical system and the quality of its components. In some cases, the grating may be the limiting component. The decision here involves the size of the grating and the angle at which it is to be used, but not on the number of grooves on the grating or the groove spacing (see chapter II).

Speed (or throughput) determines the focal length as well as the sizes of the optical elements and of the system itself. Special overcoatings become important in certain regions of the spectrum, especially the vacuum ultraviolet. For example, Al + MgF_2 is advisable in the 100-170 nm region, and Au and Pt in the 30-110 nm region.

There are other criteria, such as imaging (*e.g.*, astigmatism), magnification and thermal stability. When thermal stability is important, gratings should be made on a low expansion material, such as ZeroDur™ or ULE® fused silica.

Care in Handling Gratings

Most diffraction gratings have an aluminum coating on the active surface, because no other material reflects so well over so much of the electromagnetic spectrum. Unfortunately this makes gratings as vulnerable as unprotected first-surface mirrors (but no more so), and they should be treated accordingly. Every effort should be made to avoid the two worst enemies of such surfaces: fingerprints and oral spray. Scrubbing is not permissible and even gentle swabbing under a liquid should be performed by an expert. If fingerprints are accidentally deposited on a ruling, they should be removed immediately by rinsing from a squeeze bottle containing spectroscopic-grade solvents, such as xylene or toluene. Even CP grades of solvent should not be used, as they may leave residues. A final rinse with isopropyl alcohol is recommended.

As the surface of a diffraction grating is delicate, the grating must be unpacked with care to avoid accidental scratching, and should be stored in the same type of environment as the instrument in which they will be used.

Grating Cleaning Service

The Richardson Grating Laboratory offers a cleaning service for contaminated gratings. Solvent cleaning is the traditional manner in which grating surfaces are cleaned,

though plasma-cleaning in an oxygen atmosphere has been shown to remove thin radiation-induced deposits. Cleaning optical surfaces with a jet of carbon dioxide snow has recently been shown to be a feasible method of removing fingerprint oils and facial grease, as well as other hydrocarbon and silicone stains.

RECOATING

Gratings last a long time in the proper environment, but sometimes hostile conditions cannot be avoided. For example, oil vapor in a vacuum system can be baked onto optical surfaces by ultraviolet light. Experience has shown that damaged gratings can sometimes be restored to almost original efficiency by careful cleaning, which may or may not be followed by recoating. Visual appearance is not always a good indicator of whether such an operation will be successful.

APPEARANCE

In the early days of diffraction grating manufacture, R.W. Wood remarked that the best gratings were nearly always the worst ones in their cosmetic or visual appearance. While no one would go so far today, it is important to realize that a grating with certain types of blemishes may well perform better than one which appears perfect to the eye.

Ruled gratings. Cosmetic defects on ruled gratings may be caused by small droplets of metal or oxide which have raised the ruling diamond, or streaks may be caused by temporary adhesion of aluminum to the sides of the diamond tool. On ruled concave gratings, one can usually detect by eye a series of concentric rings called a *target pattern.* It is caused by minor changes in tool shape as the diamond swings through the arc required to rule on a curved surface. Every effort is made to reduce the visibility of target patterns to negligible proportions.

Some ruled master gratings have visible surface defects. The most common sort of defect is a region of grooves which are burnished too lightly (in relation to the rest of the grating surface). While readily seen with the eye, such a region has little effect on spectroscopic performance.

Interference gratings. Interference gratings are susceptible to a different set of cosmetic defects. *Comets* are caused by specks on the blank; when the blank is rotated (spun) as the photoresist is applied, these specks cause the photoresist to flow around them, leaving comet-like trails. Artifacts created during the recording process are also defects; these are holograms of the optical components used in the recording of the grating.

GRATING MOUNTING

The basic rule of mounting a grating as for any precise optical element: its shape should not be changed accidentally through excessive clamping pressure. This problem can be circumvented by kinematic (three-point) cementing from the rear surface, using a nonrigid cement, or by supporting the surface opposite the point where clamping pressure is applied.

BIBLIOGRAPHY

Hunter, W.R., 1985. "Diffraction Gratings and Mountings for the Vacuum Ultraviolet Spectral Region," *Spectrometric Techniques, vol. IV.*, 63-180 (1985). This article provides a very thorough and detailed review of the use and manufacture of diffraction gratings.

Hutley, M.C., 1976. "Interference (holographic) diffraction gratings," *J. Phys. E.* **9**, 513-520 (1976). This article offers more detail on interference gratings, and compares them with ruled gratings.

Hutley, M.C., 1982. *Diffraction Gratings*, Academic Press (New York, New York). This book provides a complete and thorough tour of diffraction gratings, their manufacture and their application.

Loewen, E.G., 1983. "Diffraction Gratings, Ruled and Holographic," in *Applied Optics and Optical Engineering*, vol. IX (chapter 2), R. Shannon, ed., Academic Press (New York, New York). This chapter describes developments in grating efficiency theory as well as those in concave grating aberration reduction.

Meltzer, R.J., 1969. "Spectrographs and Monochromators," in *Applied Optics and Optical Engineering*, vol. V (chapter 3), R. Shannon, ed., Academic Press (New York, New York).

Richardson, D., 1969. "Diffraction Gratings", in *Applied Optics and Optical Engineering*, vol. V (chapter 2), R. Shannon, ed., Academic Press (New York, New York).

Schroeder, D.J., 1987. *Astronomical Optics*, Academic Press (San Diego, California). Chapters 12 through 15 serve as an excellent introduction to gratings and their instruments, with application toward stellar spectrometry. Chapters 2 through 5 form a clear and quite complete introduction to the ideas of geometrical optics used to design lens, mirror, and grating systems.

Skoog, D.A., 1988. *Principles of Instrumental Analysis*, third edition, Saunders (Philadelphia, Pennsylvania). The chapters on spectroscopy serve as a good introduction to the subject.

Stover, J.C., 1990. *Optical Scattering*, McGraw-Hill, Inc. (New York, New York).

Williard, H.H., *et al.*, 1988. *Instrumental Methods of Analysis*, seventh edition, Wadsworth. (Belmont, California). The chapters on absorption and emission spectroscopy, and ultraviolet and visible spectroscopic instrumentation, are of particular interest.

REFERENCES

HUNTER *et al.* 1972. W. R. Hunter, T. L. Mikes and G. Hass, "Deterioration of Reflecting Coatings by Intermetallic Diffusion," *Appl. Optics* **11**, 1594-1597 (1972).

HUTLEY AND HUNTER 1981. M. C. Hutley and W. R. Hunter, "Variation of blaze of concave diffraction gratings," *Appl. Optics* **20**, 245-250 (1981).

LOEWEN *et al.* 1977. E.G. Loewen, M. Nevière and D. Maystre, "Grating Efficiency Theory as it applies to Blazed and Holographic Gratings," *Applied Optics* **16**, 2711-2721 (1977).

NAMIOKA 1959. T. Namioka, "Theory of the Concave Grating," *J. Opt. Soc. Am.* **49**, 446 (1959).

NODA *et al.* 1974. H. Noda, T. Namioka and M. Seya, "Geometric Theory of the Grating," *J. Opt. Soc. Am.* **64**, 1031 (1974).

RIFE *et al.* 1989. Jack C. Rife, W. R. Hunter, Troy W. Barbee, Jr., and R. G. Cruddace, "Multilayer-coated blazed grating performance in the soft x-ray region," *Appl. Optics* **28**, 1984 (1989).

SCHROEDER 1982. Daniel J. Schroeder, "Optimization of Converging-Beam Grating Monochromators," *J. Opt. Soc. Am.* **60**, 1022 (1970).

RICHARDSON GRATING LABORATORY TECHNICAL PUBLICATIONS

Below is a partial list of publications by our scientists and engineers pertaining to diffraction gratings and their uses. Please call us at 716/262-1331 to receive a reprint of any that interest you.

GRATINGS IN GENERAL

A-1 D. Richardson, "Diffraction Gratings", chapter 2, volume II of *Applied Optics and Optical Engineering*, R. Kingslake, ed. (Academic Press, New York: 1969)

A-2 E.G. Loewen, *Diffraction Gratings for Spectroscopy*, *J. Physics E* **3**, 953-961 (1970).

A-3 E.G. Loewen, "Diffraction Gratings, Ruled and Holographic", chapter 2, volume IX of *Applied Optics and Optical Engineering*, R. Shannon, ed. (Academic Press, New York: 1983), *pp.* 33-71.

A-4 E.G. Loewen, "The Ruling and Replication of Diffraction Gratings", *Optics and Photonics News*, May 1991.

A-5 *Diffraction Grating Handbook*, third edition, Richardson Grating Laboratory (1996).

A-6 C. Palmer, "Diffraction Gratings: The Crucial Dispersive Component," *Spectroscopy* **10**, 14-15 (1995).

GRATING EFFICIENCY

B-1 E.G. Loewen, M. Nevière and D. Maystre, "Grating Efficiency Theory as it applies to Blazed and Holographic Gratings," *Applied Optics* **16**, 2711-2721 (1977).

B-2 E.G. Loewen and M. Nevière, "Simple Selection Rules for VUV and XUV Diffraction Gratings," *Applied Optics* **17**, 1087-1092 (1978).

B-3 L.B. Mashev, E.K. Popov and E.G. Loewen, "Optimization of Grating Efficiency in Grazing Incidence", *Applied Optics* **26**, 4738-4741 (1987).

GRATING IMAGING

C-1 W.R. McKinney and C. Palmer, "Numerical design method for aberration-reduced concave grating spectrometers," *Applied Optics* **26**, 3108-3118 (1987).

C-2 C. Palmer, "Theory of second generation holographic gratings," *J. Opt. Soc. Am. A* **6**, 1175-1188 (1989).

C-3 C. Palmer and W.R. McKinney, "Equivalence of focusing conditions for holographic and varied line-space gratings", *Applied Optics* **29**, 47-51 (1990).

C-4 C. Palmer, "Deviation of second-order focal curves in common spectrometer mounts", *J. Opt. Soc. Am. A* **7**, 1770-1778 (1990).

C-5 C. Palmer and W. McKinney, "Imaging Theory of Plane-symmetric Varied Line-space Grating Systems", *Optical Engineering* **33**, 820-829 (1994).

ECHELLE GRATINGS

D-1 G.R. Harrison, E.G. Loewen and R.S. Wiley, "Echelle gratings: their testing and improvement," *Applied Optics* **15**, 971-976 (1976).

D-2 E.G. Loewen, D. Maystre, E. Popov and L. Tsonev, "Echelles: scalar, electromagnetic and real-groove properties," *Applied Optics* **34**, 1707-1727 (1995).

D-3 E. Loewen, D. Maystre, E. Popov and L. Tsonev, "Diffraction efficiency of echelles working in extremely high orders," *Applied Optics* **35**, 1700-1704 (1996).

INDEX

Definitions are found on **bold-face** pages.

aberration **29**
aberration coefficient **29**
Abney mount *33*
alignment, in invisible spectral regions *60*
anamorphic magnification **10**
angle, sign convention for *3*, *29*
angular deviation *4*, **34**, *44*
angular dispersion **6**
anomalies **42**
astigmatism **30**
astronomical grating *59*
B engine *13*
bandpass **8**
bandwidth *38*
blaze wavelength **41**
blazing *2*, **41**, *49*
camera **23**
Carpenter prism - *see grism*
classical diffraction **4**
classical equivalent grating **16**
classical grating **27**
collimator **23**
comets **62**
concave grating **27**
conical diffraction **4**
constant-deviation monochromator **34**
cross-rulings **59**
curvature, of concave blank **28**
Czerny-Turner mount **23**, *55*
defocus **30**
deviation angle *4*, **34**
diffraction *1*, *3*
  classical **4**
  conical **4**
  in-plane **4**
diffraction angle *29*
diffraction grating – *see grating*
diffraction limit **36**
diffraction order **4**
  existence *5*
  overlapping *5*
  zero *5*
dispersion **6**
  angular **6**
  linear **7**
  of light by grating *4*
  plane of **28**
  reciprocal linear **7**
dispersion plane **28**
double monochromator **25**
Eagle mount *33*
Ebert-Fastie mount **24**, *55*
echelle *10*, *14*, **57**
effective spectral bandwidth **38**
efficiency **41**
  absolute **41**, *52*
  anomalies *53*
  curve **41**, *53*
  relative **41**, *52*
errors of run **53**
f/number **9**
facility *17*
fanning error **53**
far scatter *54*
Fermat's principle *28*
filter (grating) *59*
first generation interference grating **17**, *27*, *31*
flat-field spectrograph **33**
focal distance *30*
focal length **9**
focal ratio **9**
Foucault knife-edge test *53*
free spectral range **10**
fringe pattern **15**
full spectral bandwidth **38**
full width at half maximum **38**
full width at zero height **38**
FWHM **38**
FWZH **38**
ghosts *11*, *13*
  Lyman *51*, **52**
  Rowland *13*, *51*
grass **52**
grating **1**, *3*
  as a beam divider *60*
  as a filter *59*
  astronomical *59*
  blazing *14*
  care *21*, *61*
  choice *61*
  classical **27**
  cleaning *50*, *61*
  coating *21*
  concave *27*, *55*
  crossed groove patterns on *59*
  damage *21*
  echelle **57**
  fingerprints on *50*
  first generation interference **17**, *27*
  for electron microscope calibration *59*
  for laser tuning *59*
  for space-borne spectrometry *60*
  grazing incidence *57*
  groove frequency **4**, *18*
  groove pattern *19*
  groove profile *18*
  holographic - *see grating, interference*
  identification of blaze direction *21*
  interference *2*, **15**
    blazing *49*
    classification **16**
    recording process *17*
    versus ruled *18*
  manufacture time *19*
  mount **23**
    terminology *23*
    with concave grating *32*
    with plane grating *23*
  normal **3**, **28**
  overcoating *49*
  pitch **4**
  plane *23*, *55*

recoating *62*
reflection **1**
replica *19, 21*
rotation *5*
ruled **13**
second generation interference *17, 27*
Sheridon *16*
special overcoatings *55*
special sizes *60*
stray light *18*
substrate shape *19*
tangent plane **28**
testing *14*
transmission **1**
varied line-space (VLS) *27*
VLS *27*
grating equation **4**
for Littrow configuration *4*
in optical media other than air *56*
grating normal **3**
grating prism – *see grism*
grazing incidence system *57*
grism **56**
groove frequency **4**
groove spacing *2*, **3**
errors of run *53*
fanning error *53*
precision (ruled grating) *2*
variations in *51, 52*
grooves per millimeter **4**
holographic grating - *see grating, interference*
in-plane diffraction **4**
incidence angle *3, 29*
instrument function *8*
interference grating - *see grating, interference*
interferometric control *13*
ion etching *18*, **49**
knife-edge test, Foucault *53*
laser tuning *24, 59*
limit of resolution **7**, – *see resolution*
line curvature **30**
linear dispersion **7**
reciprocal **7**
linespread function **36**
Littrow configuration **4**
angular dispersion *6*
for laser tuning *59*
Rowland ghosts in *52*
Littrow mount **24**
Lyman ghosts **52**
magnification
anamorphic **10**
sagittal **36**
tangential **36**
Mann engine *13*
Michelson engine *13*
molecular laser tuning *59*
Monk-Gillieson mount **24**
monochromator **23**
double **25**
triple **25**
near scatter *54*
obliquity factor **7**
order – *see diffraction order*
order sorting **6**, *11*
Paschen-Runge *39*
Paschen-Runge mount **33**
peak wavelength **41**
photoresist **16**
pitch **4**
plane grating *23*, **28**
plate factor **7**
polarization **42**, *53*
polychromator **23**
principal plane **28**
prism *56*
radius, of concave blank *28*
Raman gratings *52*
Raman spectroscopy of solid samples *25*
reciprocal linear dispersion **7**
reflection grating **3**
replica *2*, **21**
replication *2*, **21**
resolution **8**
resolution, spectral **8**
and resolving power *9*
resolving power **7**, *13, 55*
and spectral resolution *9*
maximum theoretical *8*
Richardson Grating Laboratory *2*
Rowland circle mount **32**
Rowland ghosts – *see ghosts*, **51**
ruling engine **13**
S-plane *59*
sagittal focal distance **30**
sagittal focusing *31*
sagittal plane **28**
sagittal radius, of blank **28**
satellites *51*, **52**
scan angle *4*
scattered light *54*
second generation interference grating **17**, *27*
servo control systems *2*
Seya-Namioka monochromator **34**
Sheridon grating **16**
signal-to-noise ratio (SNR) **12**
sine bar *5*
Snell's law *56*
SNR (signal-to-noise ratio) *12*
solvents (for cleaning gratings) *50, 61*
spectral order – *see diffraction order*
spectrograph **23**
spectrometer **23**
specular reflection **4**
spot diagram **35**
stigmatic image **29**
stray light *11, 18, 54*
surface microroughness *11*
tangent plane, of grating **28**
tangential focal distance **30**
tangential focusing *31*
tangential plane **28**
tangential radius, of blank **28**
target pattern *62*
temperature control *2*
transmission grating **3**
triple monochromator **25**
varied line-space (VLS) grating **14**, *27*
vibration *2*
VLS (varied line-space) grating **14**, *27*
Wadsworth mount **33**
wavefront testing *53*
Wood's anomalies **42**
zero order **4, 5**

Richardson Grating Laboratory
Formerly a Unit of Milton Roy Company

820 Linden Avenue, Rochester, New York 14625 USA; Tel: 800-654-9955 or 716-262-1331; Fax: 716-454-1568
E-Mail: gratings@spectronic.com; Web Site: http://www.gratinglab.com

35-2047 • MP • 6/96

Printed in